STUDY ON THE PYROLYSIS BEHAVIOR OF SOME MONOTERPENES AND MONOTERPENOIDS

– A MECHANISTIC AND KINETIC OVERVIEW

Dissertation

zur Erlangung des akademischen Grades

doctor rerum naturalium (Dr. rer. nat.)

vorgelegt dem Rat der Chemisch-Geowissenschaftlichen Fakultät

der Friedrich-Schiller-Universität Jena

von Dipl.-Chem. Achim Stolle

geboren am 20. November 1980 in Eisenach

Gutachter:

1. Prof. Dr. Bernd Ondruschka (Friedrich-Schiller-Universität Jena)

2. Prof. Dr. Rainer Beckert (Friedrich-Schiller-Universität Jena)

3. Prof. Dr. Henning Hopf (Technische Universität Braunschweig))

Tag der öffentlichen Verteidigung: 23. Juli 2008

Preface

Since the time of alchemists in the outgoing middle age pyrolysis processes own their place in synthetic organic as well as inorganic chemistry. Until the time modern analytical methods (GC, NMR) become available for every chemist pyrolysis reactions were rediscovered as unique methods for the kinetic investigations of high temperature processes, the isolation or synthesis of highly active species (carbenes, nitrenes) and their spectroscopical characterization. Very low pressure pyrolysis ($p > 1$ mbar) offers the opportunity to study the chemistry of single molecules without the presence of intermolecular reactions.

In the field of the thermal rearrangement of monoterpenes pyrolysis processes are the irreplaceable method of choice since gas- as well as liquid-phase thermolysis allows for the discrete regulation of reaction temperature and residence time. Hence, much research in this field of chemistry of natural products is published until today there is still the need for systematical comparative pyrolysis studies under similar or at least comparable experimental conditions. With this study an approach will be made in this direction. Six different pinane-type monoterpenes (α-pinene, β-pinene) and monoterpenoids (*cis*-pinane, *trans*-pinane, *cis*-2-pinanol, nopinone) will be subjected to explorative as well as kinetic gas-phase pyrolysis studies in a flow-type reactor using nitrogen as carrier gas. In order to unravel consecutive products which most of the acyclic primary pyrolysis products of theses bicyclic starting materials form, thermal isomerization experiments with the acyclic monoterpenes were conducted also. Calculation of Arrhenius as well as Eyring parameters allows for a deeper insight in the reaction mechanism and the nature of the transition states the reactions passing through. Studying the effects of substituents next to the bridge-head carbon atoms each of the six bicyclic starting materials represents a class of substituents.

This dissertation is prepared as a cumulative PhD-thesis. Therefore, the thermal behavior of some of the bicyclic starting materials (pinane, β-pinene, nopinone) is discussed in several papers already published or accepted for publication. In these cases the respective chapters are supposed to be a summary of the corresponding papers which can be found in the appendix of this dissertation. Hence, the results of the thermal rearrangement of α-pinene and *cis*-2-pinanol are not published yet the corresponding chapters are more comprehensive than the other parts.

Achim Stolle

Jena, June 2008

Preface Electronic Version

This dissertation is prepared as a cumulative PhD-thesis. Therefore, the thermal behavior of some of the bicyclic starting materials (pinane, β-pinene, nopinone) is discussed in several papers already published or accepted for publication. Due to copyright regulations it is not possible to include the respective papers in the electronic version of this thesis. For easy finding of the articles already published, please use the links given in the Reference List starting on page 96.

Achim Stolle

Jena, September 2008

Acknowledgement – Danksagung

Mein herzlichster Dank gilt folgenden Personen:

Prof. Dr. Bernd Ondruschka für die Vergabe des interessanten Promotionsthemas, die gewährte finanzielle als auch wissenschaftliche Unterstützung, sowie den gewährten Freiraum zur Planung und Durchführung der Arbeiten und für die Anfertigung des Erstgutachtens.

Prof. Dr. Rainer Beckert und Prof. Dr. Henning Hopf danke ich für ihr Interesse an meiner Arbeit und die Anfertigung des Zweit- bzw. Drittgutachtens.

Spezieller Dank richtet sich an PD Dr. Werner Bonrath und Dr. Thomas Netscher (beide DSM Nutritional Products) für die interessanten Diskussionen, ihren Beitrag zu den jeweiligen Manuskripten, ihre Geduld and die finanzielle Unterstützung insbesondere das Ermöglichen eines Arbeitsaufenthaltes bei DSM Nutritional Products in Kaiseraugst (CH).

Dr. Annegret Stark und Dr. Marcus M. Hoffmann für ihre Unterstützung bei der Übersetzung und / oder Korrektur der einzelnen Manuskripte.

Dr. Matthias Findeisen und Dr. Manfred Friedrich für NMR-Messungen, deren Auswertung und für interessante Diskussionen.

Die Hilfe von Dr. Nils Theyssen für die Realisierung der präparativen GC-Messung an seinem Institut und die Durchführung der daraus resultierenden Analysen soll an dieser Stelle besonders betont werden.

Daniel Kinzel und Prof. Dr. Leticia González möchte ich an dieser Stelle für ihre Zusammenarbeit auf dem Gebiet der Aufklärung des Reaktionsmechanismus der thermischen Umwandlung von Pinan mit *ab initio* Methoden danken.

Für die Beiträge zu dieser Arbeit durch Simon Prickler, Anja Baumgärtel und Lars Krantz während ihrer Tutorpraktika möchte ich mich bedanken.

Da diese Arbeit ohne technische Unterstützung nicht zustande gekommen wäre, möchte ich mich bei Gisela Gottschalt, Antje Tied, Erwin Maeder und Heike Süß bedanken.

Für die großartige und ungezwungene Arbeitsatmosphäre und die hoffentlich anhaltende Zusammenarbeit im Labor möchte ich mich ausdrücklich und herzlich bei Franzi, Christine, Silke, Tony, Antje T und Antje W bedanken. Da es in ihrer Anwesenheit oft zu schönen Momenten und lustigen Begebenheiten kam, an denen ich glücklicherweise oft teilhaben konnte, wäre das Anfertigen dieser Arbeit ohne sie nicht möglich gewesen – Danke Schön.

Bei allen früheren und aktuellen Kollegen am Institut für Technische Chemie und Umweltchemie der Friedrich-Schiller-Universität Jena möchte ich mich bedanken.

Last, but definitely not least; möchte ich mich bei meiner Familie, bei meinen Freunden und Bekannten für die Unterstützung und die teils immer mal wieder notwendige Motivation während der letzten drei Jahren bedanken.

Content

Preface iii

Preface ElectronicVersion v

Acknowledgement – Danksagung vi

Content viii

List of Abbreviations x

Chapter 1: Introduction 1

1.1 Pyrolysis in Synthetic Organic Chemistry 3
1.2 Monoterpenes and their Biosynthesis 5
1.3 Thermally induced Rearrangements of Pinane-Type Terpenes 8
1.4 Purpose of the Investigation 14

Chapter 2: Methods and Techniques 17

2.1 Materials 17
2.2 Analyses 18
2.3 Synthesis 19
2.4 Pyrolysis Experiments 20
2.5 Kinetic Experiments 22

Chapter 3: Pyrolysis of *cis*-Pinane, *trans*-Pinane and of *cis*-2-Pinanol 25

3.1 Thermal Behavior of (+)-*cis*- and (-)-*trans*-Pinane 26
3.2 Kinetic Considerations in the Field of Pyrolysis of Pinane 28
3.3 Thermal Behavior of *cis*-2-Pinanol and of (-)-Linalool 30
3.4 Kinetic Studies of the Thermal Rearrangement of 2-Pinanol and of Linalool 33

Chapter 4: Pyrolysis of α-Pinene 38

4.1 Background 39
4.2 Pyrolysis of α-Pinene 40
4.3 Pyrolysis of Ocimene 43
4.4 Pyrolysis of Alloocimene 44
4.5 Elucidation of Kinetic Steps in the Pyrolysis of α-Pinene 46

4.6 Pyrolysis Mechanisms of α-Pinene, Ocimene and Alloocimene 53

Chapter 5: Pyrolysis of β-Pinene and of Nopinone 61

5.1 Thermal Behavior of β-Pinene and Myrcene 62
5.2 Kinetic Analysis the Pyrolysis Reaction of β-Pinene and Myrcene 64
5.3 Synthesis of Nopinone 65
5.4 Pyrolysis of Nopinone and its Kinetic Analysis 66

Chapter 6: Comparison of the Results 70

6.1 Reactivity of the Compounds Investigated 71
6.2 Product Selectivity of the Compounds Investigated 75
6.3 Reactivity of the Acyclic Main Products 78
6.4 Prediction of the Pyrolysis Behavior of Bifunctional Pinane-Type Substrates 81

Chapter 7: Conclusion 86

Abstract in German – Zusammenfassung 90

References and Notes 96

Declaration of Authorship – Selbstständigkeitserklärung 102

Appendix I

Curriculum Vitae – Lebenslauf II

Documentation of Authorship III

Conference Contributions and List of Publication V

List of Abbreviations

Constants

h	Planck constant	$6.62606876\ 10^{-34}$ J s
k_b	Boltzmann constant	$1.3806503\ 10^{-23}$ J K^{-1}
R	universal gas constant	8.3144712 J mol^{-1} K^{-1}

Formula Signs

$\Delta_R G$	free reaction energy (eq. 4.2) / kJ mol^{-1}
$\Delta^{\ddagger} H$	Eyring enthalpy of activation (eq. 2.8) / kJ mol^{-1}
$\Delta_R H$	reaction enthalpy / kJ mol^{-1}
$\Delta^{\ddagger} S$	Eyring entropy of activation (eq. 2.8) / J mol^{-1} K^{-1}
$\Delta_R S$	reaction entropy / J K^{-1} mol^{-1}
τ	average residence time (eq. 2.6) / s
[*i*]	corrected concentration of reaction product *i* from GC-analysis / %
[*s*]	corrected concentration of non-converted starting material *s* from GC-analysis / %
i	reaction product *i*
s	starting material *s*
A, $\log_{10} A$	Arrhenius (frequency) factor (eq. 2.7) / s^{-1}
A_{cs}	cross-sectional area of the reactor / cm^2
A_R	reactor surface area / cm^2
d_A	outer diameter of quartz insert / mm
E_a	Arrhenius activation energy (eq. 2.7) / kJ mol^{-1}

ee	enantiomeric excess (eq. 2.1) / %
K	equilibrium constant
$k_{j,T}$	first-order rate constant for reaction *j* and at temperature *T* / s^{-1}
S_i	selectivity for reaction product *i* (eq. 2.4) / %
$S_{cp,i}$	selectivity for reaction product *i* considering consecutive reaction products of product *i* (eq. 2.5) / %
S/*V*	surface-to-volume-ratio / cm^{-1} ($S/V = A_R/V_R$)
t	retention time / min
T	temperature / °C – temperature range / K
V_R	reactor volume / mL
X_s	conversion of starting material *s* (eq. 2.3) / %
Y_i	yield of pyrolysis product *i* (eq. 2.2) / %
Y_s	yield of non-converted starting material *s* (eq. 2.2) / %

Abbreviations

ATR	attenuated total reflection
cp	consecutive product
eq.	equation
FVP	flash vacuum pyrolysis
FVT	flash vacuum thermolysis
GC	capillary gas chromatography
GC-FID	GC with flame ionization detector
GC-MSD	GC with mass selective detector
GLC	gas-liquid chromatography
(FT)-IR	(fourier transform) infrared spectroscopy
MS	mass spectrometry (here: in connection with GC)
NMR	nuclear magnetic resonance spectrometry
NOE	nuclear Ovenhauser effect
t.s.	transition states
VLPP	very low pressure pyrolysis

CHAPTER 1

Introduction

The role of chemical industry is from growing importance for everybody's everyday live. Without chemistry the today's population has to cut out modern achievements for instance individual transportation or the use of plastics. Growing earth population in combination with a growth in standard of living in population-rich developing countries (China, India) and the reach of "peak oil" faces modern chemists with special challenges to overcome these problems. Generally, industrial syntheses of bulk and even fine chemicals or commodities base on the usage of non-regenerative resources like natural oil or gas. On the other hand these play a major role in today's energy management also (production of fuels). This is one of the biggest problems our society has to face with and solve. The fact that on one hand natural non-regenerative resources are the irreplaceable basis for chemistry and on the other hand they are converted into carbon dioxide and water for energy providing is contradictorily. To overcome this discrepancy in the last ten years many strategies with various goals and approaches were developed focusing in different directions:

a) Replacement (partial or complete) of natural oil and gas for fuel production by regenerative resources (fuels from biomass, "sun fuels", biomass-to-liquid process).[1]
b) Utilization of regenerative resources (carbohydrates, proteins, fatty acids, glycerin) for the syntheses of bulk as well as fine chemicals.[1a-e,2]
c) Energy and fuel saving in industry, traffic, trade, and household.
d) Implementation of new or improved processes in chemistry with higher conversions and selectivities for a more sustainable use of rare non-regenerative resources.[3]

Facing and solving these problems by developing new sustainable strategies or improving traditional processes with respect to higher yields and selectivities should be one of the main foci of every modern chemist. Various branches of industrial as well as academic chemical research (*e.g.* catalysis, process development, reactor design) are aware of these problems and contributing to this social world-wide challenge.[1a,3]

The utilization of regenerative resources as basis for the industrial syntheses of chemicals is one of the most promising ways for solving the resource and energy problematic.[1a,3b,4] Various biomaterials can be or are used already as starting materials in chemical industry for the production of fine chemicals as well as of commodities. Carbohydrates (*e.g.* starch, glucose, fructose) are widely used for the syntheses of pharmaceuticals, vitamins and other products for animal and human nutrition. In addition carbohydrates in combination with enzymes are applied in the biosynthesis of products from pharmaceutical interest. Methyl esters of fatty acids *via* alkaline methanolysis of natural occurring animal or vegetable triglycerids are the basis for regenerative fuels or fuel additives. This process yields glycerol in high amounts as side product which can be applied for the synthesis of various multifunctional C_3 building blocks for chemical synthesis (dihydroxyacetone, methyl acrylate).[2]

A minor class of natural occurring substances are the terpenes or terpenoids. They are classified as oligomers or polymers of isoprene (C_5H_8) having the general formula $(C_5H_8)_n$ with n ranging from 1 to 8 (terpenes). Derivatives with heteroatomaric functionalizations (alcohols, aldehydes, amines) and compounds with variable carbon and hydrogen content (*e.g.* norterpenes: $C_{5n-1}H_{8n-2}$ or homoterpenes: $C_{5n+1}H_{8n+2}$) are commonly known as terpenoids. Solely important for the assignation as terpenes is the connection to its biosynthetical origin. This substance class is widely used in flavor and fragrance industry due to the fact that many terpenes and terpenoids have a typical unique odor and / or flavor (*e.g.* menthol, limonene).[5-9] Due to the fact that terpenes and terpenoids are natural occurring materials and its production from plants or parts of them (leafs, fruits) by distillation, cold-pressing, or extraction are well established methods, they can serve as interesting starting materials for the synthesis of fine chemicals.[8,9] Monoterpenes ($C_{10}H_{16}$; limonene, pinene) and monoterpenoids (citronellol, menthol, camphor) are worthy starting materials in pharmacy as well as in flavor and fragrance industry. Besides acid-catalyzed or transition metal catalyzed isomerizations or

functionalizations, thermally induced rearrangements of pinenes (pyrolysis) play a major role in synthetic processes based on these educts.

1.1 Pyrolysis in Synthetic Organic Chemistry

Since the beginning of the existence of chemistry as accepted branch of natural science in the outgoing eighteenth century pyrolysis processes play an important role for the development of this field of research. Destructive distillation of minerals or organic materials was one of the earliest preparative methods available to the first chemists (*e.g.* H_2SO_4 from ferrous sulphate). Due to the lack of analytical methods for direct observation of experiments and characterization of product mixtures pyrolysis were used to characterize the chemical behavior of organic materials until the end of the nineteenth century. Decarboxylation of benzoic acid by Mitscherlich yielding benzene was one of the first examples for the use of pyrolysis in organic synthesis.[10] Widespread introduction of modern analytic techniques in the 1950's (*e.g.* GLC, mass spectrometry, NMR) opened the field of synthetic pyrolysis reactions for more sophisticated mechanistic investigations due to its capability to analyze volatile compounds and elucidate structures without complex chemical derivatization. The application of molecular orbital theory in 1950 (Woodward-Hoffmann rules) allows for comparison of thermal and photochemical behavior thus being an tool of interest for mechanistical explorations.[11] Combining short times in reaction zone and times of flight in order to study transient species leads to the introduction of very low pressure pyrolysis (VLPP)[12] or flash vacuum pyrolysis (thermolysis) [FVP(T)],[13,14] making it an interesting tool for gas kineticists.

The use of both terms: pyrolysis[12,13] and thermolysis[14] for the description of similar experiments is confusing. From a more logical point of view, thermolysis (*thermos*: heat, *lysis*: break down) is the generic term and is defined as: a chemical reaction whereby chemical substances being broken up into at least two chemical substances when heated. From a more general point of view: it is a reaction including the breakage of at least one bond in an organic molecule induced by heating. This would suggest that all reactions are thermolysis reactions because the breakage of bonds requires "heat". Anyhow, leading to a more precise definition the term "pyrolysis" was introduced in chemistry. Pyrolysis (*pyros*: fire, *lysis*: break down) is defined as: the chemical decomposition of organic

matter by heating in the absence of oxygen or any other reagent, or more generally: chemical reactions which can be thermally induced in the temperature range of a fire (150-1200 °C).[15] From experimental viewpoint pyrolysis reactions are reactions carried out in the absence of solvents, oxygen, or catalysts at temperatures higher than used ordinary in laboratory (0-300 °C), meaning a temperature range between 350-900 °C.[15,16] If oxygen is present in the thermal reaction it is called combustion and if carbon is the only residue of a pyrolysis the term carbonization has to be used. Additionally and with respect to industrial chemistry pyrolysis can also be comprehended as the process of thermal cracking of hydrocarbons for the production of acetylene or ethylene.

However, the scope of pyrolysis reactions is focused on monomolecular reactions, for instance: isomerizations,[17-19] eliminations,[20] cyclizations,[19,21-24] aromatizations,[19,22-24] or pericyclic reactions,[19,20,23] whereby monomolecular merely means intramolecular and not in terms of a kinetic viewpoint activation without collision partners (collision theory, theory of activated complex). This is due to the fact, that the residence times in thermally induced reactions are very short and the reactants are present in low concentration either by the application of vacuum[12-14,25] or dilution with an inert gas.[17,18,21,22] Therefore, intermolecular reactions are not possible caused to the low probability of collision and often these bimolecular reactions are undesirable because the formation of polymers or soot resulting in lower selectivities and yields of the desired products. Industrial production of charcoal and of activated carbon take advantage of this yielding carbonized products. Silicon based ceramics can be synthesized by pyrolysis of silicon containing precursors (polysilane, polysiloxane).[26] Focusing on synthetic organic chemistry pyrolysis reactions play a major role in the production of polyaromatic hydrocarbons and fullerenes *via* intramolecular ring-closure reactions and elimination of hydrogen (aromatization).[23,24,27] Various other products as for instance heterocycles or ketenes can be generated using pyrolytic methods.[15,19,20,27] The synthesis of ketene intermediates *via* thermal cleavage of Meldrum's acid is one of the most utilized pyrolysis reaction in high-temperature organic synthesis.[28]

Pyrolysis reactions can be performed in both gaseous or condensed phase.[15,25] Gas-phase reactions have the great advantage that side-reactions yielding soot or coke can be suppressed due to low concentration of educt molecules in the gas phase and short residence times in the reaction zones. Often gas-phase reactions are carried out in flow

type reactors or sealed quartz tubes either at reduced pressure (FVP, VLPP)[12-14,25] or with the presence of an inert carrier gas (N_2, Ar, CO_2).[17,18,21,22] Flow systems are preferred if low contact times are necessary or the heat and residence time regulation is important for the process at all. Investigation of transient species often require the use of trapping agents which can either be introduced with the feed stream[17,18,22] or by separate injection.[25,29] Generally, pyrolysis reactions in liquid-phase can be carried out in sealed tubes made of an inert material (quartz, pyrex, steel) under reduced or atmospheric pressure with or without the presence of an inert gas. Pyrolyses in liquid phase are preferred if long reaction times at temperatures below 300 °C are necessary or desirable.

1.2 Monoterpenes and their Biosynthesis

A huge heterogeneous class of natural occurring substances are the terpenes and terpenoids. Beside condensed hydrocarbon rings, within this group acyclic, mono-, bi-, tri- and tetracyclic hydrocarbon compounds can be found with various functionalizations for instance alcohols, ethers, carbonyls, and heterocyclic compounds. Formally terpenes are oligomeric or polymeric hydrocarbons consisting of n isoprene units (2-methyl-1,3-butadiene; C_5H_8), whereas terpenoids are functionalized terpenes with molecular formulas different to $C_{5n}H_{8n}$ but with similar (bio)synthetic backgrounds.[30,31] Depending on the number of isoprene units the terpenes can be classified in different groups:

Hemiterpenes	one isoprene unit	C_5H_8,
Monoterpenes	two isoprene units	$C_{10}H_{16}$,
Sesquiterpenes	three isoprene units	$C_{15}H_{24}$, and so on.

Therefore, monoterpenes and monoterpenoids generally have a C_{10} skeleton, but also compounds with less then ten carbons (C_9, *e.g.* nopinone) belong to this class. A classification of monoterpenes from structural viewpoints is possible and widely utilized. In this connection, the internal linkage of the saturated hydrocarbons is considered.[32] Scheme 1.1 pictures the eight main structural motives of monoterpenes found for natural occurring compounds. Beware of this α-pinene (**9**), β-pinene (**10**), 2-pinanol (**11**), and nopinone (**12**; scheme 1.1) are compounds from pinane-type monoterpenes (**3**) and their main rearrangement products ocimene and myrcene are derivatives of 3,7-dimethyloctane

(**1**), whereas the flavor active compounds limonene and menthol are representatives of *p*-menthane-type monoterpenes (**2**).[33]

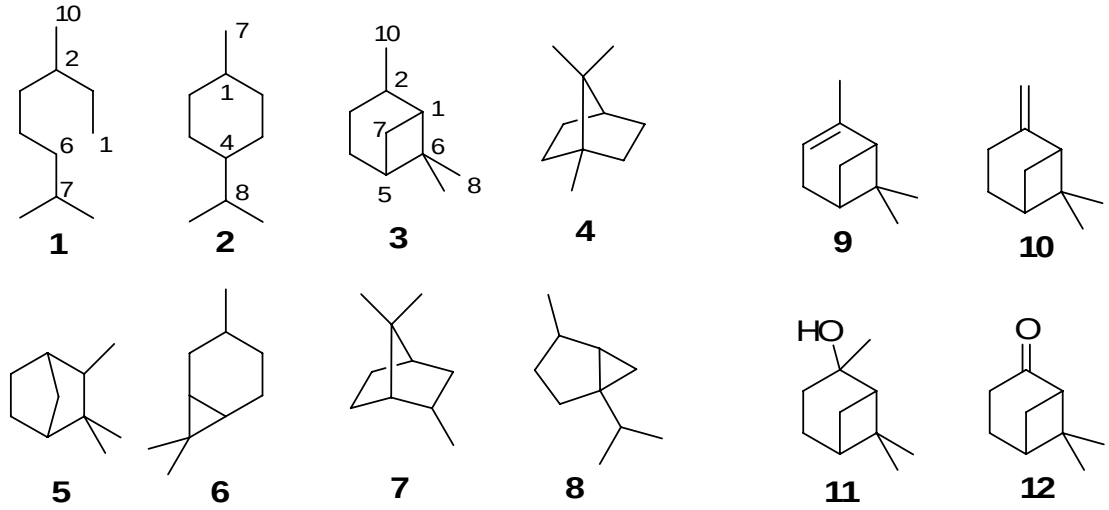

Scheme 1.1. Main classes of structural motives of natural occurring monoterpenes (**1**: 3,7-dimethyloctane, **2**: *p*-menthane, **3**: pinane, **4**: bornane, **5**: isocamphane, **6**: carane, **7**: fenchane, **8**: thujane) and important bicyclic monoterpenes (**9**: α-pinene, **10**: β-pinene, **11**: 2-pinanol, **12**: nopinone).

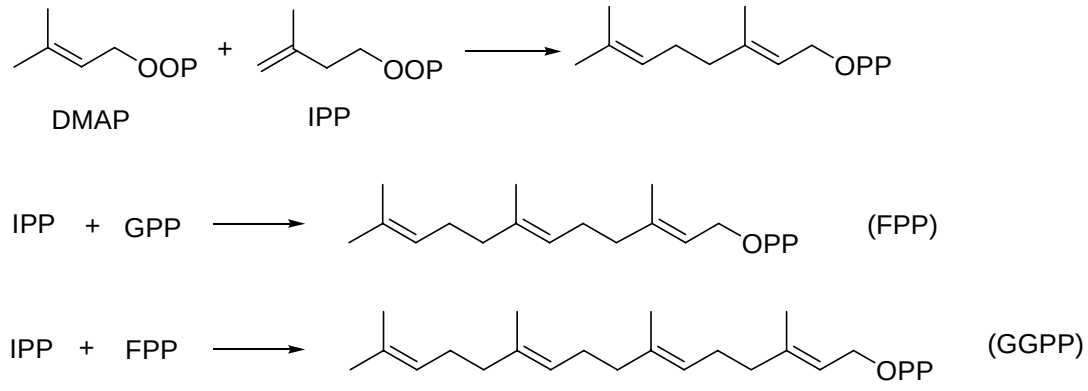

Scheme 1.2. Formation of biological terpene building blocks *via* enzymatical driven "head-to-tail" linkage of 3,3-dimethylallyl-pyrophosphate (DMAP) and 3-isopentenyl-pyrophosphate (IPP; GPP: geranyl-pyrophosphate, FPP: farnesyl-pyrophosphate, GGPP: geranylgeranyl-pyrophosphate).

Biosynthesis of terpenes and terpenoids follows a general structural principle known as "biogenetic isoprene rule", meaning that terpenes and terpenoids are not directly built from isoprene units, rather they yield from primarily formed terpene alcohols (geraniol – C_{10}, farnesol – C_{15}).[30,31,34] The biological synthesis of these natural building blocks is based on two C_5-intermediates: 3,3-dimethylallyl-pyrophosphat (DMAPP) and 3-

isopentenyl-pyrophosphat (IPP). Scheme 1.2 describes the enzymatically driven “head-to-tail” linkage leading to the formation of geranyl-pyrophosphate (GPP) as a C_{10} building block. Higher terpenes yield from additional linkage with IPP- or GPP-units.[30,31] Subsequently enzymatic functionalization (hydrolysis) leads to the formation of the corresponding alcohols almost all other natural occurring terpenes and terpenoids are based on. For instance, the cyclization of these alcohols results in cyclic terpenes (limonene, camphor) or the transformation of the hydroxyl-group into a carbonyl group yields aldehydes or ketones (citral).[31] Other combinations then “head-to-tail” are possible but not widely utilized in nature so that these products are rarely occurring.

Terpenes and terpenoids in general and terpene alcohols in special play a major role in both nature and chemical industry.[32,35] Importance in nature is based on the fact that these compounds are widely utilized in both fauna and flora with various functions. For instance they can act as repellents and due to their intensive and unmistakable odor they are important in plant-to-plant or / and plant-to-animal interactions.[34-37] Many plants contain terpenes and terpenoids in high concentrations which can be separated from the plant *via* steam-distillation, extraction cold-pressing or related processes yielding essential oils.[9] Composition of the extracts is closely related to the plant species, harvesting time, growth conditions, and locations the plants growth. To the predominant part the essential oils consist of mono- and sesquiterpenes or compounds derived from them.[32] Additional to the fact that these essential oils or the isolated terpenes (terpenoids) can be applied as flavors or as pharmacy without modifications[36] most of these substances serve as important educts for flavor and fragrance industry. Vitamins of the A-group as well as some colorants (carotenes) have their origins in terpenes or terpenoids.[38]

Essential oils and products separated from them *via* fractional distillation play a major role in the synthesis of flavors and fragrances.[8,9,38-41] Important monoterpene key components are limonene (from lime or citrus oil), **9** and **10** (from turpentine), and Δ3-carene (from Indian turpentine) which are the basis for the syntheses of other terpene hydrocarbons derived from them by acid catalyzed or thermally induced rearrangements (myrcene, camphene).[9,35,42] Catalytical functionalization of these hydrocarbons leads to the formation of terpene alcohols (linalool, citronellol), terpene aldehydes (citronellal, citral), or saturated hydrocarbons (**3**).[5-9,35,39,40]

1.3 Thermally Induced Rearrangements of Pinane-Type Terpenes

The thermal rearrangement of pinane-type monoterpenes and terpenoids is a long-known thoroughly investigated class of reactions.[5,43] Within the 1930th Smith and Carlson independently published results on the racemization of **9** observed during heating.[44] In the mid fortieth of the past century Arbuzov investigated the pyrolysis of α- (**9**) and β-pinene (**10**) and found that both yield limonene and an acyclic triene.[45] In the fifth decade of the 20th century research was intensified by Goldblatt and co-workers starting to investigate the gas-phase pyrolysis of **9** and **10**, describing the formation of alloocimene and myrcene from these, respectively.[46] At the same time authors found that pyrolysis of optical active **9** yields racemic limonene (dipentene) and racemized non-converted **9**, whereas optical active **10** forms optical active limonene. Within this time range transient biradicals were formulated as transition states in the pyrolysis of both **9** and **10** allowing the explanation of their different behavior.[47] First kinetic studies on isomerization of **9** and **10** as well in gas- and liquid-phase were performed in the 1950th in the research group of Hawkins.[43b,48] Additionally, research started to focus on other pinane-type compounds also. Chemists around Pines and others investigated the pyrolysis of pinane (**3**) under different reaction conditions showing that isomerization of **3** leads to the formation of β-citronellene.[49] The introduction of modern analytical methods (*e.g.* NMR, MS) and separation techniques (*e.g.* GLC, preparative GC) in everyday life of chemical laboratories allowed for the identification of minor side products of pyrolyses and therefore a much more detailed insight in such reactions. In the mid 1970th the group of Coxon, Garland and Hartshorn focused their research efforts on the pyrolysis of derivatives of **3**, **9**, and **10** studying the influence of various substituents on the product spectra formed.[50] In the past thirty years besides some intensive kinetic studies on pyrolysis of **9**[51,52] the influence of catalysts on the pyrolysis of 2-pinanol (**11**; scheme 1.1) was investigated thoroughly.[53]

Comparison of the results on pyrolysis of pinane-derivatives allows for classification of the compounds with respect to the isomerization products formed. The types of rearrangement products are closely related to the pyrolysis mechanism and the substitution pattern of the educts. With respect to this the bicyclic pinane-type monoterpenes and monoterpenoids can be assigned to one of the five following classes:

a) compounds based on pinane (**3**),

b) compounds based on α-pinene (**9**),

c) compounds based on β-pinene (**10**),

d) compounds with different majorities, and

e) compounds with special thermal isomerization behavior.

Norpinane and some derivatives of pinane (**3**) that are listed in table 1.1 build the first class of compounds all having in common that no unsaturated centers are to be found next to the bridge-head carbon atoms (C(1) and C(5); *cf.* scheme 1.1).[49,50e-g,54] Due to this fact there is no stabilization factor for a biradical intermediate as supposed in the case of **9** and **10**,[47] thus making it practically impossible to form *p*-menthane type products (**2**; *cf.* scheme 1.1). Reaction is assumed to proceed as stepwise fragmentation of the cyclobutane ring forming two possible acyclic products which undergo further consecutive reactions.[50e] With respect to the Woodward-Hoffmann rules a concerted mechanism (retro-[2+2]-cycloaddition) *via* a 4π-antiaromatic transition state is unlikely due to the fact that those reactions are thermally forbidden.[11]

Table 1.1. Compounds with similar behavior to pinane (**3**) concerning their thermal isomerization (colors of the reaction arrows correspond to the bonds in the bicyclus that had to be cut forming either of the two possible acyclic isomers).

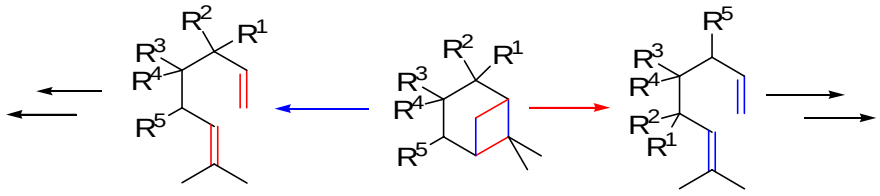

Name	R^1	R^2	R^3	R^4	R^5	Ref.
Norpinane	H	H	H	H	H	[54a,b]
Pinane (**3**)	CH_3	H	H	H	H	*e.g.* [49,55]
Nopinol	OH	H	H	H	H	[50f]
2-Pinanol (**11**)	CH_3	OH	H	H	H	[50e,53]
Isopinocampheol	CH_3	H	OH	H	H	[50f,54c]
Isopinocamphone	CH_3	H	=O		H	[50g,54c]
Neoisoverbanol	CH_3	H	H	H	OH	[50f]

Because of the similar substitution next to the bridge-head atoms fragmentation can proceed in both either ways (scission of blue or of red bonds; table 1.1) leading to two primary products.[49e,50e-g] The probability for both reaction pathways is expressed as the ratio between the two acyclic products and depends on both substitution pattern[50e-f,54d] and relative configuration of the substituents in α-position to the bridge-head carbon atoms (R^1, R^2, R^5).[49e,50e,53] Substitution with unsaturated functional groups at C(3) (R^3, R^4) has no influence on the reaction mechanism at all but affect the ratio of the two main products.[50g,54c]

Except for nopinol and 2-acetoxy-10-norpin-2-ene all α-pinene derivatives listed in table 1.2 yield from oxidation of either **9** or **10**. They have in common that in α-position to one of the two bridge-head carbon atoms an endocyclic double bond is located. This allows for the formation of a biradical wherein one radical position is stabilized *via* delocalization of the π-electrons as an allyl radical (table 1.2).[47,48c,49b,d,52,56]

Table 1.2. Reaction pathway for the thermal isomerization of α-pinene-type compounds.

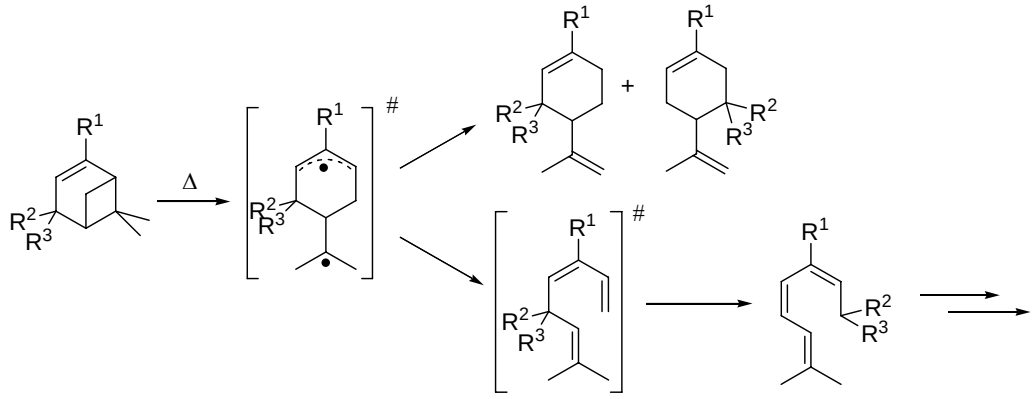

Name	R^1	R^2	R^3	Ref.
α-Pinene (**9**)	CH_3	H	H	*e.g.* [46a,47,51,52]
Myrtenal	CHO	H	H	[56a]
Myrtenol	CH_2OH	H	H	[50d]
2-Acetoxy-10-norpin-2-ene	OAc	H	H	[50b]
Nopol	C_2H_4OH	H	H	[56b]
Verbenol	CH_3	H	OH	[56c]
Verbenone	CH_3	=O		[56d]

Based on this biradical transition states two possible paths are discussed in literature.[47] One leading to *p*-menthane-type compounds and the other one yielding a 1,3,6-octatriene which rapidly rearranges forming a fully conjugated 2,4,6-octatriene. Following this route pyrolysis of **9** lead to the formation of limonene and alloocimene (**22**), whereby the last one yields from isomerization of the primarily formed ocimene (**21**).[46a,47,51,52] Only for the case of **9** the initially formed triene (**21**) could be isolated.[57] Otherwise its consecutive reaction to the fully conjugated product is very fast and the resulted conjugated triene often undergoes further side reactions leading to cyclic, aromatic or elimination products.[53b,d,56b]

Table 1.3. Products of the thermal induced isomerization of β-pinene-type compounds.

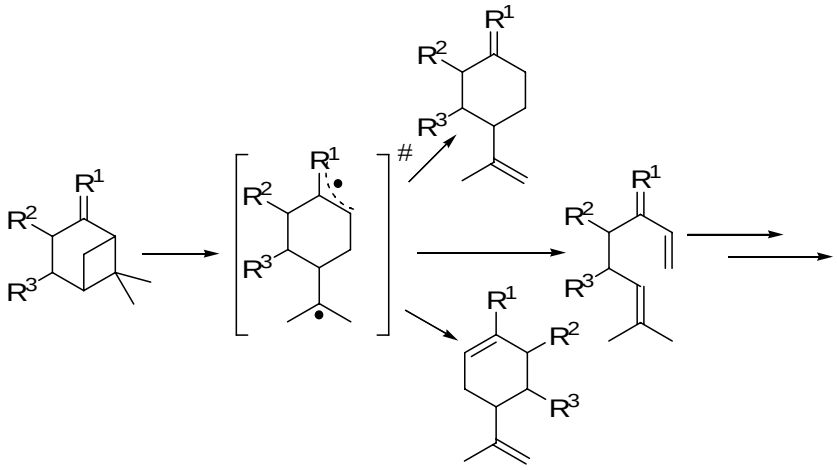

Name	R^1	R^2	R^3	Ref.
β-Pinene (**10**)	CH_2	H	H	*e.g.* [46c,47,48,58a]
Nopinone (**12**)	O	H	H	[50g,58b]
Pinocarveol	CH_2	OH	H	[50a,d]
Pinocarvylacetate	CH_2	OAc	H	[50d]
2(10)-pinen-4-ol	CH_2	H	OH	[58c]

Pinane-type monoterpenoids with an exocyclic double bond system in α-position to either of the two bridge-head carbon atoms of the pinane-skeleton (*e.g.* nopinone, **12**; table 1.3) can be assigned to the group of compounds showing similar isomerization behavior as β-pinene (**10**).[47,48c,d,50,a,d,58] Unlike for the case of α-pinene-type compounds (table 1.2) one radical position of the initially formed biradical is delocalized beyond the cyclohexane skeleton.[47,50a,d] Therefore, further reactions based on this transition state

lead to the formation of at least one monocyclic *p*-menthane-type educt and an acyclic one. The acyclic products are able to undergo consecutive reactions similar to those resulted from pyrolysis of compounds from the pinane-type (table 1.1).[48d,50a,d,58] Depending on substituents R^1 (table 1.3) more than one *p*-menthane-type product can be formed. If R^1 is CH_2 the resulted *p*-menthane-type product with an endocyclic double-bond is stable,[47,50a,d,58c] whereas in case R^1 being O the resulted enol rearranges to the corresponding ketone.[50g,58b]

Beside the compounds listed in tables 1.1-1.3 various monoterpenoids with pinane-skeleton showed behaviors different to those described before. For instance, the thermal isomerization of verbanone (**13**; scheme 1.3) primarily yields one *p*-menthane-type product and two acyclic products which undergo consecutive reactions.[50c,g] Apparently, the two structural majorities ("pinane" and "nopinone") contribute both to the formation of the products observed. Whereas the formation of the cyclic and of one monocyclic product can be explained *via* biradical reaction similar to nopinone[47,50g,58b] the formation of the other acyclic product arise from cleavage of the cyclobutane ring described for **3**.[49e]

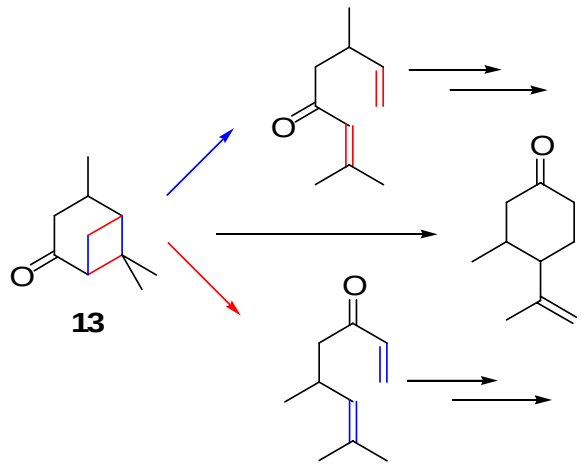

Scheme 1.3. Main products yield from thermal rearrangement of verbanone (**13**; colors of the reaction arrows correspond to the bonds in **13** that had to be cut forming either of the two possible acyclic isomers).

Verbenene (**14**) is another compound showing a curious product spectrum when pyrolyzed. The products observed seem to result from consecutive reactions of two monocyclic trienes (scheme 1.4).[50d,59] The *p*-menthatriene yields from rearrangement *via* a biradical formed in the same way as described for **10** (table 1.3), whereas the other

possible pathway for formation of a biradical similar to **9** (table 1.2) yields *o*-menthatriene.[47]

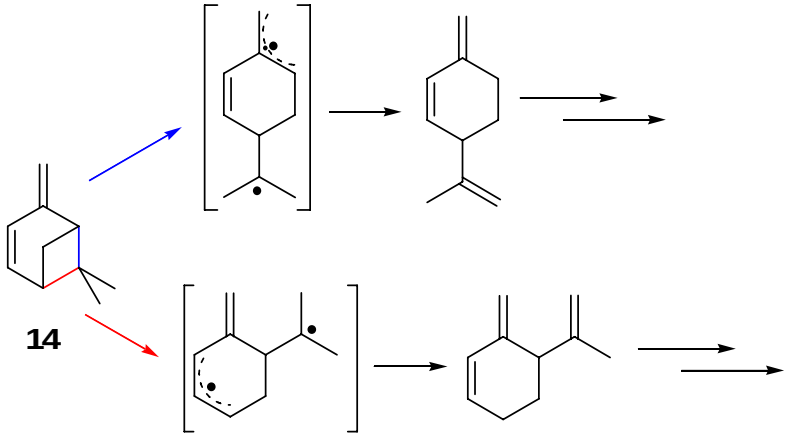

Scheme 1.4. Products of formed *via* pyrolysis of verbenene (**14**; colors of the reaction arrows correspond to the bonds in **14** that had to be cut forming either of the two possible monocyclic isomers).

Scheme 1.5 lists four monoterpenoids (**15**-**18**) that show a behavior concerning their thermal rearrangement not being in agreement with those classes of compounds described in tables 1.1-1.3. Due to their special functional group verbenone oxide (**15**) and β-pinene oxide (**16**) formed isomerization products arising from rearrangement of the epoxide followed by isomerization sequences being typical for **9** or **10**, respectively.[55,56d] FVP of pinane-2,10-diol (**17**) showed nearly the same results as observed for **16**, indicating that initial functional group interconversion accompanied by dehydatization in case of **17** leading to the same reaction intermediate (probably myrtanal).[53] Thermal treatment by means of pyrolysis of apopinen-2-ol (**18**) yields a complex product spectrum not explainable simply assuming a substituted α-pinene or pinane being transformed.[50e]

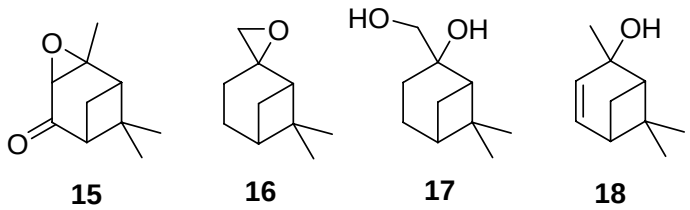

Scheme 1.5. Pinane-type monoterpenoids with special thermal isomerization pathways (**15**: verbenone oxide, **16**: β-pinene oxide, **17**: pinane-2,10-diol, **18**: apopinen-2-ol).

1.4 Purpose of the Investigation

In this study an attempt is made to unravel the mechanistic principles ruling the thermal isomerization of pinane-type monoterpenes and terpenoids. The initial point of interest was the reaction mechanisms of the different types of compounds listed in tables 1.1-1.3 and the substituents influence obviously being responsible for different product spectra formed during pyrolysis. For reasons of differentiation of products primarily formed from the pinane-type compound and those resulted from consecutive reactions of these products experiments have to conducted investigating the thermal behavior of the main acyclic products. In order to give a plausible explanation for the different reactivities and product spectra formed *via* pyrolysis it is very important to determine kinetic parameters (E_a, $\log_{10}A$) for the initial reactions allowing for direct comparison of the results. Literature reports some kinetic data but unfortunately these are hardly comparable due to the fact that experimental conditions used for their determination are extremely different.[49-51,54-56,60] On the one hand studies were undertaken investigating the behavior of **9** or **10** in gas-phase,[51,54,55] in liquid-phase,[49,50] or in supercritical alcohols.[60] Therefore the results published were estimated under different pressure regimes, either in vacuum,[55,56] atmospheric pressure[51,54] or high-pressure.[49,50,60] Additionally, the set-up of the experiments differ concerning *modus operandi* (static[49,50,55] or flow conditions[51,54,56,60]) and residence time.

To establish more systematical conditions and therefore the possibility to compare the results with respect to reactivity, selectivity, and kinetic parameters, experiments with six different monoterpenes (scheme 1.6) were carried out in a flow-type apparatus under atmospheric pressure in a temperature range between 250-600 °C. Besides the technical important pyrolyses of α-pinene (**9**), β-pinene (**10**), and 2-pinanol (**11**), the thermal behavior of both diastereomers (+)-*cis*- [(+)-**3a**] and (-)-*trans*-pinane [(-)-**3b**] was investigated as well as the rearrangement of the oxygenated nor-monoterpenoid nopinone (**12**). These compounds were chosen due to the facts that they are either lead compounds for this type of reactions (**3**,**9**,**10**) or investigation of their pyrolysis behavior is from industrial importance (**9**,**10**,**11**). Studying both the influence of substituents located next to the bridge-head carbon atoms and the influence of the relative configuration of these substituents towards the cyclobutane ring on the reactivity and selectivity experiments

were conducted investigating the thermal isomerization of **11** and **12** and of **3a** and **3b**, respectively.

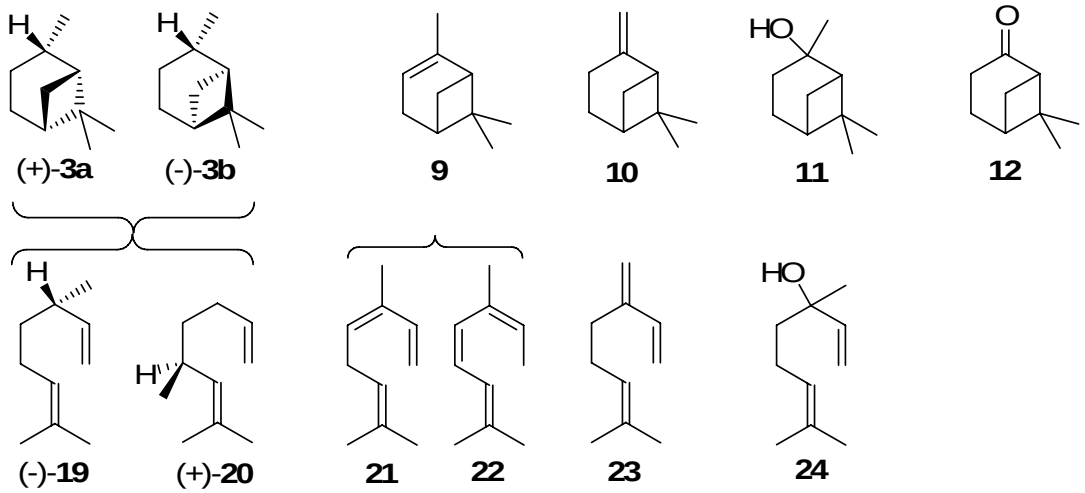

Scheme 1.6. Monoterpenes and monoterpenoids used as starting materials for the investigations [(+)-**3a**: (+)-*cis*-pinane, (-)-**3b**: (-)-*trans*-pinane, **9**: α-pinene, **10**: β-pinene, **11**: 2-pinanol, **12**: nopinone, (-)-**19**: (-)-β-citronellene, (+)-**20**: (+)-isocitronellene, **21**: ocimene, **22**, alloocimene, **23**: myrcene, **24**: linalool].

Taking care of consecutive reactions of the primarily formed main acyclic products (scheme 1.6) leading to undesirable side products their behavior under identical experimental conditions was investigated to. Thereby, this study is restricted to the main products formed *via* isomerization of **3**, **9**, **10** and **11**. Ocimene (**21**) yields from pyrolysis of **9** and rapidly undergoes rearrangement to alloocimene (**22**), whereas myrcene (**23**) is the main product from thermal rearrangement of **10**. Thermal treatment of **3** leads to β-citronellene (**19**) and isocitronellene (**20**), whereby the ratio of **19** and **20** depends on the diastereomer (**3a** or **3b**) used as starting material. The matter the fact that linalool (**24**) generated *via* pyrolysis of **11** is an important building block in synthesis of flavors and fragrances its behavior under pyrolysis conditions has to be considered.

Based on pyrolysis experiments of the compounds depicted in scheme 1.6 rate constants for the most important reaction pathways were estimated allowing for the calculation of activation parameters (E_a, $\log_{10}A$, $\Delta^{\ddagger}H$, $\Delta^{\ddagger}S$). Side reactions leading to consecutive products and therefore to a lost of the primarily formed products were considered as well as reaction channels leading to racemization of the starting materials (**9**).

In chapters 3-5 results from the pyrolysis of the pinane-type compounds listed in scheme 1.6 as well as of their corresponding acyclic main isomerization products are discussed. Chapter 3 deals with compounds which are closely related to pinane: (+)-*cis*-pinane (**3a**), (-)-*trans*-pinane (**3b**) and *cis*-2-pinanol (**11**) as well as with their rearrangement products (-)-β-citronellene (**19**), isocitronellene (**20**) and linalool (**24**). The thermally induced isomerizations of α-pinene (**9**), ocimene (**21**) and of alloocimene (**22**) will be discussed in chapter 4. Additionally, investigations concerning racemization of both (-)-**9** and (+)-**9** are reported. Considerations in the field of β-pinene (**10**) rearrangement are reported together with results of nopinone (**12**) and myrcene (**23**) pyrolysis in chapter 5. Experimental set-up, analytical methods and basics concerning the pyrolysis experiments conducted are presented in chapter 2, whereas chapter 6 will compare the results reported in the sections before.

CHAPTER 2

Methods and Techniques †

2.1 Materials

Table 2.1 lists the compounds used as starting materials for the pyrolysis experiments. If not otherwise stated all substances were purchased from Sigma-Aldrich and were used without further purification. Purity was determined by capillary gas chromatography. Optical purities expressed as enantiomeric excess (*ee*) were calculated according to eq. 2.1, whereby the ratios of the optical antipodes were determined by gas chromatography. Commercially available solvents were used without drying.

$$ee_{(-)} = \frac{[(-)]-[(+)]}{[(-)]+[(+)]} \qquad (2.1)$$

Table 2.1. Compounds used as starting materials for the pyrolysis experiments.

Entry	No.	purity (%)[a]	*ee* (%)[b]
(1*R*,2*S*,5*R*)-(+)-*cis*-pinane	(+)-**3a**	99	94
(1*S*,2*S*,5*S*)-(-)-*trans*-pinane	(-)-**3b**	99	93
(1*S*,5*S*)-(-)-α-pinene	(-)-**9**	99	80
(1*R*,5*R*)-(+)-α-pinene	(+)-**9**	99	95
(1*S*,5*S*)-(-)-β-pinene	(-)-**10**	99	97
(1*R*,5*R*)-(+)-β-pinene	(+)-**10**	99	97
cis-2-pinanol[c]	**11**	93	

† synthesis of nopinone presented within this chapter and the flow-type apparatus used for experiments were published as part of Ref. [61,62] which are given in the appendix of this dissertation.

Table 2.1. Continuation.

(3*S*)-(-)-β–citronellene	(-)-**19**	95	95
(5*S*)-(+)-isocitronellene	(+)-**20**	99	98
3*Z*- and 3*E*-ocimene[d]	**21**	86	
(4*E*,6*Z*)- and (4*E*,6*E*)-alloocimene[e]	**22**	95	
Myrcene	**23**	90	
(3*R*)-(-)-linalool	(-)-**24**	99	98

[a] Determined with GC. [b] Determined with GC and calculated according to eq. 2.1. [c] DSM Nutritional Products (Kaiseraugst, CH). [d] International Flavors and Fragrances (New York, USA); 3*Z*/3*E*: 50%; **22**: < 4%. [e] (4*E*,6*E*)/(4*E*,6*Z*): 11%.

2.2 Analyses

Analyses were carried out in a 6890 Series GC and 5890 Series II / 5972 Series MSD GC from Agilent Technologies. Products were identified by comparing either retention time and / or mass spectra of pure reference compounds. GC-FID: HP 5, 30 m × 0.32 mm × 0.25 µm, H_2 – 5 psi, program: 35 °C (hold 1 min), 4 K min^{-1} up to 80 °C, 4.5 K min^{-1} up to 90 °C, 35 K min^{-1} up to 280 °C (hold 3 min), injector temperature: 250 °C, detector temperature: 280 °C. GC-MSD: HP 5, 30 m × 0.32 mm × 0.25 µm, He – 7 psi, program: 55 °C (hold 1 min), 5 K min^{-1} up to 150 °C, 20 K min^{-1} up to 280 °C (hold 5 min), injector temperature: 280 °C, EI (70 eV).

The concentrations of the optical antipodes were determined with a permethylated β-cyclodextrine column (Supelco Beta-Dex™ 120, 30 m × 0.25 mm × 0.25 µm). Analyses were carried out with a HP 6890: H_2 – 12 psi, program: 68 °C (hold 13.12 min), 25 K min^{-1} up to 240 °C (hold 10 min), split ratio: 3.4, injector temperature: 240 °C, detector temperature: 280 °C.

NMR spectra were recorded with a Bruker Avance 200 MHz system (measurement frequency was 200 MHz for ^{1}H NMR and 50 MHz for ^{13}C NMR) in a 5-mm tube at room temperature. Measurements were carried out using trichloromethane-D ($CDCl_3$) as solvent. IR spectra were measured with a Perkin–Elmer FT-IR spectrum 100 series device equipped with a universal ATR sampling accessory.

2.3 Synthesis[61,62]

(1*R*,5*S*)-(+)-6,6-Dimethylbicyclo[3.1.1]heptan-2-one [(+)-Nopinone; 16]: Potassium permanganate (26.4 g, 0.17 mol) was added to a mixture of (-)-β-pinene (6 g, 44 mmol), aluminium oxide (60 g, 0.59 mol) and water (5 g, 0.28 mol). The mixture was transferred into a beaker (agate) with seven agate balls, inserted into a planetary ball mill "Pulverisette 5" (Fritsch GmbH, Idar-Oberstein, Germany) and milled at 300 rpm for 20 min. Subsequently, the reaction mixture was extracted with dichloromethane (400 mL). After removal of the solvent, the crude product was purified by column chromatography (silica gel 40, 0.063–0.2 mm, Merck) using a mixture of ethyl acetate/*n*-hexane (1:3) as eluent. Yield: 3.4 g per grinding beaker (56% based on β-pinene after purification). n^{D}_{20} = 1.480 (reference (1*R*)-(+)-nopinone: 1.479); ^{13}C NMR ($CDCl_3$): δ = 21.3, 21.9, 25.3, 25.7, 32.7, 40.2, 41.0, 57.7, 214.8 ppm; ^{1}H NMR ($CDCl_3$): δ = 0.85 (s, 3 H), 1.33 (s, 3 H), 1.59 (d, 1 H), 1.96–2.06 (m, 2 H), 2.24–2.25 (m, 1 H), 2.35–2.38 (dd, 1 H), 2.51–2.58 (m, 3 H) ppm; IR (ATR): ν = 2949, 2928, 2837 ($\nu_{aliph.}$ C–H), 1706 ($\nu_{C=O}$), 1459 ($\delta_{C–H}$) cm^{-1}; MS (EI 70 eV, $C_9H_{14}O$): *m*/*z* (%) = 139 (0.9) [M^++1], 138 (8.6) [M^+], 123 (16.5), 109 (26.3), 95 (40.8), 83 (100), 81 (37.3), 67 (23.1), 55 (41.4).

2.4 Pyrolysis Experiments

Dilution gas pyrolyses were carried out in an electrically heated quartz tube of 500 mm length and with a pyrolysis zone of approximately 200 mm, using the apparatus depicted in figure 2.1.[61] Within this reaction zone the discrepancies between adjusted temperature (*T*; red curve in figure 2.1) and measured temperature inside the reactor (dashed line in figure 2.1) are minimal and due to heat transfer phenomena.

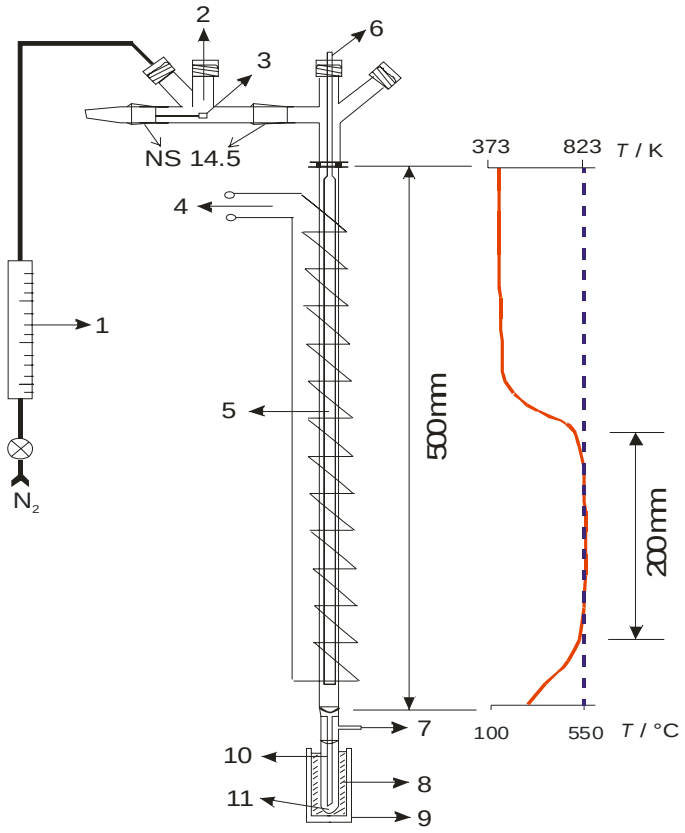

Figure 2.1. Schematic experimental setup for dilution-gas pyrolysis apparatus; 1 – rotameter for carrier gas regulation, 2 – septum for dosing substrate, 3 – quartz ladle, 4 – electrical heating, 5 – quartz reactor, 6 – variable insert, 7 – exhaust for pyrolysis and carrier gas, 8 – coolant (liquid N_2), 9 – Dewar vessel, 10 – cold finger, 11 – liquid pyrolysis product collector. [dashed line: adjusted temperature (*T*); solid curve: measured *T* (550 °C, 1.2 L min^{-1} N_2)].

Temperature was able to be regulated in-between 250-800 °C with thermocouples and in addition the actual *T* was measured inside the reactor. The temperature gradient vertical to the flow direction is below 20 K and was measured on the maximum temperature (800 °C) and the maximal flow-rate (1.2 L min^{-1} N_2). In all experiments, oxygen-free nitrogen with a purity of > 99.999% was used as the carrier gas. The carrier

gas velocity was regulated within 0.4 to 1.2 L min^{-1}. The substrates (15 µL) were introduced onto a quartz ladle at the top part of the pyrolysis apparatus using a glass syringe (50 µL) and carried along with the nitrogen stream into the reactor. Vaporization of the starting material was supported by heating the ladle to 200 °C with a hot blast. Pyrolysis products were collected in a cold trap (liquid nitrogen) and were dissolved in 1.5 mL of ethyl acetate.

Investigating the influence of the surface-to-volume-ratio (S/V) on the pyrolysis behavior of (-)-**10**, **11**, **23**, and of (-)-**24** different ratios were realized by putting a hollow quartz tube (insert I-IV) inside the reactor. The outer diameter d_A of these inserts varied between 6.2 and 13.6 mm (table 2.2). If not otherwise stated in the standard set-up insert II was used (9.1 mm). Therefore, the actual reactor geometry was similar to a hollow cylinder. Calculated reactor volumes (V_R) and surface-to-volume-ratios based on a reaction zone with an approximate length of 200 mm. Within this zone the temperature gradient in flow-direction was lower than 10 K (figure 2.1).

Table 2.2. Properties of the pyrolysis reactor depending on the quartz inserts used.

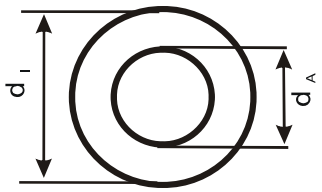

Entry	d_I (mm)[a]	d_A (mm)[b]	V_R (mL)[c]	A_R (cm^2)[d]	A_{cs} (cm^2)[e]	S/V (cm^{-1})[f]
no Insert	15.2	-	36.1	95.2	1.80	2.64
Insert I	15.2	6.2	30.0	134.1	1.50	4.47
Insert II	15.2	9.1	23.0	152.4	1.15	6.61
Insert III	15.2	10.3	19.4	159.9	0.97	8.25
Insert IV	15.2	13.6	7.0	180.6	0.35	25.8

[a] Inner reactor diameter. [b] Outer diameter of the quartz insert. [c] Reactor volume. [d] Surface area of the reactor. [e] Cross-sectional area of the reactor. [f] Surface-to-volume-ratio (A_R/V_R).

The liquid products obtained were analyzed by GC-FID and GC-MS adding 5 µL hexadecane as internal standard. Comparison of both residence times and mass spectra with those of reference compounds allowed for identification of the main products. The yields Y_i of reaction products i and of non-converted starting material s (Y_s) are expressed by the corrected peak areas from the GC-analyses (eq. 2.2). Conversions of the reactants

(X_s) were calculated according to eq. 2.3, wherein [*s*] are the corrected and normalized peak areas of non-converted starting material *s*. Eq. 2.4 was used for calculation of the selectivities (S_i) for the pyrolysis products formed *via* rearrangement of the starting materials. Selectivities calculated according to eq. 2.4 did not include products formed consecutively. Therefore, $S_{cp,i}$ (eq. 2.5) considers the side-reactions of the acyclic pyrolysis products by considering the concentration of the consecutive products [cp] yielded from their isomerization. Every data-point presented herein representing either yield, conversion, or selectivity represents mean values of at least two individual pyrolysis experiments.

$$Y_{i,s} = [i,s] \tag{2.2}$$

$$X_s = 1 - \frac{[s]}{100} \tag{2.3}$$

$$S_i = \frac{Y_i}{X_s} = \frac{[i]}{X_s} \tag{2.4}$$

$$S_{cp,i} = \frac{[i] + \sum[cp]}{X_s} \tag{2.5}$$

2.5 Kinetic Experiments

The kinetic experiments were carried out in different temperature ranges depending on the starting materials used for experiments (table 2.3). Lower and upper boundaries for the experiments were chosen with respect to those regions in the respective temperature-conversion-plots whereas the slope of the curve is linear. Variation of the carrier gas velocity in a range from 0.4 up to 1.2 L min^{-1} N_2 allows for the modulation of the average residence time (τ). Calculations of τ were accomplished according to eq. 2.6, wherein V_R is the reactor volume (table 2.2), V^*_E the substrate flow rate, V^*_{N2} the carrier gas flow rate, T_R and T_{rt} are the reactor and ambient temperatures, both in K.[25] V^*_E was calculated assuming that all liquid starting material is vaporized. The overall volumetric gas flow-rate (V^*_E+V^*_{N2}) was corrected by means of volume expansion at higher temperatures according to the law of Gay-Lussac. Due to the fact that pyrolyses were carried out using

nitrogen as carrier gas with nitrogen to substrate rations higher than 3,000 the contact time is mainly affected by changes made in the carrier gas flow-rate $\dot{V}^{*}_{N2}$. Therefore and because of the absence of gaseous products within the investigated temperature ranges eq. 2.6 can be used for calculation of the residence time τ. Unless otherwise stated experiments were carried out using insert II (V_R: 23.0 mL).

Table 2.3. Pyrolysis temperatures (T) for kinetic experiments.

Starting material		T (°C) for kinetic measurements
(+)-*cis*-pinane	(+)-**3a**	450, 462, 475, 487, 500, 512
(-)-*trans*-pinane	(-)-**3b**	500, 512, 525, 537, 550
α-pinene	**9**	337, 350, 362, 375, 387, 400
(-)-/(+)-α-pinene[a]	(-)-**9** / (+)-**9**	350, 362, 375, 387
β-pinene	**10**	375, 387, 400, 412, 425
cis-2-pinanol	**11**	450, 463, 475, 487, 500
nopinone	**12**	475, 487, 500, 512
(-)-β-citronellene	(-)-**19**	462, 475, 487, 500, 512, 525, 537, 550
(+)-isocitronellene	(+)-**20**	487, 500, 512, 525, 537
ocimene	**21**	287, 300, 312, 325, 337
alloocimene	**22**	412, 425, 437, 450, 462, 475
myrcene	**23**	482, 485, 490, 495, 500, 510
(-)-linalool[b]	**24**	463, 475, 487, 500, 512
(-)-linalool[c]	**24**	450, 475, 500, 525, 550

[a] Racemization studies. [b] Variation of carrier-gas velocity. [c] Variation of V_R.

$$\tau = \frac{V_R}{\left(\dot{V}_E + \dot{V}_{N2}\right)\frac{T_R}{T_{rt}}} \qquad (2.6)$$

Pyrolysis experiments used for calculation of rate constants were individually carried out three times. For calculation of the parameters all experimental results were considered. If outliers were present within a data-set the corresponding experiments were redone individually four times and the data were recalculated considering the additional experiments. Determination of various rate constants by performing kinetic pyrolysis

experiments at various temperatures, allows for the calculation of both Arrhenius (E_a, $\log_{10}A$) as well as Eyring activation parameters ($\Delta^{\ddagger}H$, $\Delta^{\ddagger}S$; eq. 2.7 and 2.8).

$$k_T = A \cdot e^{-\frac{E_a}{RT}} \tag{2.7}$$

$$k_T = \frac{k_B T}{h} \cdot e^{-\frac{\Delta^{\ddagger}H}{RT}} \cdot e^{\frac{\Delta^{\ddagger}S}{R}} \tag{2.8}$$

CHAPTER 3

Pyrolysis of *cis*-Pinane, *trans*-Pinane and of *cis*-2-Pinanol

This chapter investigates the thermal isomerization of (-)-*cis*-pinane, (+)-*trans*-pinane, and of the monoterpene alcohol *cis*-2-pinanol. In order to gain a deeper insight into the reaction mechanisms and the kinetics of the rearrangements pyrolyses with the acyclic products of pinane and 2-pinanol – (-)-β-citronellene, (+)-isocitronellene and (-)-linalool – were performed. Experiments reveal that the formation of the products is enantiospecific and the reaction proceeds as stepwise fragmentation of the cyclobutane ring in pinane or 2-pinanol. Kinetic experiments allow for the calculation of activation parameters according to Arrhenius and Eyring equations. Comparison of activation entropies and frequency factors supports the hypothesis that the main reactions proceed as stepwise fragmentation of the cyclobutane ring passing through biradical transition states.

Results presented in this chapter concerning the thermal rearrangement of *cis*- and *trans*-pinane are summarized results from two articles published which are given in the appendix of this dissertation.[63,64]

3.1 Thermal Behavior of (+)-*cis*- and (-)-*trans*-Pinane

Studying the thermal isomerization behavior of both (+)-*cis*-pinane [(+)-**3a**] and of (-)-*trans*-pinane [(-)-**3b**] pyrolysis experiments were carried out within a temperature range of 300-600 °C. Analysis of the yielded liquid mixtures of reaction products leads to the identification of (-)-β-citronellene (**19**)[49b-e,55,65] and of (+)-isocitronellene (**20**)[49e,55] as the main products, whose formation proceeds enantiospecifically, hence the *ee* (eq. 2.1) found for (+)-**3a** and (-)-**3b** were as high as in case of **19** and **20**.[49d] This leads to the conclusion that within the process of thermal isomerization of **3** the absolute configuration of the carbon atom C(2) next to the bridge-head carbon C(1) remains unchanged as shown in scheme 3.1.

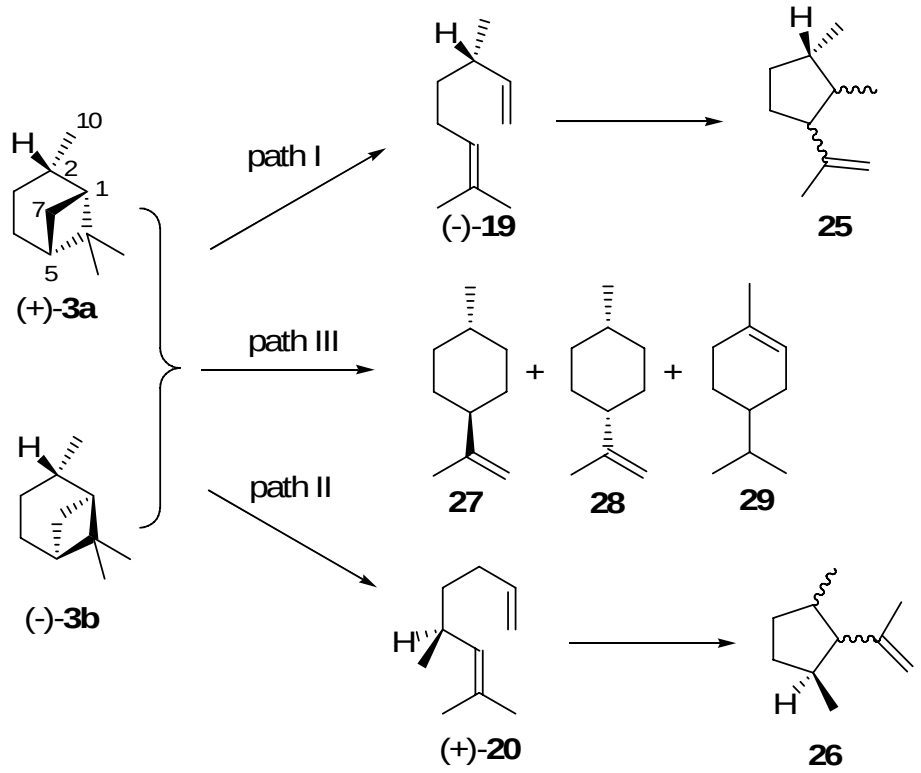

Scheme 3.1. Reaction network for the thermally induced rearrangements of (+)-*cis*- (**3a**) and (-)-*trans*-pinane (**3b**) including the main reaction pathways.

The formation of **19** and **20** has to proceed *via* stepwise fragmentation of the cyclobutane ring in either **3a** or **3b** with 1,4-carbon-centered biradicals as transition states.[49e] Cleavage of bonds C(1)-C(6) and C(5)-C(7) in **3** yields **19**, whereas the

formation of **20** appears for scission of bonds C(1)-C(7) and C(5)-C(6). Besides the acyclic main products *p*-menthenes **27**-**29** were found in the product mixture. Obviously their formation proceeds *via* a biradical transition state followed by [1,n]H-shift (path III in scheme 3.1).[62] Consecutive reactions of **19** and **20** leading to products **25** and **26**, result in decreased yields of the acyclic primarily formed products.

The relative configuration of the methyl group attached to C(2) towards the dimethyl substituted carbon C(6) seems to tremendously influence the reactivity and selectivity of **3a** and **3b**. In figure 3.1 the dependency of pinane-conversion $X_{\mathbf{3i}}$ *vs.* temperature *T* is depicted, revealing that **3a** is more reactive than **3b**. The temperatures for equal conversions of **3a** and **3b** are shifted about 40 K to higher values in case of **3b** compared to the *cis*-isomer.[49e,66] At reaction temperatures lower than 400 °C neither for **3a** nor for **3b** detectable conversions are observed, whereas at temperatures higher than 600 °C the conversions for both are complete, and besides isomerization further decomposition of the $C_{10}H_{18}$-hydrocarbons to lower weight compounds takes place.

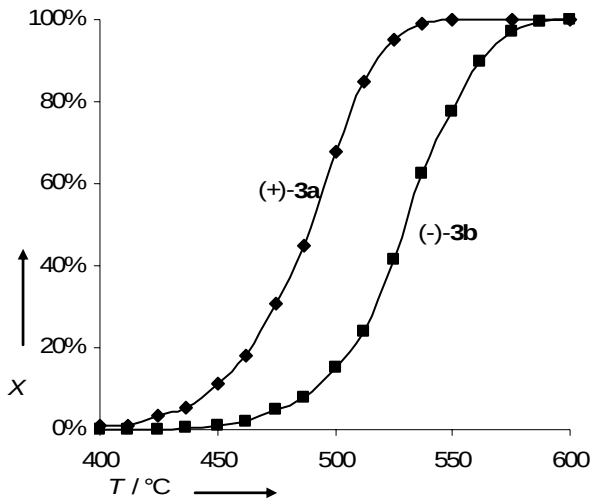

Figure 3.1. Conversion (*X*) of (+)-*cis*-pinane (**3a**), (-)-*trans*-pinane (**3b**) depending on the reaction temperature (*T*; 15 µL starting material, carrier gas: N_2, flow rate: 1.0 L min^{-1}, τ: 0.47-0.61 s).

Besides their behavior concerning the overall conversion, **3a** and **3b** differ in selectivity. Three different types of major products are formed within the pyrolysis of **3** arising from different reaction pathways (scheme 3.1): (-)-β-citronellene (**19**; path I), (+)-isocitronellene (**20**; path II) and monocyclic products (**27**-**29**; path III). Despite the fact that **27**-**29** are formed in low amounts only (overall < 5%) pyrolyzing either **3a** or **3b**,

pyrolysis of **3a** leads to the formation of **19** predominantly, whereas the ratio of reaction pathways leading to **19** and **20** (*cf.* scheme 3.1) are *pari passu* in case of the thermal isomerization of **3b**.

Consecutive reaction products **25** and **26** formed *via* rearrangement of **19** and **20**, respectively, were isolated by preparative GC and their structures were elucidated using NMR techniques (^{1}H, ^{13}C, HSQC, HMBC). Ene-reaction of **19** leads to diastereomers **25a-d**,[49e,54b,65,67] whereas cyclization of **20** yields **26a** as the main product (scheme 3.2). Both reactions proceed without an inversion of the configuration at C(3) or C(1) in **25** or **26**, respectively, allowing for the conclusion that the chiral center in **3** remains unchanged even in the side reactions of the acyclic main products. Configurations of the other chiral carbon atoms in **25** and **26** which are formed during the reaction and their distribution depend on the relative stability of the transition states leading to their formation.

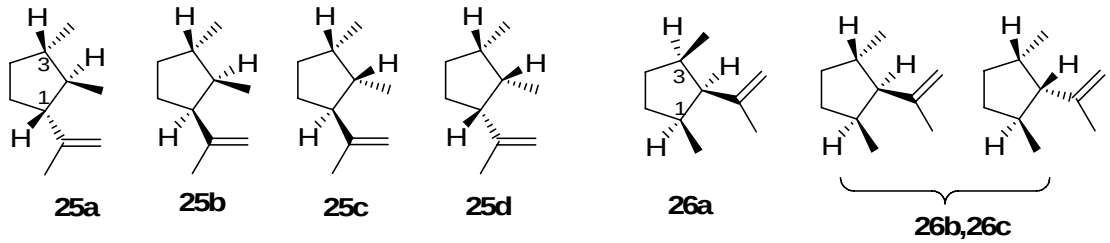

Scheme 3.2. Configuration of the rearrangement products (**25**, **26**) yielding from isomerization of (-)-β-citronellene (**19**) and of (+)-isocitronellene (**20**), respectively.

3.2 Kinetic Considerations in the Field of Pyrolysis of Pinane

Table 3.1 lists the calculated activation parameters for both the Arrhenius equation (2.7) and the Eyring equation (2.8). The lower activation energy E_a for the transformation of **3a** (201 kJ mol^{-1}) compared to **3b** (213 kJ mol^{-1}) underlines the higher reactivity of the *cis*-isomer (figure 3.1). The observed differences are in accordance with differences in the ring-strain energies form **3a** and **3b**, calculated on the basis of *ab initio* calculations.[68] In case of *cis*-pinane (**3a**) the ground-state confirmation of the cyclohexane ring seems to have a semi-chair confirmation, whereas the chair confirmation is the preferred ground state geometry for the *trans*-isomer.

Table 3.1. Kinetic data[a] for the gas-phase isomerization reactions of *cis*-pinane (**3a**), *trans*-pinane (**3b**), β-citronellene (**19**), and isocitronellene (**20**).

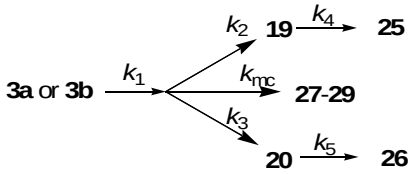

	k	E_a (kJ mol^{-1})	$\log_{10}A$ (s^{-1})	$\Delta^{\ddagger}H$ (kJ mol^{-1})	$\Delta^{\ddagger}S$ (J K^{-1} mol^{-1})
3a	$k_{1(3a)}$	201.1 ± 9.1	13.96 ± 0.63	194.8 ± 9.0	6.3 ± 0.4
19	$k_{2(3a)}$	200.1 ± 9.0	13.83 ± 0.62	193.8 ± 12.0	3.7 ± 0.2
20	$k_{3(3a)}$	233.7 ± 8.3	15.10 ± 0.58	227.4 ± 8.3	28.2 ± 1.4
mc[b]	$k_{mc(3a)}$	177.7 ± 10.8	11.17 ± 0.75	171.4 ± 11.0	-47.1 ± 4.5
3b	$k_{1(3b)}$	213.0 ± 6.9	13.94 ± 0.45	206.3 ± 6.9	6.2 ± 0.3
19	$k_{2(3b)}$	213.4 ± 7.5	13.71 ± 0.49	206.7 ± 7.4	1.1 ± 0.1
20	$k_{3(3b)}$	213.9 ± 6.3	13.68 ± 0.41	207.2 ± 6.3	0.54 ± 0.02
mc[b]	$k_{mc(3b)}$	201.0 ± 7.6	11.89 ± 0.51	194.4 ± 7.7	-33.8 ± 2.0
19	k_4	117.9 ± 1.6	7.69 ± 0.11	112.4 ± 4.7	-112.7 ± 8.0
20	k_5	137.5 ± 7.3	9.23 ± 0.48	131.0 ± 7.0	-84.6 ± 7.0

[a] Error limits are 95% certainty limits. [b] Sum of **m**ono**c**yclic *p*-menthene-type products (**27**-**29**).

Comparison of activation energies E_a for the formation of the acyclic products **19** and **20** confirms that **19** is the main product in case of **3a** ($k_{2(3a)}$), whereas the equality for the pyrolysis of **3b** supports that both reaction channels are leading together.[49e] Due to the fact that the activation barriers for the formation of the *p*-menthene-type products (**27**-**29**) are lower than for the formation of the other main products and the activation entropies are negative underlines that these products yield from different reaction intermediates than those assumed transition states leading to the acyclic products.[49e] The error margins of the activation parameters listed in table 3.1 reflect the experimental uncertainty with error limits of ± 8.3 kJ mol^{-1} in E_a and ± 0.7 in $\log_{10}A$ being reported as typical for gas-phase thermal decomposition reactions.[69a] The negative activation entropies $\Delta S^{\#}$ for the rearrangement reactions of **19** and **20** leading to **25** and **26**, respectively, support the hypothesis, that these reactions follow other mechanisms as described for the isomerization of **3**. It is well known that frequency factors $\log_{10}A$ less than 11.5 combined with negative activation entropies are typical for reactions with six-membered-ring

transition states.[69] Hence, the cyclization of **19** and **20** proceeds *via* an ene-type reaction, the reported kinetic data listed in table 3.1 support this hypothesis.[49a,49e,54b,62,65,70]

3.3 Thermal Behavior of *cis*-2-Pinanol and of (-)-Linalool

The monoterpene alcohol linalool (**24**) is an important building block in syntheses of vitamins as well as for the production of flavors and fragrances.[9,38b,40] Technical synthesis based on 2-methyl-2-heptenon which yields **24** after addition of acetylene und Lindlar-type hydrogenation of the intermediate dehydrolinalool.[38b,40] An alternative route leading to **24** starts with α- (**9**) or β-pinene (**10**) which can be obtained from distillation of turpentine. Hydrogenation of **9** or / and **10** leads to **3** and subsequently oxidation forms pinane hydroperoxide which can be reduced to *cis*- or *trans*-2-pinanol (**11**) using Pd/H_2 or Na_2SO_3, whereby **24** can be generated from **11** *via* thermal rearrangement.[50e,53,71,72] Depending on reaction temperature, residence time, and reactor geometry pyrolysis of **11** yields more or less side-products, which can be classified to their origin. The formation of monoterpenes ($C_{10}H_{16}$) formed *via* acid-catalyzed dehydratization of the monoterpenes alcohols can be suppressed by adding pyridine to the feed-stream.[53,72a] Other monoterpene alcohols ($C_{10}H_{18}O$) then **11** or **24** predominately yield form undesirable consecutive or parallel reactions of **11** or **24**. The amount of these products depend on the reaction conditions (T, τ, catalyst) the pyrolysis is carried out with.

The herein presented investigations deal with the thermal rearrangement of *cis*-2-pinanol (**11**) and of (-)-linalool (**24**) in the flow-type apparatus sketched in figure 2.1. Experiments were carried out using N_2 as carrier gas without the presence of any catalyst or additive added to the feed stream. Scheme 3.3 pictures the main pyrolysis products found in the mixture of products yielding from thermal treatment of **11**. Beside the target product **24** 1,2-dimethyl-3-isopropenylcyclopentanols **31**[50e,71-73] were identified as well as the ketone **32**.[50e] In accordance to the predominant formation of **19** within the isomerization of (+)-**3a**, pyrolysis of **11** leads to the formation of **24** (path I in scheme 3.3). Apparently this reaction proceeds as stepwise fragmentation of the cyclobutane ring in **11** by bond scissions between C(1)-C(6) and C(5)-C(7). Hence a retro-[2+2]-cycloreversion mechanism is thermally forbidden according to the Woodward-Hoffmann rules, a stepwise mechanism is the most plausible way.[11] Breakage of carbon-carbon

bonds C(1)-C(7) and C(5)-C(6) should actually yield alcohol **30** in accordance to the formation of **20** from **3**. Nevertheless, this product was not found but ketone **32** was present in the mixture of pyrolysis products. **32** is formed from intermediate **30** by a reaction sequence pictured in Scheme 3.4.[50e] In agreement with the formation of **31** from **24** initially formed **30** undergoes ene-cyclization forming the cyclopentenol **33**, whose subsequent rearrangement *via* hetero-ene-reaction yields **32** in amounts lower than 5%. Dehydratization products were found with overall yields not exceeding 3% demonstrating either that no acidic groups are present on the surface of the reactor or that the reaction took place predominantly in the gas-phase. The wall-effect on the reaction course seems to be negligible. Due to high dilution of the reactants with N_2 collisions of reactant molecules are suppressed and activation proceeds *via* collision of nitrogen-molecules with the reactants.

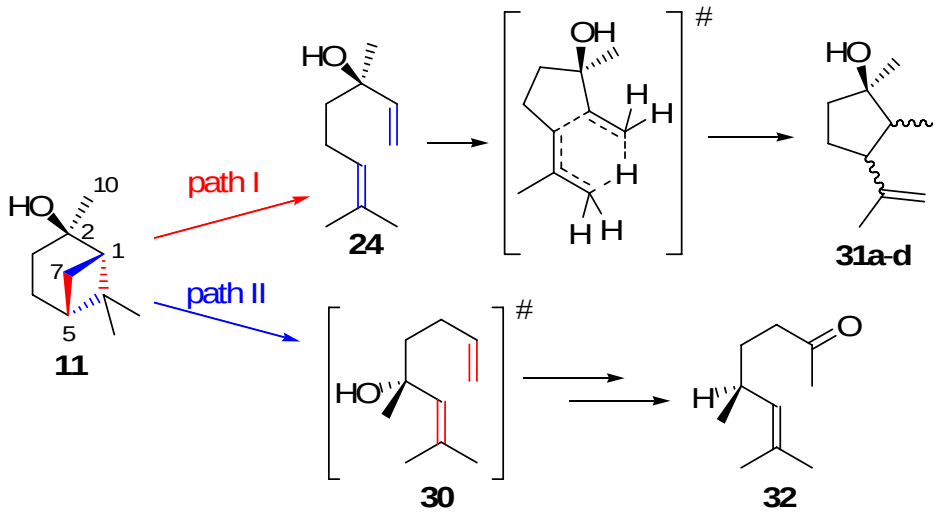

Scheme 3.3. Reaction network for the thermal rearrangement of *cis*-2-pinanol (**11**) including the main reaction pathways (a racemic mixture of **11** was used within the experiments, but for better understanding the (2*R*)-enantiomer of **11** is shown only. Colors of the reaction arrows correspond to the bonds in **11** that had to be cut forming either **24** or **30**.)

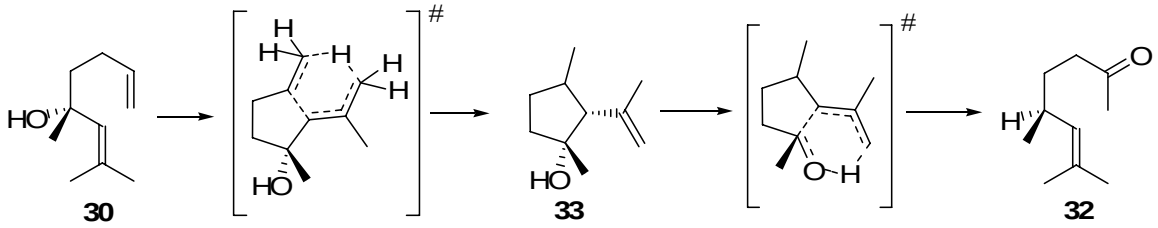

Scheme 3.4. Formation of (*S*)-5,7-dimethyloct-6-ene-2-one (**32**) form the initially formed (*R*)-2,4-dimethyl-octa-2,7-dien-4-ol (**30**).

Figure 3.2a pictures the conversion of **11** (X_{11}), the selectivity of **24** (S_{24}) and the yields of products **24**, **31** and **32** (Y_i) depending on the reaction temperature T from experiments with a flow rate of 1.0 L min^{-1} N_2. Diagram reveals that starting material **11** is converted within a temperature range of 100 K starting at 450 °C and that the selectivity of **24** (S_{24}) passes through a maximum at 460 °C (X_{11}: 12%, S_{24}: 80%). At higher temperatures consecutive reactions lead to the formation of alcohols **31** (Y_{31}) resulting in a lower selectivity for **24**, whereas the yield of **24** (Y_{24}) increases. Compared to the maximum in S_{24} the corresponding maximum of Y_{24} is shifted about 50 K to higher temperatures, indicating that the formation of **24** is accompanied by its cyclization yielding products **31**.

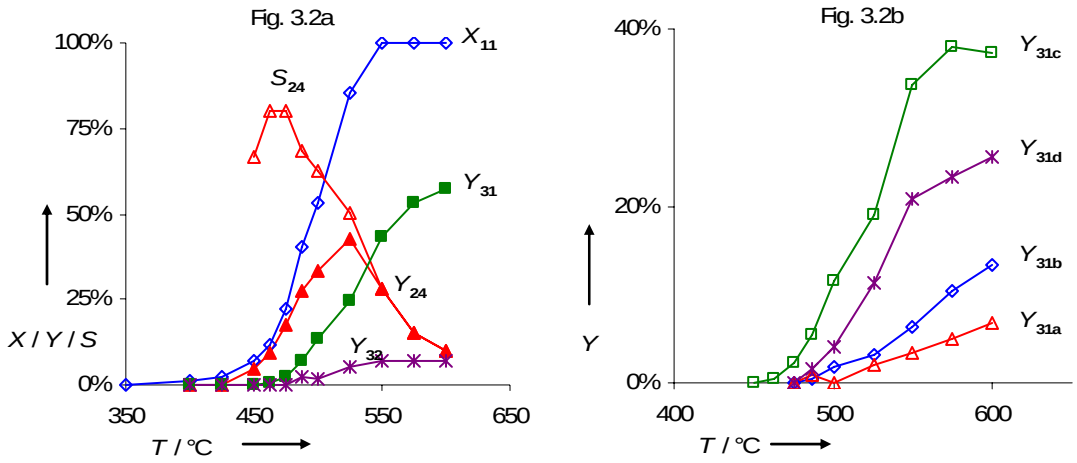

Figure 3.2a. Conversion of *cis*-2-pinane (X_{11}), selectivity for the formation of linalool (S_{24}), and yield of **24**, **31**, and **32** (Y_i) depending on the reaction temperature (T). Figure 3.2b. Yield of **31a-d** (Y_i; scheme 3.5) depending on reaction temperature (T; 40 mg starting material, carrier gas: N_2, flow rate: 1.0 L min^{-1}, τ: 0.47-0.66 s).

According to the formation of cyclopentenes **25** from **19**,[49e,63,65,66] consecutive ene-cyclization of **24** yields isomeric cyclopentenols **31a-d**, whose configurations are pictured in scheme 3.5.[50e,72-74] The assignation as alcohols **31a-d** corresponds to their retention times whereby **31a** has the lowest and **31d** elutes last on a HP5 GC-column. Figure 3.2b pictures the temperature dependency of the yields of products **31a-d** (Y), revealing a clear order whereby the following row of occurrence can be set-up: $Y_{31c} > Y_{31d} > Y_{31b} > Y_{31a}$. These order is in accordance with previously published results.[50e,73] Surprisingly, the main cyclization products **25b** (scheme 3.2) and **31c** of **19** and **24**, respectively, have the same orientation of the alkyl substituents.[63] Whereas **25b** has a *cis*,*trans*-configuration

the orientation in case of **31c** is *trans*,*cis*.[75] This is due to the different priority of the substituents in **25** (isopropenyl group) and **31** (hydroxyl group). This agreement continues considering those compounds with second highest *Y*, **25d** and **31d**, both being *cis*,*cis*-configured.[63]

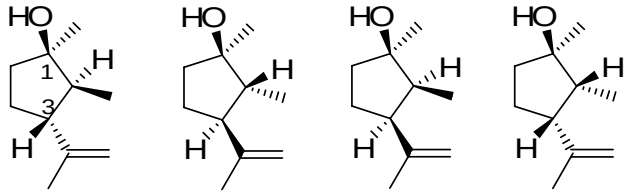

31a **31b** **31c** **31d**

Scheme 3.5. Configuration of the rearrangement products (**31a-d**) yielding from thermally induced isomerization of (-)-linalool (**24**).

2-Pinanol (**11**) used for this investigations was a racemic mixture of (1*S*,2*R*,5*R*)- and (1*R*,2*S*,5*S*)-**11**. Pointing out that *cis*-**11** was used scheme 3.3 pictures the (1*S*,2*R*,5*R*)-enantiomer only. According to the thermal isomerization of **3** the reactions occurring within the thermal reaction network based on **11** proceed enantiospecifically also. Therefore the corresponding chiral carbon-centers in **24**, **30**-**32** have the same configuration pictured for the starting material in scheme 3.3. This was proven by thermal treatment of (3*R*)-(-)-**24**, whereby the enantiomeric excess *ee* (eq. 2.1) remains unchanged while rising the reaction temperature and the optical purities found for the cyclopentenols were in the same range.

3.4 Kinetic Studies of the Thermal Rearrangement of 2-Pinanol and of Linalool

Kinetic studies concerning the gas-phase isomerization behavior of *cis*-2-pinanol (**11**) and (-)-linalool (**24**) were carried out. Due to the fact that the concentration of **32** in the product mixtures was below 5% this reaction pathway was neglected in these studies. In order to estimate activation parameters according to eq. 2.7 and 2.8 pyrolysis experiments were conducted determining the rate constants for the disappearance of **11** (k_6) and **24** (k_7) at different temperatures. Plotting $\ln k_T$ and $\ln(k_T\, T^{-1})$ against T^{-1} in K^{-1} allows for calculation of Arrhenius and Eyring parameters, respectively, from the slopes and axis intercepts of the linear regression functions. Arrhenius plots for k_6 and k_7 are shown in figure 3.3. Corresponding rate constants were determined on two different ways: a)

variation of the reactor volume V_R by use of different inserts listed in table 2.2 with a constant flow rate of 1.0 L min^{-1} N_2, and b) variation of the carrier gas flow rate, whereby the reactor volume was kept constant (V_R: 23 mL).

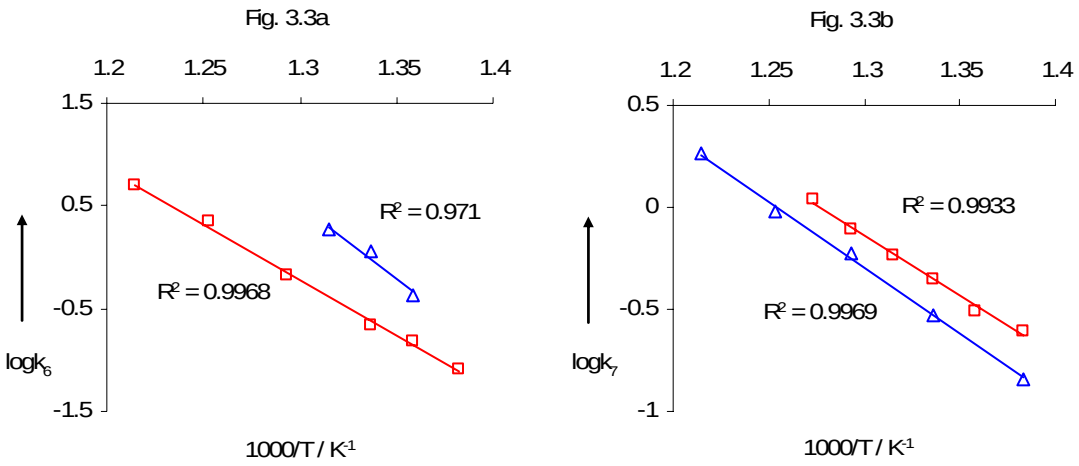

Figure 3.3. Arrhenius plots of log *k vs.* 1000/*T* for the thermal isomerization of *cis*-2-pinanol (**11**, k_6; figure 3.3a) and (-)-linalool (**24**, k_7; figure 3.3b) for either variation of reactor volume V_R (triangles; table 2.2, flow rate: 1.0 L min^{-1} N_2) or variation of carrier gas flow rate (squares; V_R: 23.0 mL).

Table 3.2. Kinetic data[a] for the gas-phase isomerization reactions of *cis*-2-pinanol (**11**; k_6) and (-)-linalool (**24**; k_7) describing the disappearances of the starting materials.

11 $\xrightarrow{k_6}$ **24** $\xrightarrow{k_7}$ **31**

	E_a (kJ mol^{-1})	log$_{10}A$ (s^{-1})	$\Delta^{\ddagger}H$ (kJ mol^{-1})	$\Delta^{\ddagger}S$ (J K^{-1} mol^{-1})
k_6[b]	207.9 ± 5.9	13.90 ± 0.40	201.5 ± 5.9	5.0 ± 0.2
k_6[c]	209.9 ± 6.7	14.70 ± 0.26	203.8 ± 3.7	20.6 ± 0.5
k_6[d]	208.9	14.3	202.7	12.8
k_7[b]	124.4 ± 4.0	8.15 ± 0.27	118.0 ± 4.1	-105.1 ± 5.9
k_7[c]	113.4 ± 4.7	7.56 ± 0.32	107.1 ± 4.6	-116.2 ± 8.8
k_7[d]	118.9	7.86	112.6	-110.7

[a] Error limits are 95% certainty limits. [b] Calculated from experiments with constant flow rate (1.0 L min^{-1} N_2) and different V_R (table 2.2). [c] Calculated from experiments with constant V_R: 23.0 mL and different flow rates. [d] Mean values of [b] and [c].

Figure 3.3 reveals differences in axis intercepts and slopes of the linear regression functions for both reactions investigated and also for both ways of determination. Those differences become manifested in the calculated activation parameters listed in table 3.2

allowing for the conclusion that the discrepancy is higher in case of experiments carried out using **24** as substrate. Obviously, the different *modus operandi* for determination of Arrhenius as well as Eyring activation parameters for the gas-phase isomerization of **11** and **24** influence the kinetic measurements. Due to the fact that in both cases temperature-corrected values of the residence times τ (eq. 2.6) were used for monitoring the time dependent disappearance of **11** and **24** the reason for discrepancies had to be found everywhere else. The only difference between the two approaches is the modification made in surface-to-volume-ratio (S/V) while changing the reactor volume V_R (table 2.2). Apparently, the surface area has an influence on both reactions, the formation of **24** from **11** *via* stepwise fragmentation of the cyclobutane ring and the lost of **24** due to the formation of **31**. For this reasons experiments were conducted, whereby the flow rate of the carrier gas was modified according to eq. 2.6 for reactor volumes listed in table 2.2 in order to keep the average contact times constant. Experimental conditions and the calculated residence times for the temperatures the reactions were performed at are listed in table 3.3.

Table 3.3. Experimental conditions for the studies investigating the influence of the surface-to-volume-ratio (S/V) on the gas-phase isomerization of *cis*-2-pinanol (**11**) and (-)-linalool (**24**).

				τ (s) for T (°C)[b]		
Entry	V_R (mL)[c]	S/V (cm^{-1})[a]	N_2 (L mi^{-1})	450	475	500
no Insert	36.1	2.64	1.2	0.74	0.72	0.69
Insert I	30.0	4.47	1.0	0.74	0.72	0.69
Insert II	23.0	6.61	0.75	0.76	0.73	0.71
Insert III	19.4	8.25	0.65	0.74	0.71	0.69
Insert IV	7.0	25.8	0.23	0.75	0.73	0.70

[a] surface-to-volume-ratio (A_R/V_R). [b] Calculated according to eq. 2.6.

Results from the gas-phase isomerization studies with constant average residence times τ are pictured in figure 3.4, indicating that there is a significant influence of the surface-to-volume-ration S/V on the rearrangement of **11** and **24**, otherwise the linear regression functions have to be parallel to the abscissas. Therefore, it can be concluded that the conversion X depends not only on residence time and reaction temperature but also on the ratio of reactor surface to reactor volume. Since the other parameters

characterizing a chemical reaction (yield, selectivity) are connected to the conversion according to eq. 2.2 and 2.4 they are also influenced by different surface areas. However, the influence of surface seems to increase while rising temperature which allows for the conclusion that this could be suppressed by performing the reaction at lower temperatures.

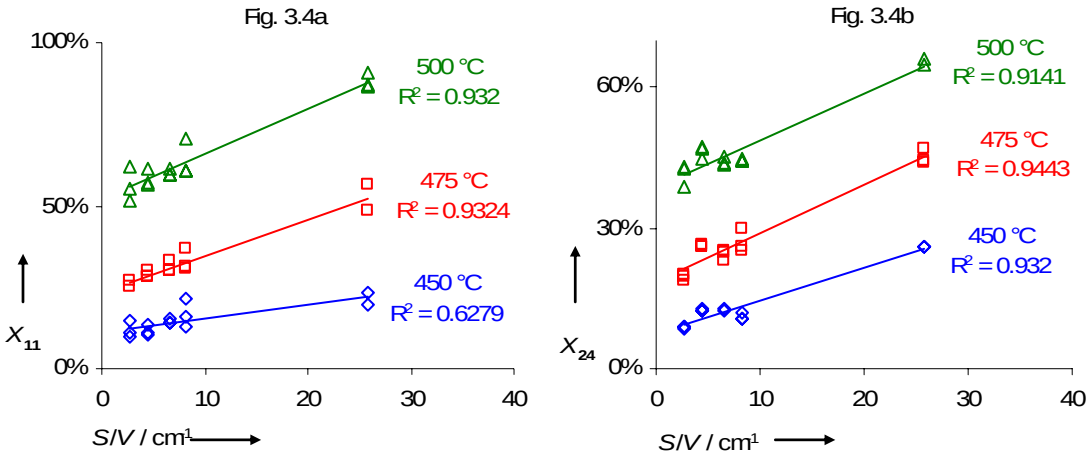

Figure 3.4. Influence of surface-to-volume-ratio (S/V; table 2.2) on the conversion of *cis*-2-pinanol (X_{11}; figure 3.4a) and on conversion of (-)-linalool (X_{24}; figure 3.4b) for different temperatures (T; carrier gas: N_2, τ at 450 °C: 0.73-0.75 s, τ at 475 °C: 0.71-0.72 s, τ at 500 °C: 0.68-0.70 s).

Comparison of frequency factors $\log_{10}A$ and of activation entropies $\Delta S^{\#}$ listed in table 3.2 with those found for the thermal reaction network of **3a** and **3b** (table 3.1) indicates that both reactions are comparable concerning the transition states (t.s.) the reactions pass through. Positive values in $\Delta S^{\#}$ and frequency factors of 13-14 in case of k_6 are reported to be typical for transition states having similar rotational and torsional degrees of freedom as found for the initial starting material.[69] Therefore, the reaction starting from **11** yielding **24** seems to proceed *via* as stepwise ring-opening of the desired cyclobutane ring. Apparently, thermally induced fragmentations of four-membered rings (cyclobutanes, oxetanes) have similar activation parameters concerning $\log_{10A}$ and $\Delta S^{\#}$ as reported herein for the cycloreversion of **3** and **11**.[69,74]

Negative activation entropies and low values for frequency factor are indicators for a "tight" t.s. the reaction passes through. Hence, the cyclization of **24** yielding **31** (scheme 3.1) is assumed to proceed as ene-reaction with a six-membered ring transition state the kinetic data reported in table 3.2 confirm this hypothesis. "Tight" t.s. have lower torsional

or rotational degrees of movement, being typical for cyclic reaction intermediates.[64,69] The values found are in the same range of order as those reported for the cyclization of **19** and **20** yielding **25** and **26**, respectively (scheme 3.1, table 3.1).[63,64,76]

CHAPTER 4

Pyrolysis of α-Pinene

This chapter reports results on the thermal isomerization of (-)- and (+)-α-pinene. Unraveling the complex rearrangement reactions of the main acyclic pyrolysis products ocimene and alloocimene those were subjected to pyrolysis studies also. Experiments reveal that the isomerization of α-pinene leading to 3*Z*-ocimene and racemic limonene (dipentene) is accompanied by a racemization of the optical active starting material. Kinetic analysis of the initial steps allows for the conclusion that these three reactions (racemization, formation of ocimene and dipentene) pass through the same biradical intermediates. Thermal isomerization studies of a mixture of 3*Z*- and 3*E*-ocimene reveal that the *Z*-isomer is more reactive and its rearrangement yields 4*E*,6*Z*-alloocimene predominantly, which themselves undergo isomerization leading to 4*E*,6*E*-alloocimene.

4.1 Background

The thermal isomerization of α-pinene (**9**) is a long known deeply investigated reaction. First studies were published in the 1930th by Smith and Carlson who independently observed racemization of the pyrolysis products yielded from thermal treatment of **9**.[44] Authors believe that this is due to the formation of racemic limonene (**34**, dipentene; Scheme 4.1), but more intensive studies reveal that beside the rearrangement of **9** to alloocimene (**22**) and **34** the pyrolysis of **9** yields non-converted α-pinene with a lower optical activity as found for the starting material.[43b,c,46a,b,48a,57a] Apparently, the initial formation of a biradical was assumed allowing for the explanation of those observations (Scheme 4.1).[47] Due to the fact that this mechanism has to lead to the formation of ocimene (**21**) and the absence of this product in the pyrolysis mixtures was proved a fast isomerization of **21** to **22** was proposed by various studies.[57a,b] α-Pinene (**9**) intensively has been subjected to kinetic studies in both gaseous and condensed phase[48b-d,51,52,77] but the consecutive reactions of **21** and **22** are rarely investigated.[51,57c] Deuterium-labeling experiments performed by Gajewski and co-workers support the hypothesis that a diradical is responsible for the formation of the primary pyrolysis products (**21**,**34**, racemic **9**) yielding from rearrangement of optical active **9**.[52,77] Recently, studies were published showing that isomerization of **9** can be carried out in supercritical alcohols without lost of the initial optical activity of **9** but accompanied by the formation of dipentene.[60,78]

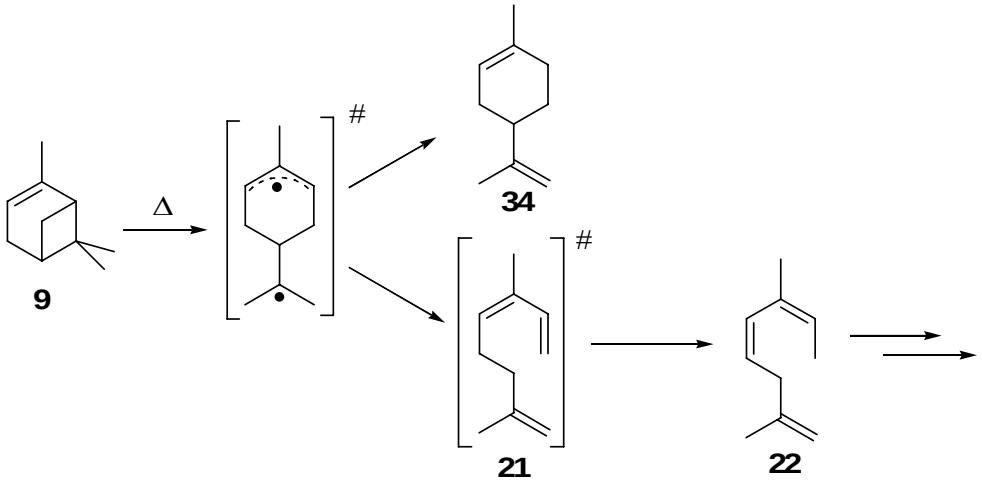

Scheme 4.1. Reaction products resulted from thermal isomerization of α-pinene (**9**).

Nevertheless, many results are published in literature concerning the thermal isomerization of α-pinene (**9**) already, it seems to be appropriate to investigate the pyrolysis once more from a mechanistic and kinetic point of view. Performing pyrolysis experiments with **9**, **21**, and **22** under identical conditions allows for a detailed study of the mechanisms of interconversions of these compounds. The calculation of activation parameters according to Arrhenius (eq. 2.7) and Eyring (eq. 2.8) on the basis of kinetic pyrolyses forces the understanding of the transition states the reactions pass through.

4.2 Pyrolysis of α-Pinene

In figure 4.1 three chromatograms (GC-FID) are shown resulting from analyses of the respective collected liquid pyrolysis products from rearrangement experiments with **9**, **21**, and **22**. Chromatograms reveal that thermally induced isomerization of **21** yields 4*E*,6*Z*-alloocimene (**22a**) exclusively, whereas experiments conducted with **9** showed an additional signal for the 4*E*,6*E*-isomer of alloocimene (**22b**). Apparently, this is due to the different pyrolysis temperatures the experiments were carried out at, because pyrolyses with **9** and **22** were performed at 462 °C and chromatogram b) result from thermal isomerization of **21** at 312 °C. Comparison of chromatograms a) and b) allows for the conclusion that the consecutive products (**cp**) formed from **9** and **22** are similar with respect to the peak pattern. Additionally, neither **21a** nor **21b** are seemed to be present in the product mixtures if **9** and **22** are pyrolyzed. Therefore, conclusion might be drawn that **21** is very reactive.

The plot of conversion of **9** (X_9) and of the yields of pyrolysis products Y_i *vs.* pyrolysis temperature T is depicted in figure 4.2. Concerning the amounts of products initially formed from **9** (**21**,**34**) significant differences were found. Whereas **34** is formed with a selectivity of approximately 45% the yield of the acyclic primary pyrolysis product **21** does not exceed 2% pointing out that **21** is a reactive molecule which rapidly rearranges to **22**. At a pyrolysis temperature of 412 °C the yield of **22** (Y_{22}) passes through a maximum and further increase of temperature gives rise to the formation of consecutive products (**cp**, *e.g.* pyronene). Decomposition and aromatization products of pyronenes built the main fraction in mixture of pyrolysis products yielded from experiments at temperatures higher than 525 °C. Interestingly, the ratio of primarily formed products **34** and **21** (incl. consecutive reaction products) practically remains constant within a

temperature range of 350-500 °C (figure 4.2). Therefore, it can be concluded that the reaction pathways starting from biradical intermediate sketched in scheme 4.1 are not affected by changes in reaction temperature.

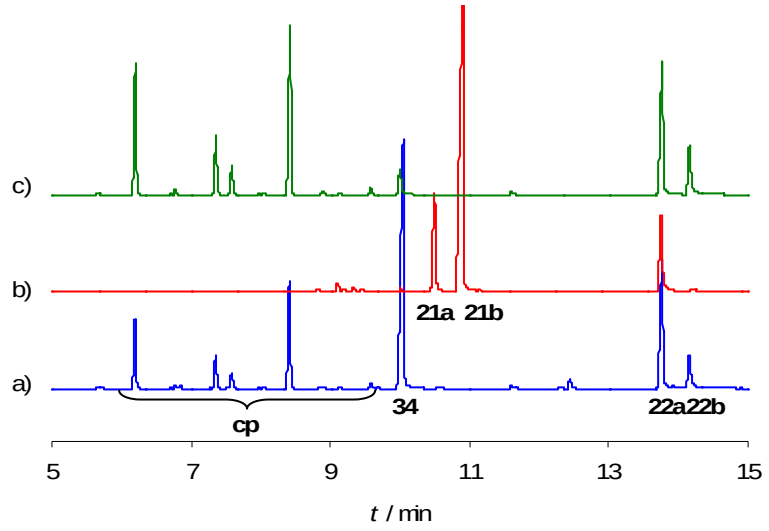

Figure 4.1. Comparative gas chromatograms (GC-FID) of product mixtures resulting from pyrolysis of α-pinene (a; **9**; 462 °C), pyrolysis of a mixture of 3*Z*- (**21a**) and 3*E*-ocimene (b; **22a**; 312 °C) and from pyrolysis of a mixture of 4*E*,6*Z*- (**22a**) and 4*E*,6*E*-alloocimene (c; **22b**; 462 °C). Product **34** is limonene and **cp** are consecutive products.

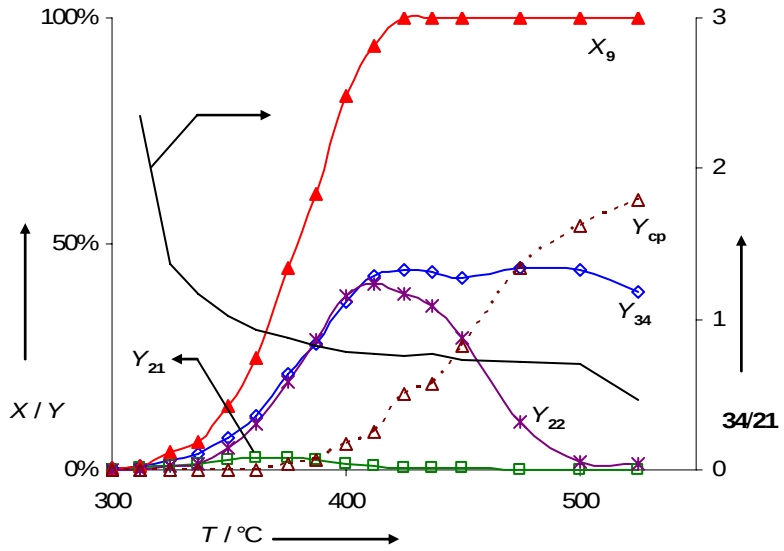

Fig. 4.2. Conversion of α-pinene (X_9), yield of primary pyrolysis products (Y_i), and ratio of Y_{34}/Y_{21} depending on the reaction temperature (T; 15 µL starting material, carrier gas: N_2, flow rate: 1.0 L min^{-1}, τ: 0.51-0.71 s).

The influence of reaction temperature on the enantiomeric ratio of both **9** and **34** was subject of these studies also. Pyrolysis experiments with optically pure (1*S*,5*S*)-(-)-**9** and (1*R*,5*R*)-(+)-**9** (scheme 4.2) were conducted, whereby the initial enantiomeric excess' *ee* (eq. 2.1), were 78 and 95%, respectively. Temperature plots of the corresponding yields of both enantiomers of **9** for pyrolysis of either (-)-**9** and (+)-**9** are pictured in figures 4.3a and 4.3b, respectively, clearly indicating that pyrolyses at elevated temperatures lead to a racemization of the starting materials. Contrarily to previous studies[44] on the lost of optical activity of **9** while heating a complete racemization was not observed in both cases, because of the fact that complete conversion (X_9) was reached first (425 °C). Additionally, the enantiomeric ratio of optical active pyrolysis product **34** was calculated based on GC-runs using the same β-cyclodextrine column as used for the determination of relative enantiomeric yields in case of **9**. Results shown in figure 4.3 for the pyrolysis of both enantiomers of **9** revealing that in both cases a racemic mixture of (-)-**34** and (+)-**34** was formed. Visible small differences are due to the chromatographic resolution.

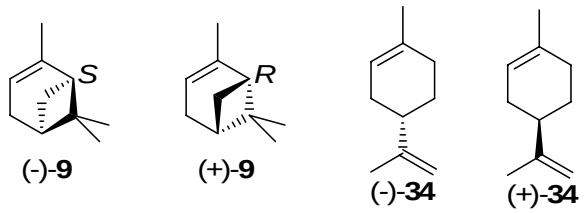

Scheme 4.2. Enatiomers of α-pinene (**9**) and limonene (**34**).

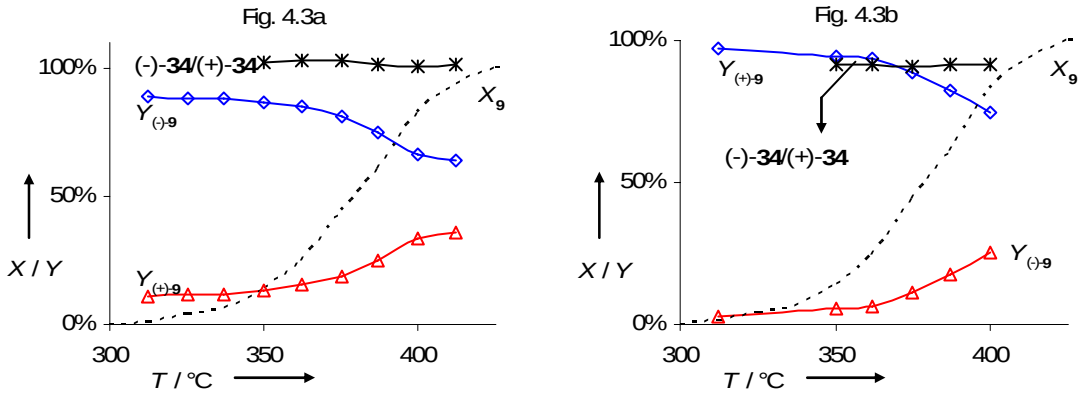

Figure 4.3. Conversion of α-pinene (X_9), relative yield of (-)-α-pinene ($Y_{(-)\text{-}9}$), relative yield of (+)-α-pinene ($Y_{(+)\text{-}9}$), and ratio of (-)- and (+)-limonene (**34**) depending on the reaction temperature (T) for the pyrolyses of (-)-**9** (figure 4.3a) and (+)-**9** (figure 4.3b; 15 µL starting material, carrier gas: N_2, flow rate: 1.0 L min^{-1}, τ: 0.60-0.70 s, enantiomeric ratios measured with a β-cyclodextrine column).

4.3 Pyrolysis of Ocimene

Pyrolysis experiments with a mixture of 3*Z*- (**21a**) and 3*E*-ocimene (**21b**; scheme 4.3) were conducted to unravel the products formed from their thermal treatment. GC analyses showed that the ratio of the two stereoisomers of **21** was approximately 0.5 in favor of **21b**. Same results were found in the ^{1}H NMR spectrum of the mixture. Structures were confirmed by one-dimensional NOESY-experiments.[79] Excitation of the protons at C(4) and at C(2) of **21a** leads to NOE (Nuclear Ovenhauser Effect) contacts with the methyl-protons at C(9) and with those at C(5), respectively (scheme 4.3). Excitation of the same protons in case of **21b** showed contacts with the respective other proton only.

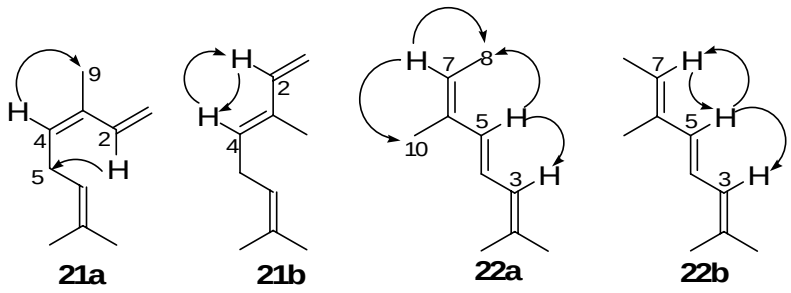

Scheme 4.3. Structures of 3*Z*-ocimene (**21a**), 3*E*-ocimene (**21b**), 4*E*,6*Z*-alloocimene (**22a**), and of 4*E*,6*E*-alloocimene (**22b**; arrows assign NOE-contacts between protons, whereby the respective excited proton is the origin of the arrow).

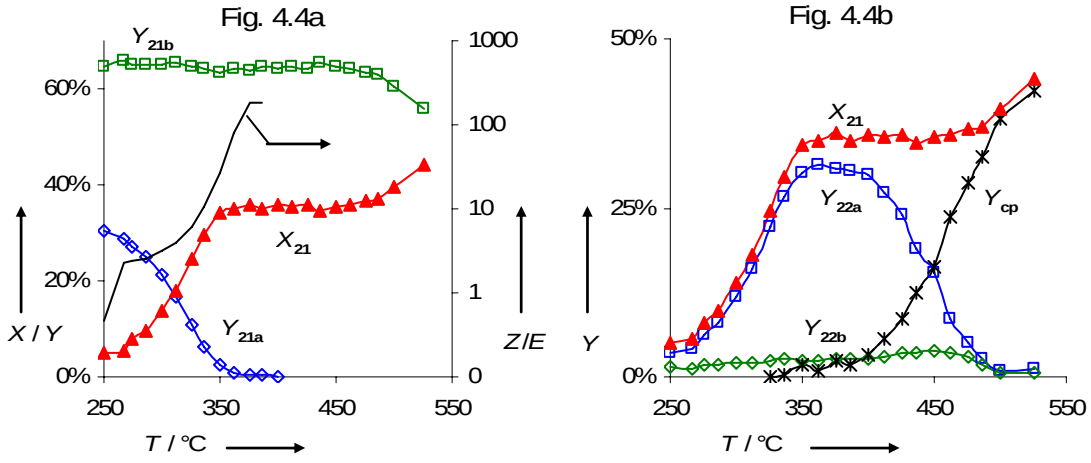

Figure 4.4. Conversion of ocimene (X_{21}), yield of 3*Z*-ocimene (Y_{21a}), yield of 3*E*-ocimene (Y_{21b}), and ratio of 3*Z*- and 3*E*-ocimene (Z/E) depending on the reaction temperature (*T*; figure 4.4a). *T*-plot of the yields (Y_i) of ocimene and pyrolysis products (figure 4.4b; 15 µL starting material, carrier gas: N_2, flow rate: 1.0 L min^{-1}, τ: 0.51-0.78 s).

Explorative pyrolyses investigating the temperature dependency of the conversion of **21** ($X_{\mathbf{21}}$) reveal differences in the thermal behavior of **21a** and **21b** pictured figure 4.4a. Whereas the *Z*-isomer (**21a**) is completely converted at a pyrolysis temperature of 375 °C **21b** is thermally stable up to 525 °C, thus indicating that pyrolysis of **9** mainly yields **21b**. Therefore the low yields reported for **21** (figure 4.2) in case of the pyrolysis of **9** have to be assigned to the formation of **21b**, because at those temperatures the *Z*-isomer is not present any more. Hence $Y_{\mathbf{21a}}$ decreases wile rising temperature from 250 to 375 °C the ratio of **21a**/**21b** increases until complete conversion of **21a**.

Figure 4.4b reports the yields Y_i of pyrolysis products of **21** depending on the reaction temperature T indicating that alloocimene (**22**) is formed in two stereoisomeric forms: 4*E*,6*Z*- (**22a**) and 4*E*,6*E*-alloocimene (**22b**, scheme 4.3), whereby **22a** is the main product. After passing through a maximum at 375 °C the yield of **22a** ($Y_{\mathbf{22a}}$) decreases in favor of the formation of consecutive products (**cp**), whereas the amount of **22b** formed from **21a** remains constant. Hence, figure 4.2 shows $Y_{\mathbf{22}}$ as sum of the two isomers its maximum is shifted to higher temperatures. Structures of the two alloocimenes were confirmed by comparison of retention times and mass spectra with those of an authentic mixture of **22a** and **22b**. ^{1}H NMR spectra in combination with NOE-experiments[79] with this authentic sample (**22a**/**22b**: 9.0) allowed for structural elucidation of the two isomers. In case of excitation of the protons at C(5) NOE-contacts were detected with protons at C(3) and C(8) or C(3) and C(7) for **22a** or **22b**, respectively. Excitation of the vinylic proton at C(7) no further contacts were detected in case of **22b**, whereas interactions with the protons of the neighbored methyl groups C(8) and C(10) were evident for the 4*E*,6*Z*-isomer (scheme 4.3).

4.4 Pyrolysis of Alloocimene

Pyrolysis experiments with a mixture of 4*E*,6*Z*- (**22a**) and 4*E*,6*E*-alloocimene (**22b**; scheme 4.3) were conducted in order to investigate the thermal behavior of these two diastereomers. As described in section 4.3 pyrolysis of **21a** yields those two isomers in favor of **22a**, whereas their structure was confirmed based on NMR-experiments with the respective authentic mixture. Figure 4.5 reports the dependency between reaction temperature and the yields of **22a** ($Y_{\mathbf{22a}}$) and **22b** ($Y_{\mathbf{22b}}$) revealing that both were converted into other $C_{10}H_{16}$ hydrocarbons (*e.g.* pyronenes). Because of the fact that

aromatization and decomposition of those consecutive products occurred at temperatures higher than 525 °C this region was not investigated. Contrarily to $Y_{\mathbf{22a}}$ the yield of **22b** seems to increase until 450 °C and after passing through this maximum $Y_{\mathbf{22b}}$ decreases in the same way as observed for the 4*E*,4*Z*-isomer. Apparently, isomerization of **22a** to the other isomer takes place being responsible for an increase of the ratio of **22b** to **22a** wile rising temperature.

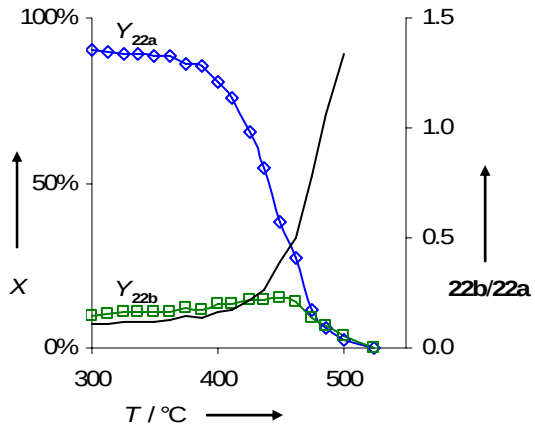

Fig. 4.5. Yield of 4*E*,6Z-alloocimene ($Y_{\mathbf{22a}}$), yield of 4*E*,6*E*-alloocimene ($Y_{\mathbf{22b}}$) and ratio of **22b**/**22a** depending on the reaction temperature (*T*, 15 µL starting material, carrier gas: N_2, flow rate: 1.0 L min^{-1}, τ: 0.51-0.71 s).

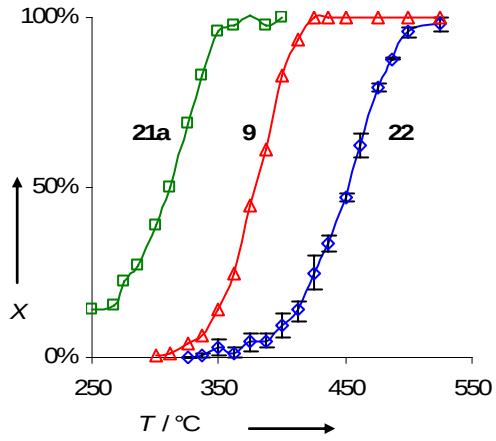

Fig. 4.6. Conversion of 3*Z*-ocimene (**21a**), of α-pinene (**9**), and of alloocimene (**22**; mean values) depending on the reaction temperature (*T*; 15 µL starting material, carrier gas: N_2, flow rate: 1.0 L min^{-1}, τ: 0.51-0.78 s).

Pyrolysis experiments with **9** and its acyclic pyrolysis products **21** and **22** reveal significant differences with respect to the temperature region they are converted (figures 4.2, 4.4, and 4.5). Comparison of these results are illustrated in figure 4.6 revealing that **21a** being the most reactive isomer and **22** the most thermally stable hydrocarbon. Results confirm the findings published that **21a** is present in very low concentrations in the mixture of pyrolysis products yielded from thermal isomerization of **9**.[46a,51,52,57a,77,80] In order to compare the yields of **22** (Y_{22}) resulted from independent pyrolysis experiments with either **9**, **21** or **22** the respective conversions were calculated from the experimental data. Mean values for each reaction temperature are depicted in figure 4.6, whereby the reported variances correspond to the maximal or minimal difference to the respective mean values. Results recalculated from pyrolysis of **9** and **21** are in good agreement with those from thermal isomerization experiments with **22** itself.

4.5 Elucidation of Kinetic Steps in the Pyrolysis of α-Pinene

α-Pinene (**9**) as well as its acyclic main isomerization products 3*Z*-ocimene (**21a**), 4*E*,6*Z*-alloocimene (**22a**), and 4*E*,6*E*-alloocimene (**22b**) were subjected to kinetic studies. Simplified reaction scheme used for calculation of the rate constants k_i is depicted in scheme 4.4. Explorative pyrolysis studies revealed that **9** primarily isomerizes to give **21a** and **34**, whereby minor amounts of 3*E*-ocimene (**22b**, Y_{22b}: < 2.5%; figure 4.2) were neglected due to its thermal stability within the temperature range investigated (250-525 °C; figure 4.4a). It has to be pointed out that the network presented in scheme 4.4 does not include the reaction(s) leading to racemized **9**. Due to the fact that the racemization of both (-)- and (+)-**9** is accompanied by isomerization to products **21a**, **22**, and **34** consideration of this reaction would complicate the reaction network. Additionally, besides **34** all products are not optically active and pyrolyses with enantiomeric pure (-)- as well as (+)-**9** reveal that both yield racemic **34**. Therefore, it seems to be appropriate to discuss the racemization of **9** separately.

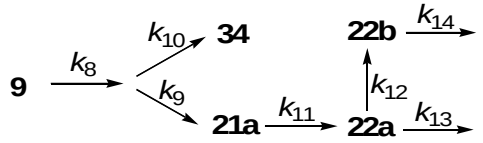

Scheme 4.4. Simplified reaction network used for calculation of rate constants $k_{8\text{-}14}$.

Arrhenius as well as Eyring activation parameters were calculated according to eq. 2.7 and 2.8, respectively. Pyrolysis experiments with pure **9** and with mixtures of diastereomeric **21** and **22** were conducted to determine the rate constants k for the disappearance of **9** (k_8), **21a** (k_{11}), **22a** (k_{13}), and **22b** (k_{14}), respectively. Based on these data it was possible to calculate the other rate constants using the model of competitive parallel first order reactions. Arrhenius plots for the reactions responsible for disappearance of the starting materials are shown in figure 4.7. Linear regression allows for the calculation of activation energies E_a and frequency factors $\log_{10}A$ from the slopes or axis intercepts, respectively. Similar to those, activation enthalpies $\Delta^{\ddagger}H$ and activation entropies $\Delta^{\ddagger}S$ were calculated form linear regression function of the Eyring-plots [T^{-1} against $\ln(k_T\ T^{-1})$]. Activation data are summarized in table 4.1. Hence, in case of calculation of k_{12} experiments at only two different temperatures were able to be considered no error limits are given.

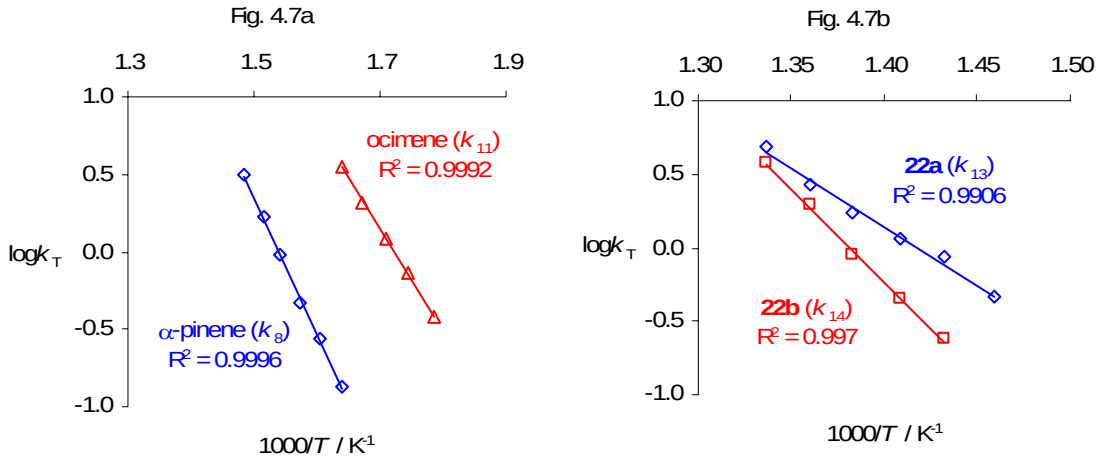

Figure 4.7. Arrhenius plots of log k *vs.* 1000/T for the thermal isomerization of α-pinene (**9**, k_8) and 3*Z*-ocimene (**21a**, k_{11}; figure 4.7a) as well as for the rearrangement of 4*E*,6*Z*-alloocimene (**22a**, k_{13}) and 4*E*,6*E*-alloocimene (**22b**, k_{14}; figure 4.7b).

Consideration of $\log_{10}A$ together with $\Delta^{\ddagger}S$ allows for characterization of the transition states the reactions presumably passing through. Typical parameters for "normal" t.s. are approximately 13 in $\log_{10}A$ and activation entropies of around 0 J K^{-1} mol^{-1} as found for k_8 describing the disappearance of **9**. Literature assumes that those t.s. have a similar geometry compared to the ground-state geometry of the starting molecule with minor differences in torsional and rotational degrees of movement.[69] Hence, "normal" t.s. are

reported to be typical for fragmentations of four-membered rings the results found herein for k_8 are in accordance to those from studies investigating the thermal decomposition of cyclobutane derivatives.[69,74a-d] Similar conclusions can be drawn for the formation of **21a** from **9** (k_9; table 4.1) but the positive activation entropies in these cases are indicators for "loose" t.s. being typical for biradical intermediates the reactions pass through. Therefore, it seems to be appropriate assuming that both reactions k_8 and k_9 are reactions involving biradical intermediates. A high Arrhenius factor and an activation entropy of 74 J K^{-1} mol^{-1} were found for the disappearance of **22b** (k_{14}) being an unequivocal indicator for the fact that this reaction passes through (a) radical reaction intermediate(s). In contrast to **22b** the activation parameters for the disappearance of the 4*E*,6*Z*-isomer of **22** (k_{13}; table 4.1) are typical for reactions passing through rigid six-membered ring t.s.. Those are characterized by a lower degree of freedom for torsional and / or rotational movement.[69] Therefore it can be concluded, that beside k_{13} the formation of **34** from **9** (k_{10}), the isomerization of **21a** to **22a** (k_{11}), and the reaction of **22a** leading to **22b** (k_{12}) are reactions passing through six-membered ring transitional states (*e.g.* [1,5]H-shift, ene-reaction).

Table 4.1. Kinetic data[a] for the gas-phase isomerization reactions of α-pinene (**9**; $k_{8\text{-}10}$), 3*Z*-ocimene (**21a**; k_{11}), and of alloocimene (**22**; $k_{12\text{-}14}$; *cf.* scheme 4.4).

	E_a (kJ mol^{-1})	$\log_{10}A$ (s^{-1})	$\Delta^{\ddagger}H$ (kJ mol^{-1})	$\Delta^{\ddagger}S$ (J K^{-1} mol^{-1})
k_8	170.0 ± 1.7	13.70 ± 0.14	165.2 ± 1.6	3.0 ± 0.04
k_9	178.5 ± 1.8	14.11 ± 0.15	173.7 ± 1.8	11.0 ± 0.2
k_{10}	160.8 ± 2.4	12.61 ± 0.19	155.9 ± 2.3	-17.7 ± 0.4
k_{11}	125.72.1	11.31 ± 0.18	120.8 ± 2.1	-42.4 ± 1.0
k_{12}[b]	181	12.4	175	-23
k_{13}	150.9 ± 7.4	11.18 ± 0.54	144.9 ± 7.3	-46.6 ± 3.2
k_{14}	242.4 ± 7.6	17.49 ± 0.55	236.4 ± 7.6	74.3 ± 2.9

[a] Error limits are 95% certainty limits. [b] Based on experiments at only two different temperatures.

Comparison of the kinetic data calculated on the basis of pyrolysis experiments with the herein described reactor (table 4.1) with those reported in literature (table 4.2) reveals a high accordance.[48d,51,52,57a,b,77,78] The network of reactions based on pyrolysis of **9** has been subjected to kinetic studies since the 1950th but there is only one study investigating

the isomerization of **9** in the gas-phase using a flow-type reactor.[57a] Unfortunately, this study reported data for the isomerization of **21** leading to **22** only (k_{11}). Nevertheless, those results are in agreement with those reported herein and found for pyrolysis experiments in liquid-phase.[51,57c] Due to different experimental conditions the results concerning initial reactions of **9** ($k_{8\text{-}10}$; table 4.2) differ from each other, but the absolute differences of the Arrhenius activation parameters (E_a, $\log_{10}A$) are in accordance with those listed in table 4.1.[48d,51,52,77]

Table 4.2. Comparison of kinetic data (E_a, $\log_{10}A$)[a] for isomerization reactions in the reaction network based on pyrolysis of α-pinene (**9**).

Reaction conditions		E_a (kJ mol^{-1})	$\log_{10}A$ (s^{-1})
flow-type rector, gas-phase, vacuum [57a]	k_{11}	108.9	9.49
glass ampoules, liquid-phase[b] [48d]	k_9	178.6	15.6
	k_{10}	154.9	13.3
liquid-phase[c] [57c]	k_{11}	118.5	10.41
glass ampoules, liquid-phase, N_2 [51]	k_8	179	14.37
	k_9	171	13.30
	k_{10}	186	14.70
	k_{11}	118	10.50
	k_{13+14}	136	11.34
batch reactor, gas-phase, vacuum[b] [52,77]	k_8	178.8	14.2
	k_9	181.3	14.1
	k_{10}	175.0	13.6
flow-type reactor, supercritical EtOH[d] [78]	k_9	136.6 ± 9.2	
	k_{10}	118.0 ± 8.1	
flow-type reactor, supercritical EtOH[d] [81]	k_{13+14}	129.4 ± 31.0	

[a] Respective rate constants k_i according to scheme 4.4. [b] Racemization of **9** is included in the model. [c] No experimental detail. Eyring parameters calculated on basis of Arrhenius parameters for 423 K: $\Delta H^{\#}$: 113.0 kJ mol^{-1}, $\Delta S^{\#}$: -14.7 J K^{-1} mol^{-1}. [d] Activation energies calculated on the basis of a model of the reactor used for the experiments.

Activation energies E_a calculated on the basis of pyrolysis experiments with **9** in a flow-type reactor using supercritical ethanol as fluent shows significant differences to all other values reported in table 4.2.[78] Obviously, other reaction mechanisms are present

when the reaction is carried out in a high-pressure regime. Activation parameters available from literature for the disappearance of **22**[51,81] indicate that mostly **22a** is formed from **21a**, thus being in agreement with the pyrolysis studies on **21** and **22** presented in figures 4.4b and 4.5.

Consideration of the gas-phase racemization of both enantiomers of **9** within the simplified model described in scheme 4.4 is difficult from various points of view. As reported in figure 4.3 both (-)-**9** as well as (+)-**9** undergo beside their racemization isomerization reactions leading to **21** and racemic **34** as primary pyrolysis products with selectivities being independent from the enantiomer used. This allows for the conclusion that both molecules take part in the isomerization reaction and therefore it seems to be impossible to combine the kinetics for rearrangement and racemization. Combination of both processes would lead to rate equations with feedback routes because if some molecules of (+)-**9** are formed from the (-)-enantiomer those can either undergo isomerization or can be converted to give again (-)-**9**. Decoupling of these reaction pathways and separate determination of the kinetic parameters seem to be appropriate. scheme 4.5 shows the network for gas-phase racemization of **9**. Due to the fact that racemic **34** is formed in either of both ways and the other products (**21**,**22**; *cf.* scheme 4.4) are not optical active those reactions ($k_{8\text{-}14}$; *cf.* table 4.1) are independent from the enantiomeric ratio of the starting material and a decoupling of the reaction pathways is possible.

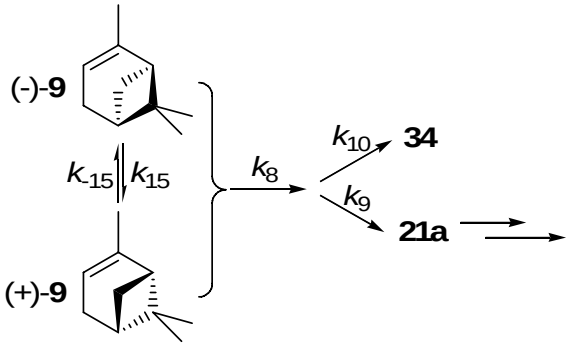

Scheme 4.5. Gas-phase racemization of α-pinene (**9**).

Hence, pyrolysis experiments proven the fact that both enantiomers can be interconverted (figure 4.3) it seems appropriate assuming that this reaction is a chemical equilibrium as described in scheme 4.5. Equilibrium constant K is defined as the ratio of the forward reaction (k_{15}) to the back reaction ($k_{\text{-}15}$; eq. 4.1). Rate constants for both the

forward and the back reaction can be calculated on the basis of pyrolysis experiments with (-)- or (+)-**9**, respectively. Contrarily to the calculation of the rate constants listed in table 4.1 which based on concentrations, in this case the changes of the enantiomeric excess' *ee* (eq. 2.1) were monitored while the residence time τ (eq. 2.6) was varied.

$$K = \frac{k_{15}}{k_{-15}} \tag{4.1}$$

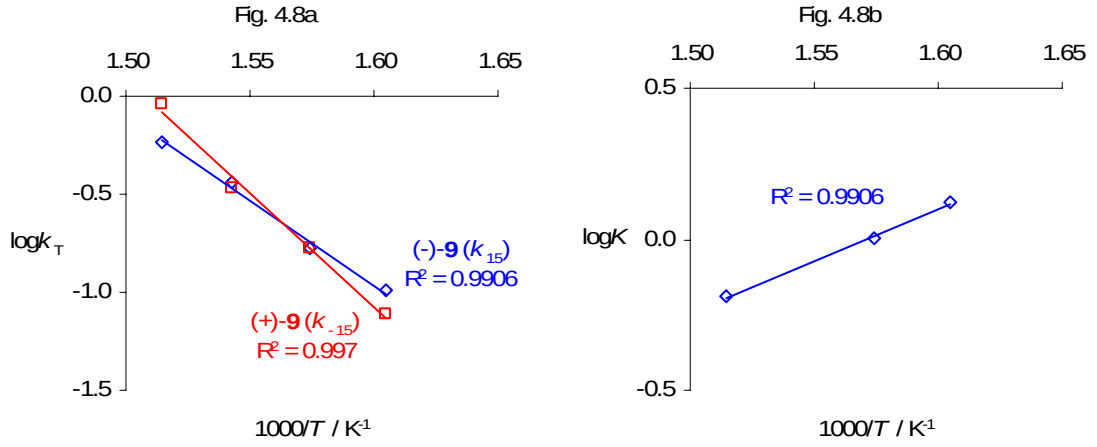

Figure 4.8. Arrhenius plots of log *k vs.* 1000/*T* for the lost of optical activity in case of (-)-**9** (k_{15}) and (+)-**9** (k_{-15}; figure 4.8a) as well as plot of the logarithmic equilibrium constant log*K vs.* 1000/*T* for the racemization of (-)-**9** to (+)-**9** (figure 4.8b).

Table 4.3. Kinetic data[a] for the gas-phase racemization of (-)- and (+)-α-pinene (**9**; *cf.* scheme 4.5).

	E_a (kJ mol^{-1})	$\log_{10}A$ (s^{-1})	$\Delta^{\ddagger}H$ (kJ mol^{-1})	$\Delta^{\ddagger}S$ (J K^{-1} mol^{-1})	Ref.
k_{15}	166.8 ± 9.9	12.97 ± 0.80	161.4 ± 9.9	-11.3 ± 0.9	This work
k_{-15}	223.4 ± 15.4	17.59 ± 1.26	218.0 ± 15.4	77.1 ± 6.8	This work
k_{-15}[b]	184.8	15.8			[48b]
k_{15}[c]	188.4	14.4			[52,77]

[a] Error limits are 95% certainty limits. [b] Racemization of (+)-**9** carried out in sealed quartz ampoules in liquid phase. [c] Racemization of (-)-**9** in gas-phase (vacuum) using a batch system.

Arrhenius plots for the decrease in *ee* for both enantiomers are pictured in figure 4.8a. The corresponding activation parameters according to Arrhenius and Eyring equations are listed in table 4.3. Surprisingly, these parameters significantly differ from each other and comparison with data published within earlier studies reveals huge

differences.[47,52,77] One would expect that reactions being part of a chemical equilibrium have the same or even similar activation parameters. Apparently, this is not the fact for the racemization of **9** in the gas-phase. It has to be stated that values reported in literature result from static experiments in either glass ampoules[48b] or in a batch-reactor under vacuum conditions.[52,77] Due to this experimental differences the temperature and residence time regimes the pyrolysis experiments were carried out are not comparable. Herein pyrolyses were conducted within a temperature range of 350 to 387 °C with contact times of 0.5-1.8 s, whereas reactions in the batch system were carried out at 180-200[48b] or at 225-250 °C for vacuum conditions.[52,77] Reaction times range from 40 min to 7.5 h.

Equilibrium constant K is related to the Gibbs free energy of activation ($\Delta_R G$) by eq. 4.2. With respect to the first law of thermodynamics K is related to the reaction enthalpy ($\Delta_R H$) and reaction entropy ($\Delta_R S$). Transformation of eq. 4.2 leading to eq. 4.3 and plotting ln$K$ against inverse temperature T^{-1} in K^{-1} and linear regression allows for the calculation of $\Delta_R H$ and $\Delta_R S$ from the slope and axis intercept, respectively. Corresponding plot is pictured in figure 4.8b and calculation gives the reaction enthalpy and entropy for the formation of the transition state with values of (-65.9 ± 3.1) kJ mol^{-1} and (103.5 ± 4.9) J K^{-1} mol^{-1}, respectively.

$$-RT \ln K = \Delta_R G = \Delta_R H - T \Delta_R S \tag{4.2}$$

$$\ln K = -\frac{\Delta_R H}{T \cdot R} + \frac{\Delta_R S}{R} \tag{4.3}$$

Figure 4.8b suggests that there exists a point whereat both the forward and the back reaction have equal rate constants (K = 1.0). With respect to eq. 4.2 this point is equal to $\Delta_R G$ of 0 kJ mol^{-1} and using the first law of thermodynamics (4.3) the corresponding temperature is 363 °C. Pyrolysis experiments at 362 °C with (-)- and (+)-**9** lead to rate constants of 0.1677 s^{-1} and of 0.1659 s^{-1} for k_{15} and k_{-15}, respectively.

4.5 Pyrolysis Mechanisms of α-Pinene, Ocimene and Alloocimene

Pyrolysis experiments as well as kinetic analysis of the most important reactions in the thermal reaction network based on **9** allow for mechanistic evaluations of the initial reaction steps. Pyrolyses with **9** (figure 4.2) reveal that the ratio of primary formed pyrolysis products **21** and **34** remains constant while increasing temperature and conversion of **9** from 300 to 500 °C or 0 to 100%, respectively. Additionally, enantiomerically pure (-)- as well as (+)-**9** were subjected to pyrolysis studies in order to investigate the temperature dependency of the enantiomeric excess' (figure 4.3) showing that independently from the enantiomer used as starting material racemization occurred. This allows for the conclusion that three major reactions contribute to the disappearance of **9** during its thermal induced rearrangement. Comparative pyrolysis experiments with a mixture of 3*Z*- (**21a**) and 3*E*-ocimene (**21b**) proofs that **21a** is formed from **9** exclusively. **21a** undergoes rapid rearrangement yielding stereospecifically **22a**. The formation of consecutive product **22b** is due to a rearrangement of the initially formed conjugated triene **22a**.

Kinetic analysis of the reactions responsible for disappearance of **9** (k_8) and the formation of **21a** (k_9) and **34** (k_{10}; *cf.* scheme 4.4 and table 4.1) allows for the conclusions that k_8 and k_9 pass through "loose" t.s., whereas the reaction leading to product **34** runs through a six-membered ring transition state. Since [2+2]-cycloadditions as well as [2+2]-cycloreversions are thermally forbidden reactions with respect to the Woodward-Hoffmann rules,[11] formation of **21a** has to proceed stepwise including a biradical intermediate **TS1** depicted in scheme 4.6.[43b,47,52,62,77] Rupture of the carbon-carbon bond between C(1) and C(2) leads initially to the biradical **TS1a** which is resonance stabilized due to the formation of an intramolecular allylic radical forming intermediate **TS1b**.

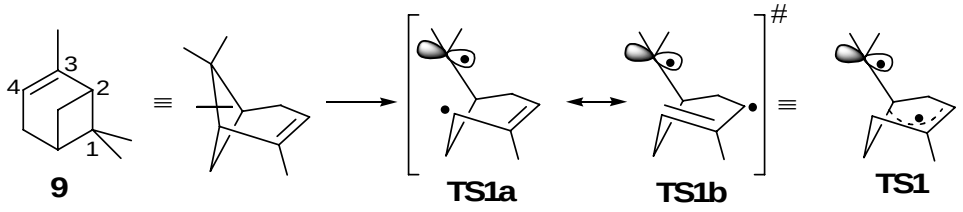

Scheme 4.6. Initial formation of the biradical intermediates **TS1** from α-pinene (**9**).

Based on the biradical **TS1** three possible reaction pathways exist leading to the formation of products **21a**, **34**, and to racemized **9**. Reconnection of the bond initially been broken in case of **TS1a** leads to **9** with the initial configuration whereas bond formation in **TS1b** yields the opposite enantiomer (scheme 4.7).[52,77] Due to the fact that pyrolysis experiments performed herein used unlabeled **9** the resulted products differ only in their optical activity. The use of **9** labeled with ^{13}C in either 2-, 3-, or 4-position would yield products which could easily be separated and identified using ^{1}H NMR- or ^{13}C NMR-spectroscopy. Unfortunately, synthetic routes leading to those labeled α-pinenes are very difficult and complex as well as time and cost consuming.

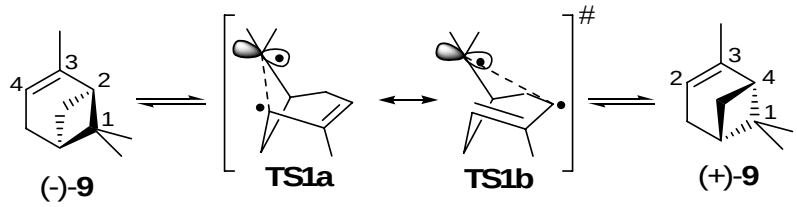

Scheme 4.7. Racemization of α-pinene (**9**) *via* biradical transitions states **TS1a** and **TS1b**.

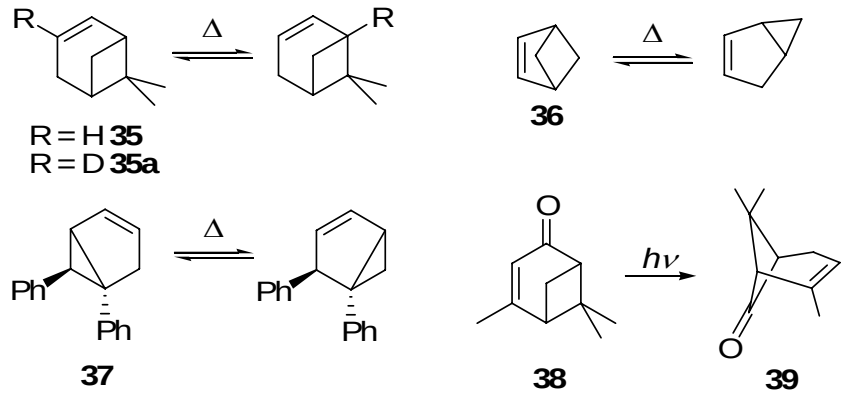

Scheme 4.8. Examples for 1,3-sigmatropic rearrangements similar to the racemization of α-pinene (**9**; *cf.* scheme 4.7).

This racemization reaction can be classified as 1,3-sigmatropic rearrangement reaction. Literature reports some examples for similar thermally as well as photochemically induced isomerizations pictured in scheme 4.8.[82] All thermally induced reactions have in common that a chemical equilibrium between starting material and rearranged product is formed. The reaction of ^{2}H-labeled norpinene **35a** exemplifies the possibility to study this reaction without the need of separation of the enantiomers.[82e] Hence, that the photochemical rearrangement of verbenone (**38**) yields chrysanthenone

(**39**) as the main product[82d,83] those 1,3-sigmatropic shift reactions pictured in schemes 4.7 and 4.8 are thermally and photochemically permitted reactions.

Analysis of the resulted pyrolysis products from thermal isomerization experiments of both enantiomers of **9** reveals that racemic **34** (dipentene) is formed independently from temperature, conversion of **9**, and from the initial enantiomeric excess (figure 4.3). Activation parameters for the formation of dipentene from **9** indicate a "tight" t.s. thus being typical for reactions passing through six-membered ring transition states. Therefore, the most plausible mechanism explaining the formation of dipentene involves a [1,5]H-shift reaction shown in scheme 4.9.[52,77] Hydrogen shift from C(9) to C(1) in case of intermediate **TS1a** yields (-)-**34**, whereas shift reaction from C(9) to C(3) in case of mesomeric **TS1b** leads to the formation of the respective other enantiomer. Racemic dipentente is formed with respect to the formation of an resonance stabilized allyl-type radical leading to a lost of optical activity, due to the fact that **TS1** (scheme 4.6) has a mirror-plane (point symmetry group: C_S).

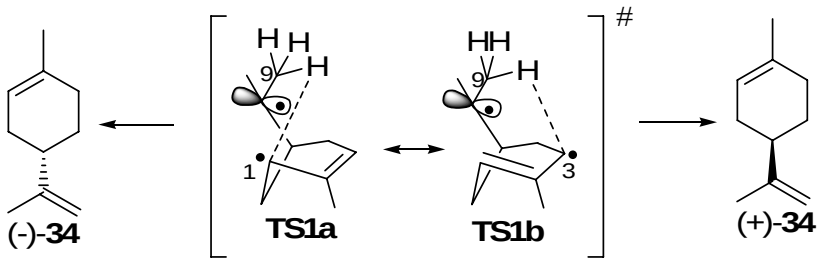

Scheme 4.9. Formation of racemic limonene (**34**; dipentene) *via* [1,5]H-shift in the initially formed biradicals **TS1a** and **TS1b** (*cf.* scheme 4.7).

The formation of **21a** from **9** *via* thermally induced rearrangement follows the known mechanisms for cyclobutane defragmentation.[74b-e,84] Rupture of the second carbon-carbon bond in intermediate **TS1** and subsequently radical recombination yields 3*Z*-ocimene (**21a**) exclusively (scheme 4.10). This reaction pathway is in accordance to the Woodward-Hoffmann rules which forbid a concerted cycloreversion mechanism.[11] The formation of **21b** is suppressed because of the rigid cyclic structure in case of **TS1**. Hence, there is no statistically firmed dependency of the formation of **21b** from either pyrolysis of **9** or **21a** (figure 4.9) conclusion is permissible that **21b** yields from a surface-catalyzed rearrangement (reactor wall) of the respective carbon-carbon double bond in **21a**. Photosensitized reactions of **9** using acetophenone as quencher reports the

exclusive formation of **21a** which themselves consecutively rearranges forming the respective *trans*-isomer **21b**.[85] Even radiolysis of **9** yields **21a** and **34** as the primary products,[86] whereby accordingly to the thermal rearrangement **21a** isomerizes to give **22**.[87]

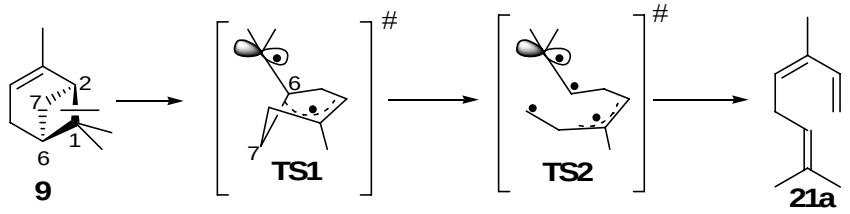

Scheme 4.10. Formation of 3*Z*-ocimene (**21a**) from α-pinene (**9**).

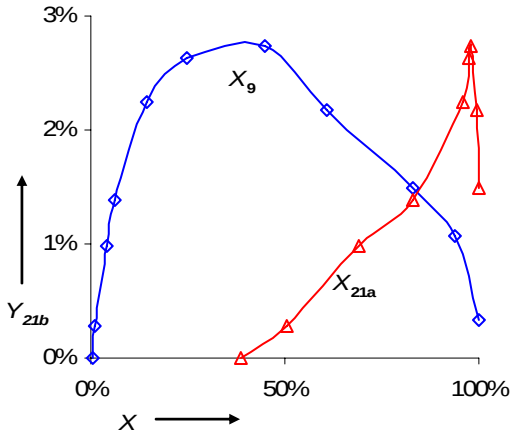

Figure 4.9. Dependency of the yield of 3*E*-ocimene ($Y_{\mathbf{21b}}$) from conversion of α-pinene ($X_{\mathbf{9}}$) and from conversion of 3*Z*-ocimene ($X_{\mathbf{21a}}$).

Results reported herein on the pyrolysis of **9** are in good agreement with thermolysis studies on 2,2-dimethyl-1-vinylcyclopropane (**40**) as non-bridged cyclobutane model for **9**.[74d] The relationship between **9** and **40** is described in scheme 4.11. Asterisks attached to **40** and its pyrolysis products assign connection points for the cyclohexane ring in **9** whereas the circle assigns the missing methyl-group. Four major reaction pathways were found by Chickos and Frey indicated by the respective rate constants in Scheme 4.11. Fragmentation of **40** (k_f) yields isobutene and 1,3-butadiene exclusively, whereby the addition of the missing methylene bridge and methyl-group leads to **21a**. Interestingly, authors report the formation of the cisoid form of 1,3-butadiene. 4,4-Dimethylcyclohexene is the 1,3-sigmatropic shift reaction product ($k_{1,3}$) from **40** being

equal to the racemized form of **9** after pyrolysis (*cf.* scheme 4.7). Both reaction pathways leading to acyclic products for the pyrolysis of **40** differ in position of one of the two carbon-carbon double bonds (scheme 4.11), thus expressing the two different enantiomers of **34** yielding from pyrolysis of **9** (*cf.* scheme 4.9). Comparison of experimental results presented herein and those found for thermolysis of **40**[74d] showed a good agreement concerning the products formed and therefore the comparability of the two compounds.

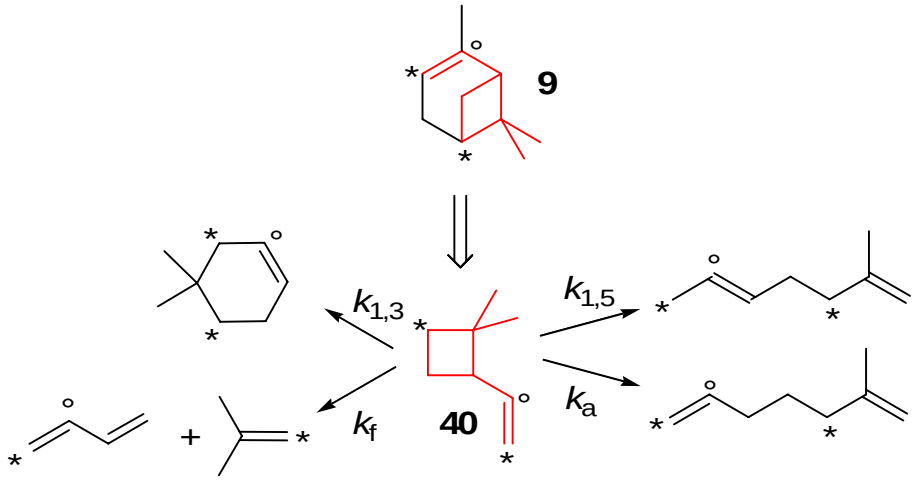

Scheme 4.11. Thermal network of pyrolysis products from thermolysis of 2,2-dimethyl-1-vinylcyclobutane (**40**) and its relationship to α-pinene (**9**).[74d]

Results of pyrolysis experiments with a mixture of 3*Z*- (**21a**) and 3*E*-ocimene (**21b**) depicted in figure 4.4 revealed that predominately the *Z*-isomer was isomerized, whereas the concentration of **21b** remains constant within the temperature range investigated. Analysis of the pyrolysis products formed showed that the formation of 4*E*,6*Z*-alloocimene (**22a**) is favored, whereby thermolysis experiments with a mixture of **22a** and **22b** allows for the conclusion that the 4*E*,6*E*-isomer (**22b**) yields from reconfiguration of the 6*Z*-double bond in **22a**. Therefore, conclusion can be drawn that both the formation of **21a** and its disappearance are highly enantiospecific reactions. Reasons for the preferred formation of **21a** from **9** have been presented in the section before (*cf.* scheme 4.10). Liquid-phase pyrolysis studies with **21a** reported similar activation parameters found for the gas-phase isomerization presented in table 4.1 (k_{11}).[57c] Activation entropy $\Delta^{\ddagger}S$ and frequency factor $\log_{10}A$ indicate a “tight” transition state as reaction intermediate typical for reactions passing through a six-membered ring

t.s.[69] Probably, the rearrangement of **21a** to **22a** proceeds as [1,5]H-shift reaction pictured in scheme 4.12. According to the Woodward-Hoffmann rules those reactions are thermally allowed if they proceed in the suprafacial version.[11,57c,74c,88] Whereas the stereospecific formation of the 6*Z*-double bond in **22a** is due to reaction mechanism and the rigid cyclic transition state the stereochemistry of the double bond at C(4)-C(5) is controlled by the nature of the reaction intermediate. Scheme 4.12 pictures two possible intermediates (**TS3a** and **TS3b**) for the suprafacial [1,5]H migration leading to either **22a** or to 4*Z*,6*Z*-alloocimene, respectively. Hence, it is evident that the thermal isomerization of **21a** exclusively yields **22a** the reaction has to pass through intermediate **TS3a**. Obviously, the preference of **TS3a** to **TS3b** could be explained by less steric repulsion of the large isobutenyl substituents in the less crowded equatorial position than in the more crowded axial.[57c] Results are in agreement with respect to stereochemistry and activation parameters to those found for the thermal rearrangement of 3*Z*-hexa-1,3-diene to 2*Z*,4*E*-hexa-2,4-diene.[89]

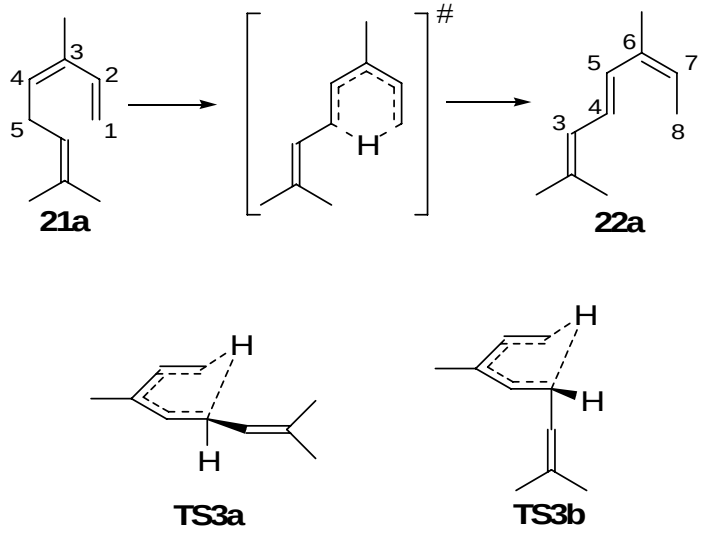

Scheme 4.12. Rearrangement of 3*Z*-ocimene (**21a**) to 4*E*,6*Z*-alloocimene (**22a**) *via* [1,5]H-shift and presumptive transition states (**TS3a** and **TS3b**).[57c]

The formation of **22b** from **22a** can be explained by acid- or base-catalyzed rearrangement of the respective double bond affected by interaction with the reactor walls. This is evident with respect to the kinetic analysis of the temperature-dependent yields of both stereoisomers of **22** reported in figure 4.5. Based on the activation parameters listed in table 4.1 for the rate constants k_{12}, k_{13}, and k_{14} (scheme 4.4) and with respect to eq. 2.7 it is possible to calculate the mole fractions of **22a** and **22b**. Assuming

that a mixture of both isomers is used with a ratio of **22a** to **22b** of 9.0 Eqs. 4.4 and 4.5 allow for the calculation of their concentrations at a desired temperature and residence time, respectively, whereby additional formation of **22b** from **22a** is neglected in this first step of approximation.

$$[\mathbf{22a}]_T = [\mathbf{22a}]_0 \cdot e^{-k_{13;T}\tau} = 0.9 \cdot e^{-k_{13;T}\tau} \qquad (4.4)$$

$$\{[\mathbf{22b}]_T\} = [\mathbf{22b}]_0 \cdot e^{-k_{14;T}\tau} = 0.1 \cdot e^{-k_{14;T}\tau} \qquad (4.5)$$

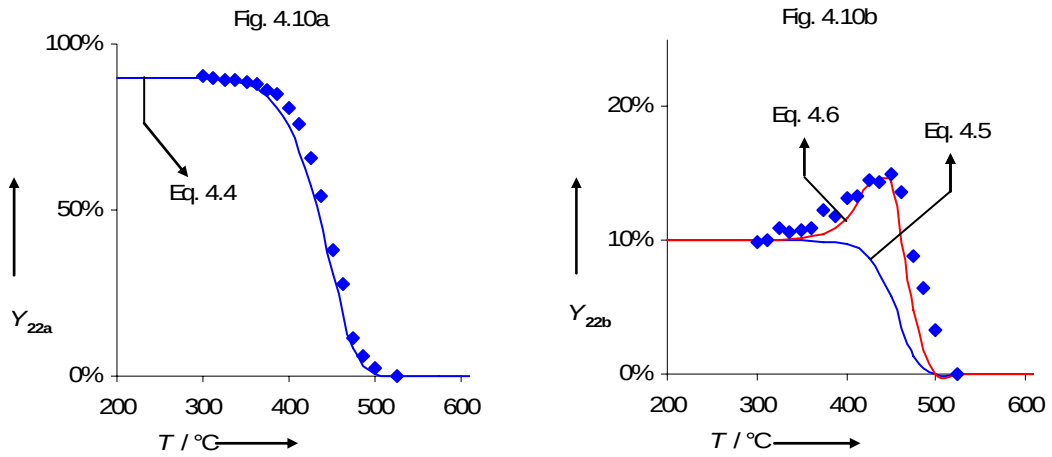

Figure 4.10. Comparison of data for the temperature dependent mole fractions of 4*E*,6*Z*-alloocimene ($Y_{\mathbf{22a}}$; figure 4.10a) and of 4*E*,6*E*-alloocimene ($Y_{\mathbf{22b}}$; figure 4.10b) from experiment (diamonds; *cf.* figure 4.5a) and for data based on kinetic parameters listed in table 4.1.

Figure 4.10a reveals that this simple kinetic is able to describe well the disappearance of the 4*E*,6*Z*-isomer, whereas it is not suitable for the modelling in case of **22b** (figure 4.10b). It is evident that consideration of the side reaction describing the isomerization of **22a** to **22b** (eq. 4.6) allows for an excellent modelling of the temperature-dependent mole fraction of **22b** ($Y_{\mathbf{22b}}$; *cf.* red line in figure 4.10b). Therefore, this *Z*-*E*-isomerization of the two isomers of alloocimene is approved to proceed as a one-directional reaction. Other isomers of **22** with a *Z*-configuration of the carbon-carbon double bond at C(4)-C(5) were not able to be identified in the reaction mixture from explorative pyrolysis of **21a** being in accordance to the proposed mechanism pictured in scheme 4.12. Consecutive reactions of both isomers of **22** yield various monocyclic products which mainly yield from cyclization reactions leading to substituted cyclohexadienes, thus being in agreement with

the reported activation data listed in tables 4.1 and 4.2 for the disappearance of **22** (k_{13}, k_{14}).[90]

$$\begin{aligned}[\mathbf{22b}]_T &= \left[[\mathbf{22b}]_0 + \frac{[\mathbf{22a}]_0 \cdot k_{12;T}}{k_{13;T}} \left(1 - e^{-k_{13;T}\tau}\right) \right] \cdot e^{-k_{14;T}\tau} \\ &= \left[0.1 + \frac{0.9 \cdot k_{12;T}}{k_{13;T}} \left(1 - e^{-k_{13;T}\tau}\right) \right] \cdot e^{-k_{14;T}\tau} \end{aligned} \tag{4.6}$$

With respect to these findings based on kinetic and mechanistic considerations a modified reaction scheme for the thermal network of $C_{10}H_{16}$ hydrocarbons based on the pyrolysis of **9** can be arranged (scheme 4.13). Most important modifications in comparison with previous studies[52,60b,77,78] concern the rearrangement reactions of 3*Z*-ocimene (**21a**). It is evident from the experimental and kinetic data that pyrolysis of **21a** yields exclusively 4*E*,6*Z*-alloocimene (**22a**) which rearranges to form the 4*E*,6*E*-isomer (**22b**). Minor reaction pathway from the initially formed biradical presumably leads to the formation of **21b**.

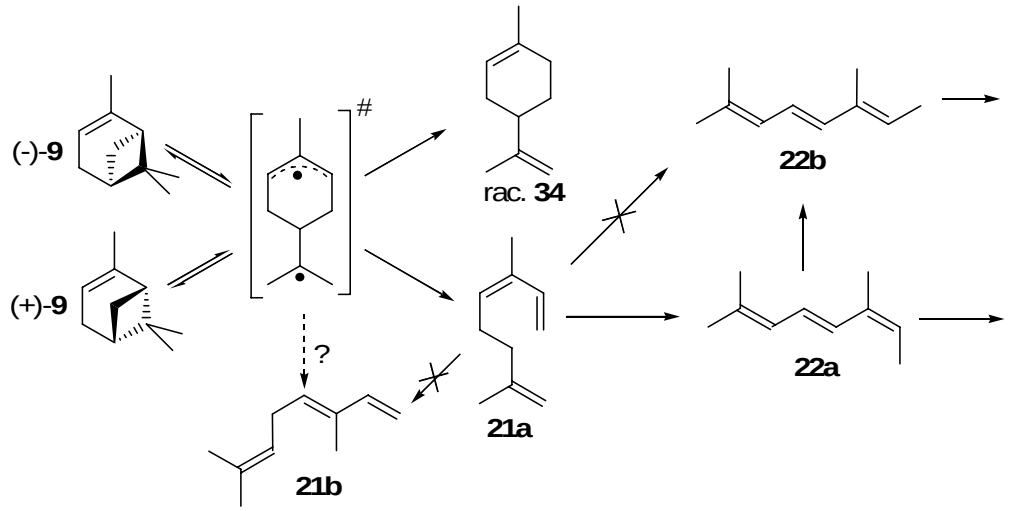

Scheme 4.13. Modified reaction network for the thermal isomerization of α-pinene (**9**).

CHAPTER 5

Pyrolysis of β-Pinene and of Nopinone

β-Pinene and nopinone as well as the main acyclic product from the thermal isomerization of β-pinene (myrcene) were subjected to pyrolysis studies. Experiments were conducted to gain a deeper insight in the reaction mechanisms responsible for the formation of the primary pyrolysis products as well as for their disappearance. Kinetic rearrangement studies reveal that biradical intermediates are the most important transition states the reactions passing through in case of β-pinene and nopinone. Arrhenius and Eyring activation parameters indicate that consecutive reactions leading to the disappearance of myrcene involve a six-membered ring transition state, thus being in agreement with mechanistical considerations. Comparison of the isomerization behavior of β-pinene and nopinone reveal differences concerning thermal stability, product spectra, and transition states reactions running through.

Results presented in this chapter concerning the thermal rearrangements of β-pinene, myrcene, and nopinone are summarized results from three articles published which are given in the appendix of this dissertation.[62,61,91]

5.1 Thermal Behavior of β-Pinene and Myrcene

The reactions within the thermal reaction network of $C_{10}H_{16}$ hydrocarbons yielded from gas-phase pyrolysis of β-pinene (**10**) are interesting from mechanistic as well as from kinetic points of view. For these reasons **10** and the reported main acyclic product from its pyrolysis myrcene (**23**) were subjected to pyrolysis studies investigating their thermal isomerization behavior. On the basis of gas-phase rearrangement experiments using **10** or **23** as substrates with varying temperatures and residence times (eq. 2.6) it was possible to calculate activation parameters according to Arrhenius (2.7) and Eyring equation (2.8). This allows for detailed studying of the transition states the reactions passes through.

Scheme 5.1 pictures the network of $C_{10}H_{16}$ hydrocarbons resulted from gas-phase pyrolysis of both **10** and **23**. The acyclic product **23** was formed as the main rearrangement product and the ratio of limonene (**34**) and ψ-limonene (**41**) was found to be 2.0 in favor of **34**.[45c,46a,48c,60b,61,62d,91,92] Apparently these primary pyrolysis products yield from reactions passing through a biradical transition state (**TS10**)[47,58a,61,62] similar to that one reported for the thermal induced isomerization of α-pinene (**9**; *cf.* chapter 4).[47,51,52,66,77,80] In contrast to the pyrolysis of **9** whereby racemic **34** is formed similar values of enantiomeric excess´ *ee* (eq. 2.1) are found for **10** used as starting material and the primary products **34** and **41**.[47,61,91] This is due to the fact that the intermediate **TS10** is optical active and has no mirror plane reported for the biradical the reaction passes through in case of **9** (*cf.* chapter 4.5).

The mole fractions of the desired products **23**, **34**, and **41**-**43** as well as of non-converted **10** expressed as yields Y_i (eq. 2.2) are pictured in figure 5.1a for a temperature range of 300 to 550 °C. Results are in agreement with those published in previous studies.[45c,46a,58a,60-62,66,92] **23** is the main product and after passing through a maximum at 440 °C its yield (Y_{23}) decreases in favor of the formation of consecutive reaction products **42** and **43**. According to the other acyclic isomerization products of pinane-type compounds (**19**-**22**,**24**) **23** undergoes reactions leading to isomerization[58a,61,62,73] and degradation products.[92] Within the temperature range the experiments were conducted the formation of isomerization products was observed exclusively, whereby several pyrolyses carried out at a pyrolysis temperature higher than 550 °C reveal that

decomposition took place also.[92] In agreement to the cyclizations of **19**, **22**, and **24** which have been thoroughly discussed in chapter 3[63] myrcene (**23**) undergoes ene-cyclization forming the substituted cyclopentane **42**.[61,62,73] A further consecutive reaction of **23** yields 5-ethylidene-1-methylcycloheptene (**43**) *via* [1,5]H-shift accompanied by cyclization.[58a,61]

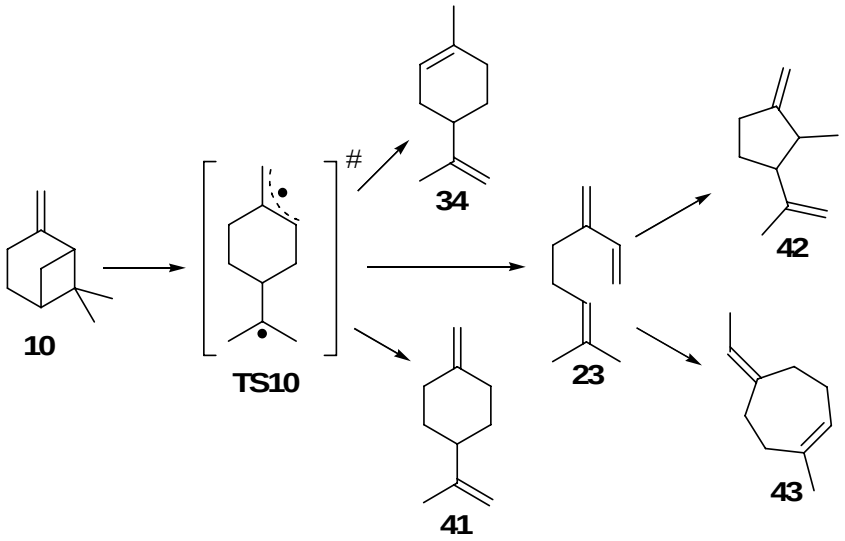

Scheme 5.1. Network of $C_{10}H_{16}$ hydrocarbons resulted form pyrolysis of β-pinene (**10**).

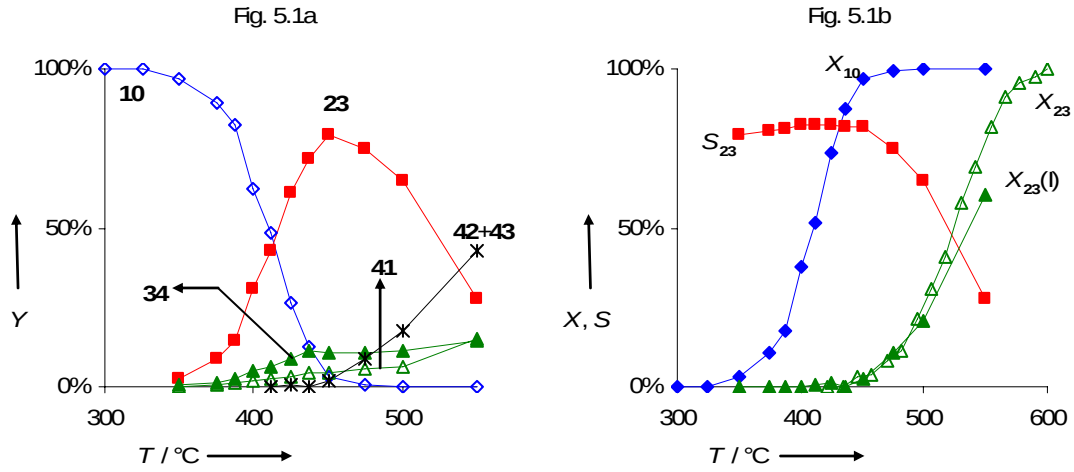

Figure 5.1. Yield Y_i of pyrolysis products depending on reaction temperature T for pyrolysis of β-pinene (**10**; figure 5.1a). Selectivity for myrcene formation (S_{23}) and conversions of **10** and **23** (X_i) in dependency of T for pyrolysis of **10** and **23** (X_{23}(I); figure 5.1b; 15 µL starting material, carrier gas: N_2, flow rate: 1.0 L min^{-1}, τ: 0.47-0.71 s).

Figure 5.1b pictures the conversion of **10** (X_{10}; eq. 2.3) and the selectivity for the formation of **23** (S_{23}; eq. 2.4) depending on the reaction temperature T, whereby

consecutive reactions of **23** yielding products **42** and **43** were not considered calculating the selectivity. Diagram indicated that the myrcene formation is independently from the conversion of **10** as S_{23} remains constant until complete conversion is reached (T: 440 °C). Interestingly, this point is equal to the maximum for the yield of **23**. This is due to the connection between the three parameters: yield, selectivity, and conversion expressed in eq. 2.5. Considering the conversion of **23** (X_{23}) pyrolysis experiments of **9** and **23** are quite comparable (*cf.* figure 5.1b), hence the differences between the two values at similar reaction temperatures are negligible.

5.2 Kinetic Analysis the Pyrolysis Reaction of β-Pinene and Myrcene

β-Pinene **10** and the major pyrolysis product myrcene **23** were subjected to kinetic pyrolysis experiments in order to investigate the thermal isomerization reactions from kinetic point of view. The model of competitive parallel first-order reactions was used for description of the formation of **10**, **34**, and **41** (scheme 5.2), whereby the respective rate constants k_{17}, k_{18}, and k_{19} were calculated on the basis of pyrolysis experiments at different residence times and constant reaction temperature. The disappearance of **10** was expressed by rate constant k_{16} being the sum of $k_{17\text{-}19}$.[91] Consecutive reactions of **23** leading to products **42** and **43** (scheme 5.1) were summarized to rate constant k_{20}.

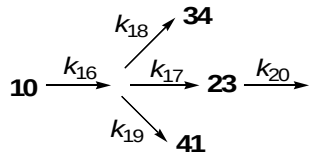

Scheme 5.2. Reaction Scheme for the pyrolysis of β-pinene (**10**) used for calculation of the rate constants and the activation parameters.

Kinetic pyrolysis experiments at different temperatures allowed for the calculation of Arrhenius and Eyring activation parameters using eqs. 2.7 and 2.8, respectively. Corresponding activation parameters for the most important kinetic reaction steps (scheme 5.2) are listed in table 5.1.[91] Positive values for activation entropy $\Delta^{\ddagger}S$ and $\log_{10}A$-values of 13.5 to 14.5 for k_{15} and k_{16} indicate that the disappearance of **10** and the formation of **23**, respectively, proceed *via* "loose" biradical transition states,[91] thus being in agreement with the assumptions made before and published in literature.[47,61,62,66,92]

Negative activation entropies are typical for “tight” t.s. characterized by a lower number of torsional or rotational degrees of movement compared to the starting material. Since the formation of **34** and **41** is assumed to proceed as [1,n]H-shift with a rigid cyclic reaction intermediate the findings are in agreement with mechanistical considerations.[61] Main reaction pathways responsible for disappearance of **23** are reactions similar to those ones reported for the thermal isomerization of **19**, **20**, and **24** (*cf.* chapter 3) thus passing through a tight six-membered ring transition state and therefore being in accordance to experimental findings.

Table 5.1. Kinetic data[a] for the gas-phase isomerization of β-pinene (**10**) and myrcene (**23**).

	E_a (kJ mol^{-1})	$\log_{10}A$ (s^{-1})	$\Delta^{\ddagger}H$ (kJ mol^{-1})	$\Delta^{\ddagger}S$ (J K^{-1} mol^{-1})
k_{16}	180.8 ± 6.4	13.94 ± 0.48	175.2 ± 6.4	6.8 ± 0.3
k_{17}	182.7 ± 6.2	14.00 ± 0.48	177.1 ± 6.2	8.1 ± 0.4
k_{18}	168.5 ± 6.6	12.09 ± 0.52	162.9 ± 6.7	-28.6 ± 1.7
k_{19}	180.7 ± 10.4	12.58 ± 0.81	175.1 ± 10.5	-19.2 ± 1.7
k_{20}	167.6 ± 6.8	11.26 ± 0.47	161.5 ± 7.0	-45.1 ± 2.7

[a] Error limits are 95% certainty limits.

5.3 Synthesis of Nopinone

Nopinone (**12**) used for the pyrolysis experiments presented in this study was synthesized by mechanochemically assisted oxidation of β-pinene (**10**) using potassium permanganate as oxidizing agent and alumina as solid additive for reasons of dilution (scheme 5.3). Reactions were performed in grinding beakers made of agate using agate grinding balls in a planetary ball mill. Reaction times of 20 min yielded **12** exclusively with overall yields of 95% (GC-analysis). Reaction mixtures were subsequently extracted with dichloromethane and after column chromatography of the crude products **12** with a purity > 98% was able to be isolated with a yield of 70% based on **10**.

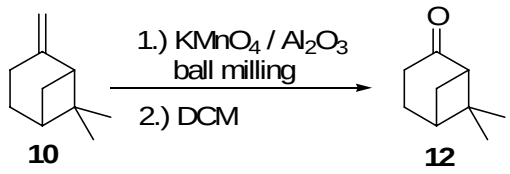

Scheme 5.3. Synthesis of nopinone (**12**) from β-pinene (**10**).

This novel reaction procedure is advantageous compared to classical oxidation methods due to short reaction times and simple work-up procedure. Additionally no further catalyst or dangerous oxidizing agents (O_3, H_2O_2) are needed. Another benefit is the high selectivity for the formation of **12** even at high degrees of conversion for **10**.

5.4 Pyrolysis of Nopinone and its Kinetic Analysis

Pyrolysis of **12** is interesting for the investigation of the influence of a hetero atom on the product spectrum and the thermal behavior compared to the corresponding hydrocarbon **10**. For this reason **12** was subjected to pyrolysis experiments allowing for the identification of the major reaction products pictured in scheme 5.4, thus revealing that the product spectrum is quite similar to that one found for **10** (scheme 5.1). Beside the primarily formed monocyclic product **34** yielded from thermal isomerization of **10** all corresponding products were found in case of **12**.[50g,58b,62] Hence, product **34** would correspond to the enol **47** (scheme 5.4) it can be concluded that this product is thermally not stable and rearranges to form ketone **45**. On the other hand conclusion is permissible that the respective hetero-allyl radical in the presumptive intermediate **TS12** is not delocalized and the mesomeric formula **TS12a** is favored (scheme 5.4). This is the first obvious difference in the pyrolysis behavior of **12** compared to **10**.

In agreement to the formation of two acyclic isomerization products in case of pyrolysis of *cis*-pinane (**3a**)[49e,63,64] Coxon, Garland and Hartshorn found ketone **48** (< 5%) within their pyrolysis studies of **12**.[50g] Performing gas-phase pyrolysis studies with the herein described reactor and experimental conditions **48** was not able to be identified. The formation of 3-isopropenyl-2-methylcyclopenatnones (**46**) as consecutive reaction products of acyclic ketone **44** was confirmed.[50g,58b,62]

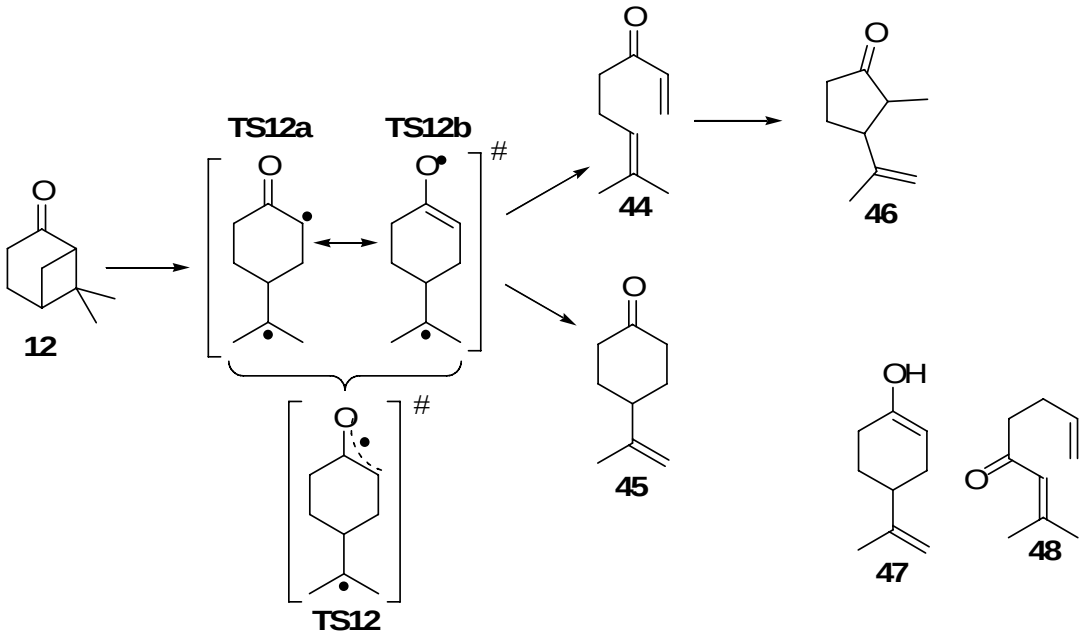

Scheme 5.4. Thermal reaction network for the pyrolysis of nopinone (**12**).

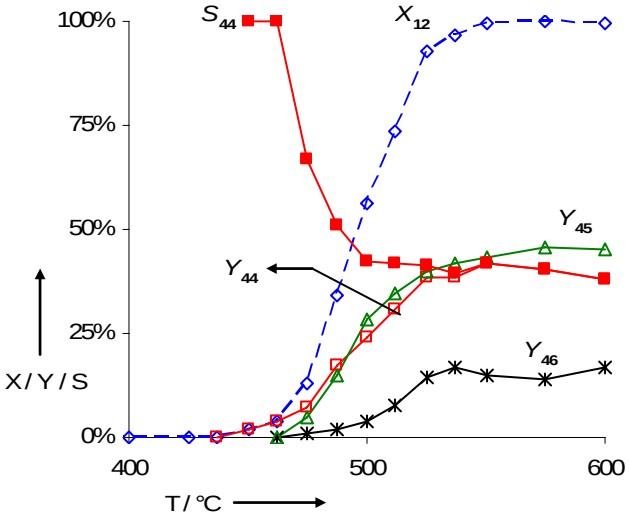

Fig. 5.2. Conversion of nopinone (**12**), selectivity for ketone **44** ($S_{cp;44}$) and yields of products **44-46** (Y_i) depending on reaction temperature (T; 15 µL starting material, carrier gas: N_2, flow rate: 1.0 L min^{-1}, τ: 0.47-0.61 s).

Figure 5.2 pictures the temperature dependency of various values important for the overall description of the pyrolysis reaction of **12** in a temperature range from of 400 - 600 °C. According to the pyrolysis of **10** (figure 5.1b) the ratio of acyclic product **44** and monocyclic ketone **45** is apparently independent from reaction temperature and also from degree of conversion of **12** (X_{12}; figure 5.2). Contrarily to the thermal isomerization of **10**

consecutive reactions of **44** leading to consecutive products **46** do not influence the yield and therefore the selectivity of **44** (Y_{44}) at temperatures higher than 500 °C. Thus it can be concluded that the introduction of an oxygen atom next to one of the bridge-head carbon atoms enhance the thermal stability of the substrate and lower the yield of acyclic rearrangement products.

Subjecting **12** to pyrolysis studies in order to estimate various rate constants allows for the calculation of both Arrhenius and Eyring activation parameters according to eqs. 2.7 and 2.8, respectively. A simple model of two parallel first order reactions was used for calculation of the rate constants for the formation of primary pyrolysis products **44** (k_{22}) and **45** (k_{23}). Consecutive reactions leading to cyclization products **46** were neglected and the respective yields were added to the concentration of **44** used for calculation of k_{22}. Similar to the disappearance of **10** the rate constant for the disappearance of starting material **12** (k_{21}) is the sum of k_{22} and k_{23}. Exemplarily for k_{21} the Arrhenius plot is depicted in figure 5.3. The corresponding activation parameters for the desired rate constants are listed in table 5.2.

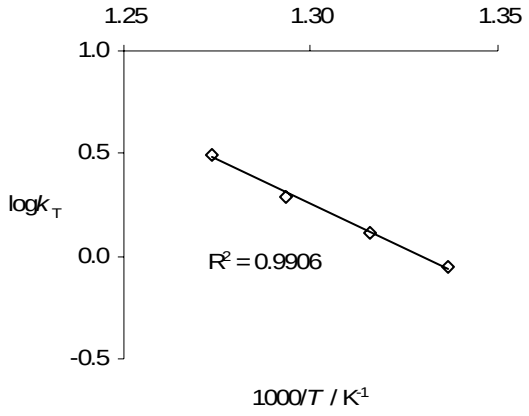

Figure 5.3. Arrhenius plot of log *k vs.* 1000/*T* for the thermal isomerization of nopinone (**12**, k_{21}).

The activation parameters for the desired rate constants describing the disappearance of **12** and the formation of ketones **44** and **46** are listed in table 5.2. Interestingly the values for the activation entropies $\Delta^{\ddagger}S$ are negative for all reactions kinetically being investigated. This would indicate that the reactions pass through “tight” transition states and therefore other reaction intermediates than biradicals **TS12a** and **TS12b** (scheme 5.4) have to be considered. Unfortunately, no further kinetic data concerning the gas- or

liquid-phase thermal rearrangement of **12** have been published yet. Comparison to photochemical isomerization studies are not possible due to the fact that other products are formed.[93] Since those activation parameters are typical for rigid transition state,[69] the only explanation is an interaction of the carbonyl group with one of the methyl-groups at C(6) pictured in scheme 5.5. This would allow the explanation of two other phenomena found within the pyrolysis studies of **12**. Due to the preferred formation of **TS12a** the mesomeric rearrangement leading to **TS12b** is suppressed and therefore the minor reaction products **47** and **48** (scheme 5.4) are not formed. On the other hand a stabilization of the TS the reaction passes through can be responsible for the low activation energies E_a listed in Tab. 5.2. Therefore, the conclusion can be drawn that the pyrolysis of **12** passes through a biradical transition state with rigid structure, due to interaction of the carbonyl-group with one of the two neighbored methyl-groups.

Table 5.2. Kinetic data[a] for the gas-phase isomerization of nopinone (**12**).

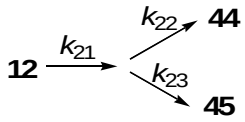

	E_a (kJ mol^{-1})	$\log_{10}A$ (s^{-1})	$\Delta^{\ddagger}H$ (kJ mol^{-1})	$\Delta^{\ddagger}S$ (J K^{-1} mol^{-1})
k_{21}	166.3 ± 7.3	11.54 ± 0.50	159.9 ± 7.3	-40.1 ± 2.4
k_{22}	169.6 ± 16.3	11.54 ± 1.11	163.2 ± 16.2	-40.2 ± 5.4
k_{23}	160.9 ± 9.7	10.80 ± 0.66	154.6 ± 9.7	-54.4 ± 4.8

[a] Error limits are 95% certainty limits.

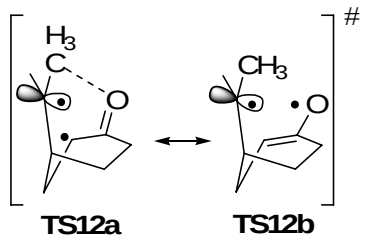

Scheme 5.5. Presumptive transition states for the thermal isomerization of nopinone (**12**).

CHAPTER 6

Comparison of the Results [†]

In this chapter the results from pyrolysis experiments as well as the calculated kinetic data of the thermal gas-phase isomerization reactions of *cis*-pinane, *trans*-pinane, *cis*-2-pinanol, α-pinene, β-pinene and nopinone are compared with each other. Analysis of the conversions reveal that the different substituents in α-position to the carbon bridge-head atoms tremendously influence the reactivity, revealing that an endocyclic carbon-carbon double bond in α-position (α-pinene) is the most effective substituent. A *trans*-methyl substituent next to the bridge-head (*trans*-pinane) leads to the substrate with the highest thermal stability.

Besides the reactivity the different substituents influence the types of pyrolysis products that are formed and its selectivity also. Whereas compounds with sp^2-carbon atoms next to the bridge-head atom of the respective pinane derivative (α-pinene, β-pinene, nopinone) yield at least one primary acyclic rearrangement product this route is suppressed in case of saturated compounds (pinane, 2-pinanol).

Based on these findings for monofunctional pinane-type compounds an attempt was made to predict the rearrangement products yield from the thermal isomerization of bifunctional monoterpenoids. Reconsideration of pyrolysis studies with verbenone and verbanone showed that this is possible.

[†] Some of the results presented within this chapter have already been published in ref. [62] which is given in the appendix of this dissertation.

6.1 Reactivity of the Compounds Investigated

Six different types of pinane-type compounds listed in scheme 6.1 have been subjected to pyrolysis studies all having in common that their thermal isomerization yields at least one acyclic main product, whereby its selectivity depends on the substituents(s) in α-position to the bridgehead-carbon atom. Experiments reveal that starting materials **3** and **9**-**12** do not differ in the product spectra only, but reactivity was significantly different also allowing for the conclusion that the nature of functionalization at C(2) influences the thermal behavior with respect to three points of issue: (a) reactivity of the substrates, (b) product spectra, and (c) selectivity for the formation of the acyclic main product.

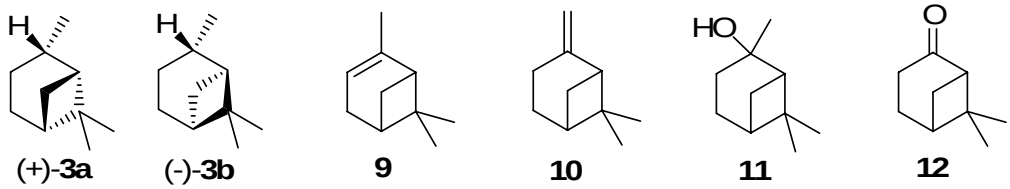

Scheme 6.1. Compounds whose thermal isomerization behavior has been investigated.

The main issue of this study was therefore studying the thermal behavior of the pinane-type compounds selected under identical experimental conditions. In contrast to previous studies in the field of pyrolysis of monoterpenes or monoterpenoids thermal rearrangement experiments were conducted in the gas-phase using N_2 as carrier gas and diluting agent suppressing undesirable side reactions like for instance polymerization. Minimization of costs for pyrolysis apparatus, easy handling, simple work-up procedures, controllable and highly reproducible pyrolysis conditions are only some advantages of carrier-gas supported thermolysis processes compared to FVP- or VLPP-techniques.[25] Another benefit is the close relationship of the experimental conditions to industrial pyrolysis processes being carried out in gas-phase at atmospheric pressures and high flow-rates. Hence, the carrier gas was used with a high molar extend compared to the substrate (3.000 at 550 °C) it allows for variation and regulation of the average residence time (eq. 2.6) by simple regulation of the carrier-gas flow-rate offering the opportunity for performing kinetic experiments under similar experimental conditions.

Due to the comparable experimental conditions and the absence of decomposition reactions in the temperature range investigated (250-600 °C) the reactivity of starting materials **3** and **9-12** are able to be compared directly without the need of any corrections. The conversion X for a desired reaction temperature is the ideal parameter for comparing reactivities of different compounds but it has to be pointed out that this is permitted only if comparable or similar conditions were chosen for the experiments. In figure 6.1 the conversions X_i (eq. 2.3) for the substrates pictured in scheme 6.1 as function of pyrolysis temperature T [$X = f(T)$] are shown indicating significant differences in their reactivity concerning their conversion within the pyrolysis studies. Obviously, α-pinene (**9**) is the most reactive compound followed by β-pinene (**10**) and the most inactive substance is *trans*-pinane (**3b**). The differences in $X = f(T)$ between the three other compounds *cis*-pinane (**3a**), *cis*-2-pinanol (**11**), and nopinone (**12**) are negligible. With respect to these observations the following order of reactivity can be seen to be: **9** > **10** >> **3a** = **11** = **12** > **3b**. With respect to the data shown in figure 6.1 for the bicyclic starting materials **3** and **9-12** table 6.1 lists those reaction temperatures whereby a conversion of 25, 50, and 75% is reached. The data are sorted according to the structural characteristics of the substituents next to the bridge-head carbon atom, starting with **9** showing the lowest temperatures needed for the respective conversions.

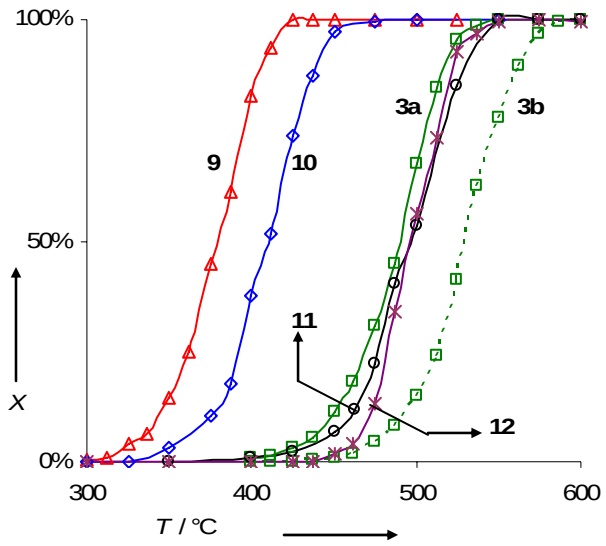

Figure 6.1. Conversion X *vs.* reaction temperature T for *cis*-pinane (**3a**), *trans*-pinane (**3b**), α-pinene (**9**), β-pinene (**10**), *cis*-2-pinanol (**11**), and nopinone (**12**).

Table 6.1. Respective temperature at which a conversion of 25, 50 or 75% is reached for the compounds shown in scheme 6.1 (*cf.* figure 6.1).

		Temperature (°C) at conversion of		
	Functional group at C(2)	25%	50%	75%
9	endocyclic C-C-double bond	362	380	395
10	exocyclic C-C-double bond	395	410	425
(+)-**3a**	*cis*-methyl group	470	490	505
11	*cis*-methyl group + *trans*-OH	475	495	515
12	carbonyl group	485	495	515
(-)-**3b**	*trans*-methyl group	515	530	535

Hence, the only difference between these compounds are the different substituents in α-position to the bridge-head carbon atom it is evident from the pyrolysis experiments that those directly influence the reactivity. Apparently, carbon-carbon double bonds are very effective for the selective ring-opening of the cyclobutane ring due to the fact that one of the radical position is resonance stabilized as an allyl type radical.[47,51,52,61,62,66,77] The higher ring tension energy in case of **9** compared to **10** due to the endocyclic in stead of an exocyclic double bond, respectively, is the reason for the higher reactivity of **9**. The difference in $X = f(T)$ for both isomeric pinanes (**3a** and **3b**) is surprising because they differ in relative orientation of the α-methyl group towards the cyclobutane ring only (table 6.1). Apparently, the *cis*-configuration is more suitable for a fragmentation of the cyclobutane ring than the *trans*-isomer. Again this is believed to be due to stereochemical effects. Since the ground-state geometry for **3a** is a "Y"-confirmation with a planar C_3-bridge the respective *trans*-isomer (**3b**) is characterized by the more stable chair-type confirmation with a bend down C_3-bridge.[63,64,68] As evident from pyrolysis experiments summarized in figure 6.1 the introduction of an hydroxyl group additional to the *cis*-methyl group in **3a** leading to **11** seems to have no further influence on the reactivity of the substrates. Therefore, the relative order of effectiveness of substituents in α-position to the bridge-head carbon atom in influencing the thermal defragmentation of the cyclobutane ring can be seen to be:

endocyclic double bond > exocyclic double bond >> *cis*-methyl group = carbonyl group > *trans*-methyl group.

Another indicator for the reactivity of any chemical compound are the Arrhenius activation parameters (E_a and $\log_{10}A$; eq. 2.7) able to be calculated from the temperature dependency of the rate constant k describing the disappearance of the respective compound. Comparison of the activation energies E_a and of the frequency factors $\log_{10}A$ listed in table 6.2 for the respective rate constants reflects the order of reactivity and the $X = f(T)$-functions for the respective compounds pictured in figure 6.1. The activation energy for k_8 describing the disappearance of **9** has the lowest value followed by the rate constant for the lost of **10** (k_{16}). Except for k_{21} (pyrolysis of **12**) all other energies of activation are in the same order of magnitude, expressing the similar reactivity of **3a** and **11**. Since that for the pyrolysis of **3b** the highest amount of activation energy was found its high thermal stability is confirmed. Low activation parameters for the thermal rearrangement of **12** is believed to be due to the interaction of the carbonyl-group with the biradical formed initially. Since, the initial reactions for all substrates require the rupture of a carbon-carbon single-bond being part of a cyclobutane system the bond-dissociation energies are the same. Differences in activation energies listed in table 6.2 are due to the concurrence of bond-dissociation energies, ring-tension energies, and stabilization energies of the resulting biradical.

Table 6.2. Kinetic data[a] for the disappearance of *cis*-pinane (**3a**), *trans*-pinane (**3b**), α-pinene (**9**), β-pinene (**10**), *cis*-2-pinanol (**11**), and of nopinone (**12**) during their gas-phase isomerization.

		E_a (kJ mol^{-1})	$\log_{10}A$ (s^{-1})	$\Delta^{\ddagger}H$ (kJ mol^{-1})	$\Delta^{\ddagger}S$ (J K^{-1} mol^{-1})
(+)-**3a**	$k_{1(3a)}$	201.1 ± 9.1	13.96 ± 0.63	194.8 ± 9.0	6.3 ± 0.4
(-)-**3b**	$k_{1(3b)}$	213.0 ± 6.9	13.94 ± 0.45	206.3 ± 6.9	6.2 ± 0.3
9	k_8	170.0 ± 1.7	13.70 ± 0.14	165.2 ± 1.6	3.0 ± 0.04
10	k_{16}	180.8 ± 6.4	13.94 ± 0.48	175.2 ± 6.4	6.8 ± 0.3
11	k_6	209.9 ± 6.7	14.70 ± 0.26	203.8 ± 3.7	20.6 ± 0.5
12	k_{21}	166.3 ± 7.3	11.54 ± 0.50	159.9 ± 7.3	-40.1 ± 2.4

[a] Error limits are 95% certainty limits.

Eyring activation parameters (eq. 2.8) listed in table 6.2 indicate that all reactions initially passing through a “normal” transition state being typical for the fragmentations of four-membered ring systems (cyclobutane, oxetane).[69,74b-e,,84,94] Hence a concerted mechanism involving a 4π antiaromatic transition state is thermally forbidden according

to the Woodward-Hoffmann rules,[11] those reactions have to proceed *via* a stepwise fragmentation mechanism including a biradical intermediate.

6.2 Product Selectivity of the Compounds Investigated

It is evident from the pyrolysis studies performed with the compounds listed in scheme 6.1 that different substituents lead to the formation of different products. As indicated by the activation entropies $\Delta S^{\#}$ listed in table. 6.2 the initial reactions proceed as stepwise fragmentation of the respective cyclobutane ring leading to biradical intermediates. As shown in scheme 6.2 degenerative pyrolysis of an unsymmetrically substituted cyclobutane offers two different fragmentation routes. Depending on the bonds primarily been broken two different biradicals **TSA** and **TSB** are formed each of them having two options to form stable products. In case of subsequent carbon-carbon bond rupture acyclic products are formed, whereas [1,n]H-shift reactions yield cyclohexanes with an isoprop(en)yl-group. Exemplarily scheme 6.2 pictures the products from [1,5]H-shift only. The ratio of theses different reaction pathways are strongly influenced by the substituents in α-position to C(1).

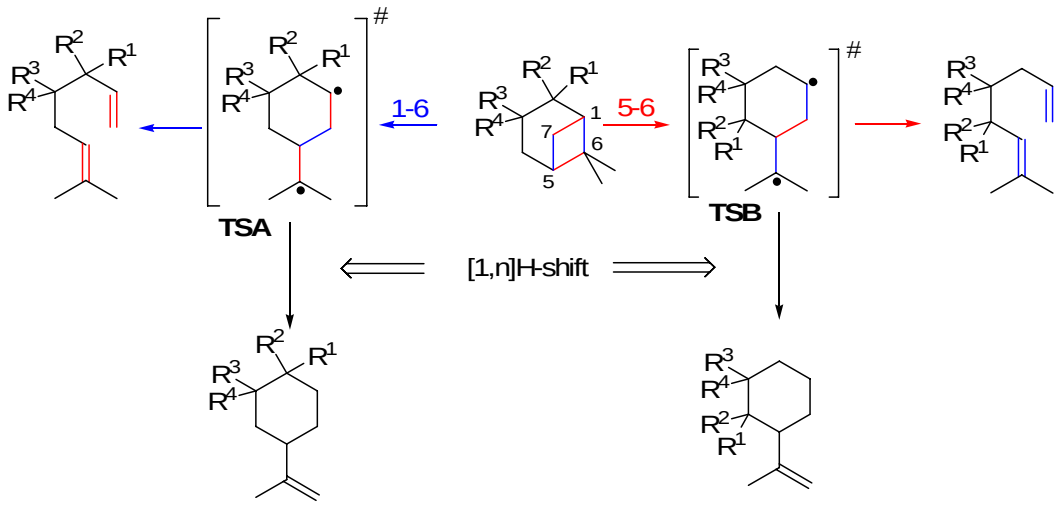

Scheme 6.2. General reaction scheme for the thermally induced rearrangement of pinane-type compounds (colors of the reaction arrows correspond to the bonds in the bicyclus that had to be cut forming the respective biradical **TSA** or **TSB**).

Generally, the compounds listed in scheme 6.1 can be divided into two main groups: (a) starting materials which yield only one type of acyclic products and (b) pinane-type

compounds leading to the formation of both acyclic products. Substances can be classified according to the formation of primarily formed monocyclic reaction products. Table 6.3 summarizes these results revealing that except for **9** and **10** acyclic products from both possible reaction intermediates have been found in the mixtures of reaction products. In case of the pyrolysis of **12** the respective open-chained product resulted from biradical **TSB** was not found in this study but a previous study indicates its formation in amounts lower than 5%.[50g] Therefore it has to be concluded that the presence of a carbon-carbon double bond in α-position of C(2) (**9**,**10**) prefers the route allowing for resonance stabilization of one radical position (allyl radical). If the substituents offer no possibility for mesomeric delocalization (**3**,**11**) or if the delocalization is not as distinct as in the case of an hetero-allyl radical (**12**) both routes are possible. This behavior is in agreement with studies dealing with the thermal decomposition of substituted cyclobutanes.[69,74b-e,84] Whereas the pyrolysis of vinyl-substituted cyclobutanes yield only one set of fragmentation products[74e] two sets of products are found for the thermolysis of four-membered rings that have no sp^2-carbon atoms attached to the ring.[74b-e,84] Additionally to the differentiation between the two possible routes, table 6.2 also indicates that a sp^2-carbon next to the bridge-head carbon atom leads to the formation of monocyclic primary pyrolysis products also. Therefore the gas-phase thermal isomerization reactions of **3** and **11** primarily yield acyclic products almost exclusively. The minor formation of *p*-menthenes in case of **3** can be attributed to undesirable side-reactions with the reactor walls.

Table 6.3. Products formed initially from pyrolysis of pinane-type compounds investigated (routes according to scheme 6.2).

	Route "1-6"		Route "5-6"	
	acyclic	monocyclic	acyclic	monocyclic
(+)-**3a**	yes	<5%	yes	no
(-)-**3b**	yes	<5%	yes	no
9	yes	yes	no	no
10	yes	yes	no	no
11	yes	no	yes	no
12	yes	yes	no (5%[50g])	no

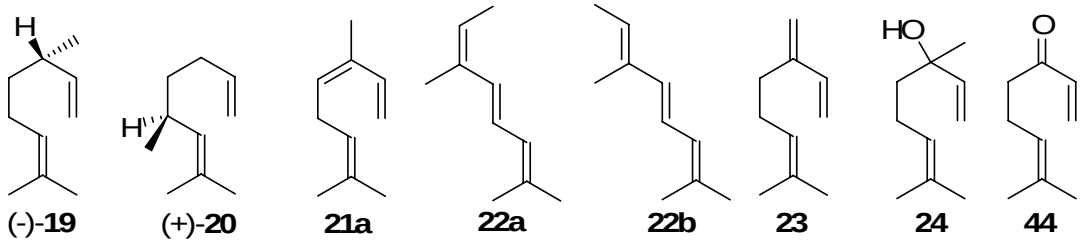

Scheme 6.3. Acyclic main rearrangement products of those pinane-type compounds pictured in Scheme 6.1 whose isomerization behavior has been studied.

In scheme 6.3 the acyclic main products are depicted which yield from the thermal gas-phase isomerizations of the pinane-type compounds investigated within this study. β-Citronellene (**19**) and isocitronellene (**20**) are the main products from pyrolysis of both **3a** and **3b**.[49e,55,63,64] The thermal rearrangement of **9** primarily yields 3*Z*-ocimene (**21a**)[51,52,62,66,77,80] which rapidly undergoes [1,5]H-shift forming 4*E*,6*Z*-alloocimene (**22a**).[57c] The formation of 4*E*,6*E*-alloocimene (**22b**) is due to an undesirable side reaction of **22a** with the reactor walls. It was evident from the pyrolysis studies that **22b** yields exclusively from **22a** and not from pyrolysis of **9** or **21a**. Thermal rearrangements of **10**, **11**, and **12** lead to the formation of myrcene (**23**),[47,58a,61,62,66,91,92] linalool (**24**),[53,72,74a] and ketone **44**,[50g,58b,62] respectively. According to the reactivity of the pinane-type compounds (figure 6.1) and the product spectra (table 6.3) the selectivity for the formation of the acyclic main products depend on the substituents being present. Figure 6.2 presents a diagram plotting the selectivity $S_{cp;i}$ (eq. 2.5) for the formation of the products **19**-**21**, **23**, and **44** against reaction temperature T revealing significant differences. The selectivity for the formation of **23** is not shown due to the fact that pyrolysis of **11** yields **23** almost exclusively ($S_{cp;\mathbf{23}}$: > 95%) without any changes while variation of the pyrolysis temperature. Figure 6.2 indicates that the formation of **23** and **19** ($S_{cp;i}$: ca. 85%) is the preferred reaction if **10** and **3a** are thermally treated in gas-phase under flow conditions using N_2 as carrier gas. Contrarily to **3a** the pathways leading to the formation of **19** and **20** from pyrolysis of the *trans*-isomer **3b** are *pari passu*. After reaching equilibrium conditions the selectivities for the formation of **21** and **44** ($S_{cp;\mathbf{21}}$ and $S_{cp;\mathbf{44}}$) remain constant at a level of approximately 50%. With respect to these results the relative order of effectiveness of substituents influencing the formation of the acyclic pyrolysis products can be seen to be:

exocyclic double bond (10) = *cis*-methyl (19 from 3a, 11) > exocyclic double bond (9) = *trans*-methyl (19 from 3b) = carbonyl (12).

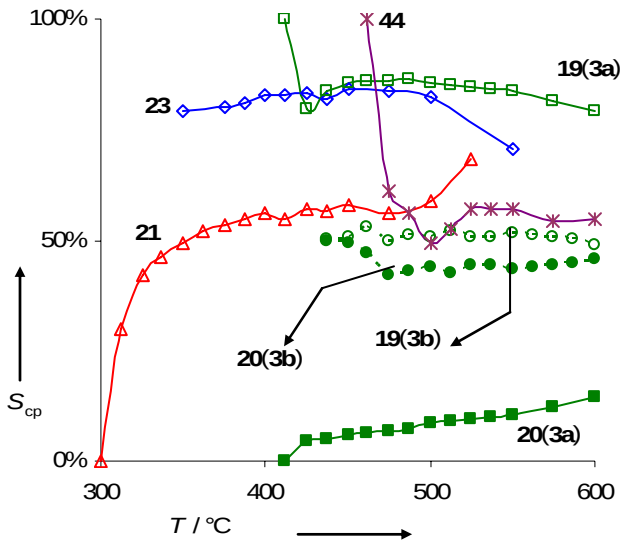

Figure 6.2. Selectivity for the formation of the acyclic main products $S_{cp;}$ (eq. 2.5) *vs.* reaction temperature T for β-citronellene [**19**; from *cis*- (**3a**) or *trans*-pinane (**3a**)], isocitronellene (**20**; from **3a** or **3b**), ocimene (**21**; from α-pinene), myrcene (**23**; from β-pinene), and 7-methyl-1,6-octadien-3-one (**44**; from nopinone).

6.3 Reactivity of the Acyclic Main Products

Due to the fact that the defragmentation of the cyclobutane ring in every pinane type compound leads to acyclic products with at least two carbon-carbon double bonds the resulting octa-1,6-dienes are reactive molecules able to undergo various reactions forming consecutive products. Those reactions are responsible for their disappearance if the pyrolysis experiments were carried out at higher temperatures or longer residence times. Investigating this behavior the acyclic products **19**-**24** pictured in scheme 6.3 were subjected to pyrolysis studies. In figure 6.3 the conversions X_i of the desired starting materials are plotted against the reaction temperature T, indicating that the compounds can be classified into three groups. The 3*Z*-isomer of ocimene (**21a**) is the most reactive followed by the two isomers of alloocimene (**22**; *cf.* scheme 6.3) and the remaining four 1,6-octadienes **19**, **20**, **23**, and **24** are the thermally most stable compounds, compared to the other two educts. Apparently, the reactivity of those four compounds does not differ from each other significantly allowing for the conclusion that the reaction pathways

responsible for their disappearance are quite similar but different from those reactions leading to the conversions in case of **21** and **22**.

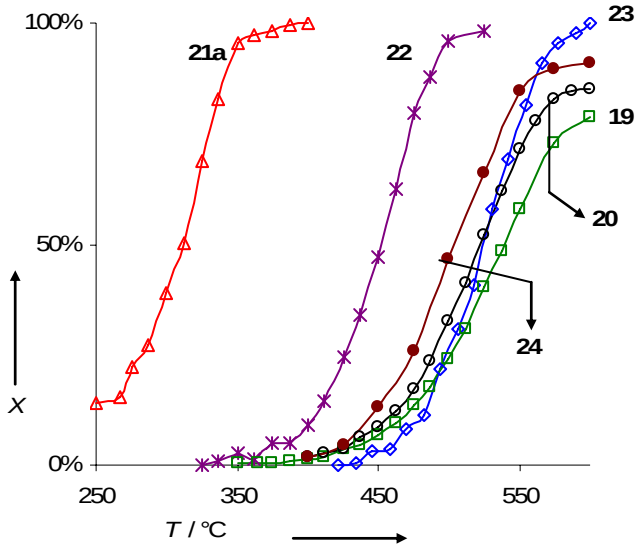

Figure 6.3. Conversion *X* of acyclic main products *vs.* reaction temperature *T* for β-citronellene (**19**), isocitronellene (**20**), 3*Z*-ocimene (**21a**), alloocimene (**22**), myrcene (**23**), and linalool (**24**).

One reason for the observed differences in the temperature-dependent conversions of the acyclic monoterpenes and –terpenoids subjected to pyrolysis studies shown in figure 6.3 are the reaction mechanisms leading to different types of products. Table 6.4 lists the nature of reaction products formed while the desired substrate is pyrolyzed and in addition the presumed type of reaction is given. It is conspicuous that those compounds that are thermally more stable form different types of substituted cyclopentanes *via* ene-type cyclizations,[46a,49e,58b,50g,62-65,66,73,74a] whereas acyclic **22a** is formed *via* [1,5]H-shift reaction, if **21a** is thermally converted.[57c] The thermal rearrangement of **22** leads to the formation of cyclohexadienes (pyronenes), which are assumed to yield from various sigmatropic shift reactions.[52,76,90] The high reactivity of **21a** compared to all other compounds is attributed to the fact that the resulted product (**22a**) is a fully conjugated triene with no external carbon-carbon double bond. Therefore, its formation is preferred from thermodynamical point of view.

Table 6.4. Types of reaction the acyclic substrates **19**-**24** and **44** undergo.

	Nature of reaction products	Type of reaction
19	cyclopentane (**25**)	ene-cyclization
20	cyclopentane (**26**)	ene-cyclization
21a	acyclic (**22a**)	[1,5]H-shift
22	cyclohexadienes (pyronenes)	sigmatropic shifts
23	cyclopentane (**42**)	ene-cyclization
	cycloheptane (**43**)	[1,5]H-shift
24	cyclopentane (**31**)	ene-cyclization
30	acyclic (**32**) *via* cyclopentane (**33**)	ene-reaction / ene-cyclization
44	cyclopentane (**46**)	ene-cyclization

The formation of cyclopentanes in case of compounds **19**, **20**, **23**, and **24** as well as from alcohol **30** and ketone **44** which were not subjected to pyrolysis studies are typical for the gas-phase isomerization of 1,6-octadienes.[50e,g,f,54a,c,58b,62,65,73,76,95-97] In contrast to 1,6-heptadienes which are not able to undergo ene-cyclization reactions due to the lack of an α-hydrogen atom at C(8) the cyclization route is the predominant reaction in case of 1,6-octadienes. Thermolysis of similar 1,6-heptadienes yield fragmentation products exclusively.[98] The only condition for those cyclizations that has to be fulfilled is the absence of an internal carbon-carbon double bond in conjugation to one of the others in 1- or 6-position (*e.g.* **21a**).

Kinetic pyrolysis studies with acyclic starting materials **19**-**24** allowed for the calculation of activation parameters listed in table 6.5. Except for the conversion of **22b** (k_{14}) the activation entropies $\Delta^{\ddagger}S$ are negative and the frequency factors $\log_{10}A$ are smaller than 12.0. Hence, those values indicate a “tight” transition state being characteristically for reactions passing through six-membered ring transition state,[69] the assumption is confirmed that the reactions responsible for the disappearance are ene-cyclizations (**19**,**20**,**23**,**24**) or in case of **21a** [1,5]H-shift reactions. The “loose” transition states for the conversion of **22b** indicated by a positive activation entropy and a logarithmic Arrhenius factor higher than 15.0 is typical for biradical intermediates. Thus conclusion can be drawn that this reaction involves biradical intermediates.

Table 6.5. Kinetic data[a] for the disappearance of β-citronellene (**19**), isocitronellene (**20**), 3*Z*-ocimene (**21a**), 4*E*,6*Z*-alloocimene (**22a**), 4*E*,6*E*-alloocimene (**22b**), myrcene (**23**), and linalool (**24**) during their gas-phase isomerization.

		E_a (kJ mol^{-1})	$\log_{10}A$ (s^{-1})	$\Delta^{\ddagger}H$ (kJ mol^{-1})	$\Delta^{\ddagger}S$ (J K^{-1} mol^{-1})
19	k_4	117.9 ± 1.6	7.69 ± 0.11	112.4 ± 4.7	-112.7 ± 8.0
20	k_5	137.5 ± 7.3	9.23 ± 0.48	131.0 ± 7.0	-84.6 ± 7.0
21a	k_{11}	125.72.1	11.31 ± 0.18	120.8 ± 2.1	-42.4 ± 1.0
22a	k_{13}	150.9 ± 7.4	11.18 ± 0.54	144.9 ± 7.3	-46.6 ± 3.2
22b	k_{14}	242.4 ± 7.6	17.49 ± 0.55	236.4 ± 7.6	74.3 ± 2.9
23	k_{20}	167.6 ± 6.8	11.26 ± 0.47	161.5 ± 7.0	-45.1 ± 2.7
24	k_7	113.4 ± 4.7	7.56 ± 0.32	107.1 ± 4.6	-116.2 ± 8.8

[a] Error limits are 95% certainty limits.

6.4 Prediction of the Pyrolysis Behavior of Bifunctional Pinane-Type Substrates

At this moment it is sure to state that substituents in α-position to one of the two bridge-head carbon atoms in a pinane-type monoterpene or monoterpenoid significantly influence the reactivity of this compound towards isomerization reactions, the spectrum of products formed *via* its pyrolysis, and also the selectivity for the formation of the acyclic products. The compounds investigated in this study represent the three classes of pinane-type compounds concerning their thermal isomerization behavior: pinane (**3**), α-pinene (**9**), and β-pinene (**10**). *cis*-2-Pinanol (**11**) and nopinone (**12**) which have been also investigated are representatives for the groups of pinane-type and β-pinene-type monoterpenoids, respectively, both having in common with the other substrates that only one out of two α-positions is functionalized. Literature reports many examples of compounds wherein both positions are functionalized.[50c,g,56d,58c,59a,99] The reader might ask what have those compounds in common with those being subjected to pyrolysis studies herein. Studying the influence of substituents of monofunctionalized pinane-type compounds might be the basis for the investigation of difuctionalized substances due to the fact that the effects caused by different substituents are able to be studied in simple systems. Starting with more complex systems would cause problems because of multiple reaction pathways and consecutive reactions that lead to products not explainable *prima*

facie. To proof the conclusions drawn from pyrolysis experiments with mono-functionalized compounds **3** and **9**-**12** the thermal isomerization of the two bifunctional monoterpenoids *cis*-verbanone (**13**) and verbenone (**38**) have been reconsidered. Those two compounds are representative for a wide class of terpenoids and they where chosen because the products formed from their pyrolysis are well described in literature.[50c,g,56d]

cis-Verbanone (**13**) the saturated eponym of verbenone (**38**) combines the two functionalities of two monofunctionalized pinanes in one molecule: the *cis*-methyl group of **3a** and the carbonyl group of **12**. As shown in figure 6.1 these two compounds (**3a**,**12**) differ not much in reactivity but in product selectivity and product spectra. Whereas the pyrolysis of **3a** yields two acyclic products (**19**,**20**) almost exclusively,[49e,63-65] the thermal isomerization of **12** primarily leads to the formation of one acyclic (**44**) and one monocyclic product (**45**).[50g,58d,62] Hence, both single compounds showed similar reactivity the pyrolysis of **13** primarily has to yield two acyclic and at least one monocyclic product. Since both acyclic products are 1,6-octadienes they consecutively have to undergo ene-cyclizations leading to the formation of cyclopentane-type products.

Scheme 6.4 pictures the network of $C_{10}H_{16}O$ ketones resulted from gas-phase pyrolysis experiments of **13** at 580 °C performed by Coxon, Garland, and Hartshorn. [50c,g] Data reveal that actually two acyclic ketones (**49**,**51**) and one 3-methyl-4-isopropenylcyclohexanone (**50**) were formed. Accordingly to the cyclization of **19**, **20**, **23**, and **24** the products **49** and **51** undergo ene-reactions leading to cyclopentanones **52** and **53**, respectively. With respect to the assumption being evident from the pyrolysis studies of **3a** and **12** reported herein the presumptions made for the thermal rearrangement of **13** proved to be correct. Coxon, Garland, and Hartshorn published in their studies selectivities for the formation of the primary pyrolysis products also. At a conversion of **13** ($X_{\mathbf{13}}$) of 86% the selectivities (S) for the formation of products **49**-**51** considering consecutive reactions to products **52** and **53** are 31, 26, and 41%, respectively.[50g] Therefore conclusion could be drawn that preferably the carbon-carbon bond between C(1) and C(6) is broken leading to a biradical (**TS13b**; scheme 6.4) offering the opportunity for resonance stabilization of one of the two radicals. For this reason the rupture of the bond between C(5) and C(6) takes place to only 31% (**TS13a**).

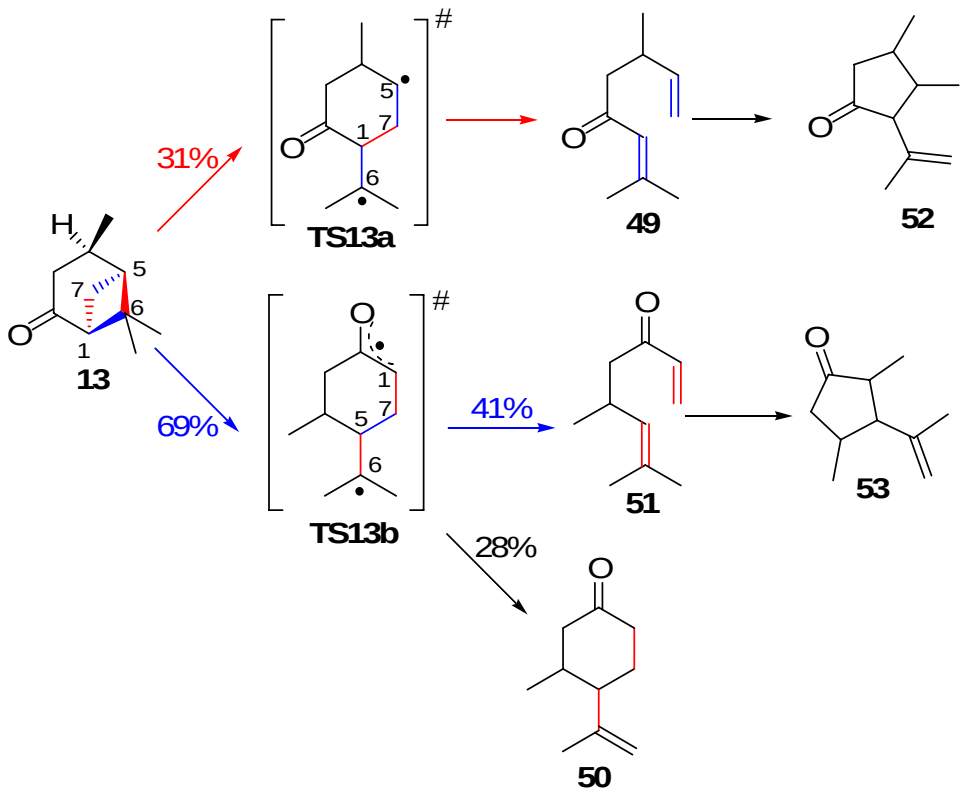

Scheme 6.4. Network of $C_{10}H_{16}O$ compounds resulted from the gas-phase pyrolysis of *cis*-verbanone (**13**; numbers represent selectivities for a conversion of **13** of 86%; colors of the reaction arrows correspond to the bonds in **13** that had to be cut forming the two possible biradicals **TS13a** or **TS13b**).[50g]

Additionally to the reactivity of these two different fragmentation pathways the resulted biradicals differ in their possibility to form finally products also. Whereas cyclic ketone **50** yield from [1,5]H-shift reaction from intermediate **TS13b**, a similar reaction products were not found in case of reaction passing through **TS13a**. These results are also in agreement with those found for the pyrolysis of **3a** and **12**. Thermal rearrangement of **3a** primarily yields monocyclic products in amount < 5%, whereby it might be that they result from undesirable reactions of the substrate with the reactor walls.[63,64] Pyrolysis of **12** lead to monocyclic ketone **45** as primary pyrolysis product, whereby an enol-type product (**47**; *cf.* scheme 5.4) was not formed neither with **12** nor with **13** as substrate.[50g,58b,62]

The second compound verbenone (**38**) chosen for revision of the transferability of the hypotheses resulted from pyrolysis studies of monofunctional pinane-type compounds **3** and **9**-**12** is quite similar to **13**. The most significant difference is the presence of an endocyclic carbon-carbon double bond in stead of the *cis*-methyl group in **13**, thus making **38** to a compound unifying the functionalizations of α-pinene (**9**) and **12**.

Comparison of the reactivity of **9** and **12** reveals that the hydrocarbon is thermally more reactive than the ketone **12** (figure 6-1), thus allowing for the conclusion that the pyrolysis of the bifunctional ketone **38** predominately yields products similar to those reported for the pyrolysis of **9**. According to the gas-phase racemization of **9**, 1,3-sigmatropic shift reaction of **38** has to yield chrysanthenone (**39**) also being the photo-isomerization product of **38** (*cf.* scheme 4.8).[83] Rupture of the C(5)-C(6) carbon-carbon bond in **38** leads to the formation of the biradical **TS38** pictured in scheme 6.5 whose subsequent fragmentation or [1,5]H-shift forms acyclic ketone **54** and isopiperitenone (**55**), respectively. Contrarily to the intermediate formed from **9** the biradical **TS38** has no mirror plain. Therefore the formation of a further acyclic ketone (**58**) has to take place. Reaction products resulted from the rupture of the C(1)-C(6) carbon-carbon bond (**59**,**60**; according to pyrolysis of **12**) would be formed in low amounts only due to the prevalence of the carbon-carbon double bond in **38**.

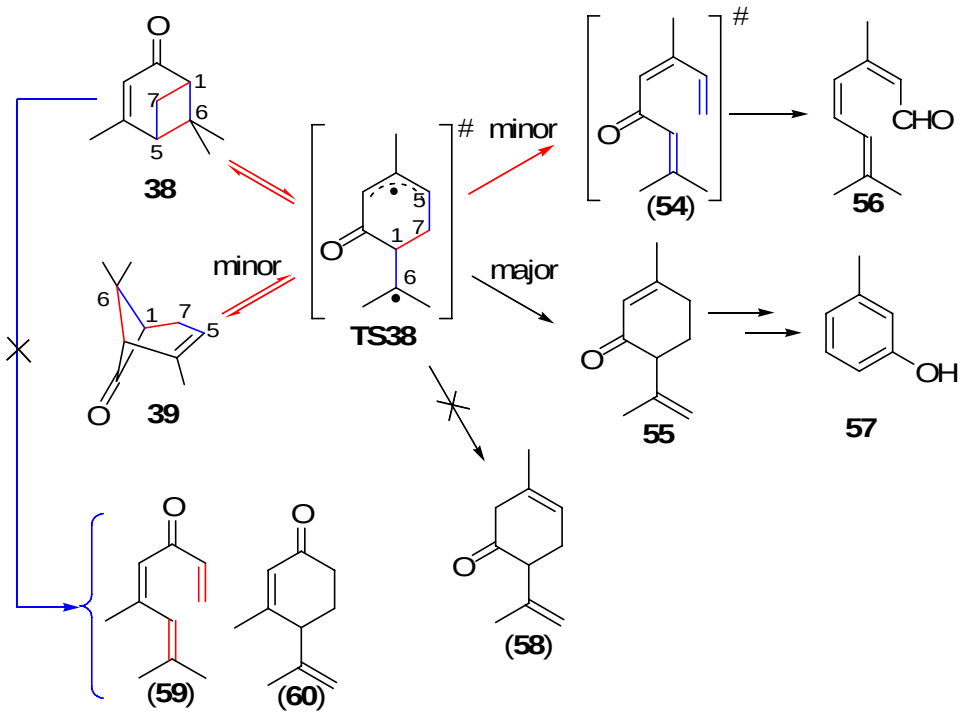

Scheme 6.5. Network of $C_{16}H_{14}O$ compounds resulted from pyrolysis of verbenone (**38**; compounds in parentheses assign presumptive pyrolysis products not being identified; colors of the reaction arrows correspond to the bonds in **38** that had to be cut forming biradical **TS38**).[56d,100]

Gas-phase pyrolysis of **38** at 500 °C and 270 mbar with an average residence time of 0.5 s were performed by Retamar,[56d] whereby product mixture consist of *p*-cresole (**57**),

propylene, ketone **55**, and aldehyde **56** as well as of minor amounts of **39** and other aromatics (scheme 6.5).[100] *Prima facie* those compounds are only partially in agreement to those ones predicted, but it has to be stated that the products observed result from consecutive reactions of the primarily formed products **54** and **55**. Apparently, according to the rapid rearrangement of **21a** to **22a** (*cf.* figure 6.3 and table 6.5) [51,57c] the initially formed ketone **54** rapidly undergoes hetero-Cope rearrangement leading to fully conjugated aldehyde **56** (scheme 6.6). The cyclic ketone **58** was not formed due to the fact that the carbonyl group and the endocyclic double bond are isolated from each other. Aromatization of the primarily formed ketone **55** yields 2-isopropenyl-5-methylphenol (thymol) which undergoes defragmentation leading to the formation of **57** and propylene.[56d]

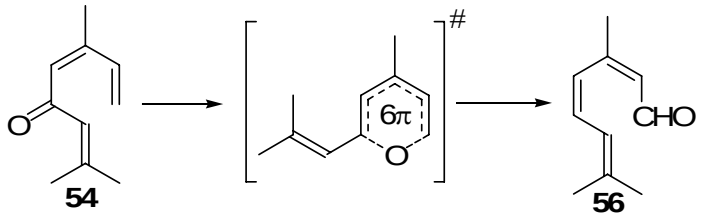

Scheme 6.6. Formation of aldehyde **56** from ketone **54** *via* hetero-Cope rearrangement.

Comparison of the results from pyrolyses of monofunctional pinane-type compounds **3** and **9**-**12** concerning reactivity, product spectra and selectivity with the results known from previous studies about the gas-phase isomerization of **13** and **38**[50g,c,56d] revealed that it is possible to use the hypotheses to predict the rearrangement behavior of pinane-type compounds with multiple functionalizations. Nevertheless, it has to be pointed out that consecutive reactions or conversions of functional groups (*e.g.* epoxides) may lead to the conclusion that the results are not comparable. In this case special attention has to be focused on these possible “side” reactions.

CHAPTER 7

Conclusion

The gas-phase pyrolysis of pinane-type monoterpenes and –terpenoids has proved to be a powerful method for the synthesis of various acyclic as well as cyclic monoterpenes and –terpenoids. Experiments were performed using a flow-type reactor with controllable reactor temperature (250-600 °C) with the addition of N_2 as carrier gas. Residence times were able to be varied by simply changing the carrier gas velocity. Due to the high N_2 to substrate ratios (3,000 at 550 °C) undesirable bimolecular reactions leading to polymerized products instead of rearrangement products were suppressed. The herein presented technique is beneficial with respect to the low amounts of substrate (< 50 µL) used for pyrolysis experiments, the simple handling, and the fact that pyrolyses lead to highly reproducible results concerning conversion, selectivity, and yield, which offers the opportunity to perform kinetic experiments also.

The variation of the residence times by changing the carrier gas flow rate allows for the calculation of rate constants and after doing this at different temperatures activation parameters according to Arrhenius as well as Eyring theory were able to be calculated. A kinetic model of competitive parallel first-order reactions was used for the estimation of the rate constants as well as of the activation parameters for the most important reactions thus allowing a deeper insight in the reaction mechanism and transition states the reactions passing through.

The six pinane derivatives **3** and **9**-**12** pictured in scheme 7.1 were subjected to pyrolysis studies in order to investigate their reactivity under controllable and quite similar reaction conditions. Explorative pyrolyses reveal that those compounds with carbon-carbon double bonds in the molecule (α-pinene **9**, β-pinene **10**) are the most reactive substrates, whereas the differences in reactivity between *cis*-pinane (**3a**), *cis*-2-pinanol (**11**), and nopinone (**12**) are negligible. *trans*-Pinane (**3b**) seem to be the compound with the highest thermal stability. Beside reactivity substituents also influence

the spectrum of products formed if starting materials being pyrolyzed. If a sp^2-carbon is in α-position to the bridge-head carbon atom of the pinane derivative (**9**,**10**,**12**) beside an acyclic main product at least one cyclic product is formed as primary pyrolysis products. This route is suppressed in case of the saturated compounds (**3**,**11**) but thermal isomerization of these leads to the formation of two different acyclic main products, which was not observed when unsaturated compounds were pyrolyzed.

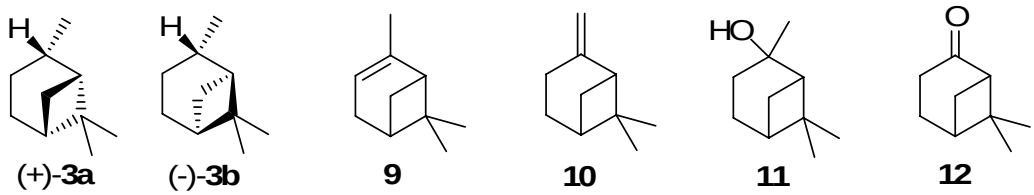

Scheme 7.1. Bicyclic pinane-type compounds whose thermal behavior has been investigated.

Kinetic analysis of the main reaction steps allows for the conclusion that the reactions responsible for the disappearance of the starting materials passing through biradical transition states, since a concerted mechanism is thermally forbidden with respect to the Woodward-Hoffmann rules for pericyclic reactions. Primary acyclic pyrolysis products are formed in a stepwise fragmentation of the cyclobutane ring in the bicyclic starting material similar to the degenerative pyrolysis of other four-membered ring systems (cyclobutane, oxetane). Apparently the formation of the cyclic reaction products in case of pyrolysis of **9**, **10**, and **12** is due to [1,n]H-shifts occurring in the initially formed biradical transition state. 1,3-sigmatropic rearrangement is supposed to be responsible for the racemization occurred in the case of thermal treatment of **9**.

In order to unravel the consecutive reactions that the at least double unsaturated acyclic pyrolysis products normally undergo those were subjected to pyrolysis studies also. Investigation of the thermal behavior of the compounds listed in scheme 7.2 allows for the conclusion that those can be classified into two categories according to the reactions they are able to undergo. The first group of 1,6-octadienes (β-citronellene **19**, isocitronellene **20**, myrcene **23**, linalool **24**) have in common that beside the two carbon-carbon double bonds at C(1) and C(6) no further internal double bonds are present in the molecule. The terminal carbon-carbon double bond in case of **23** does not participate in the reaction responsible for the disappearance of these class of substances. Ene cyclizations of **19**, **20**, **23**, and **24** lead to the formation of substituted cyclopentanes **61**

pictured in scheme 7.2, whereby the numbers of the carbon atoms in **61** correspond to the numbering in case of **19**. Rearrangement of **20**, **23**, and **24** yields similar products. GC-Analysis of the product mixtures of those isomerizations with a β-cyclodextrine column allow for the conclusion that this reaction proceed without changing the configuration of the chiral carbon atoms in **19**, **20**, and **24**.

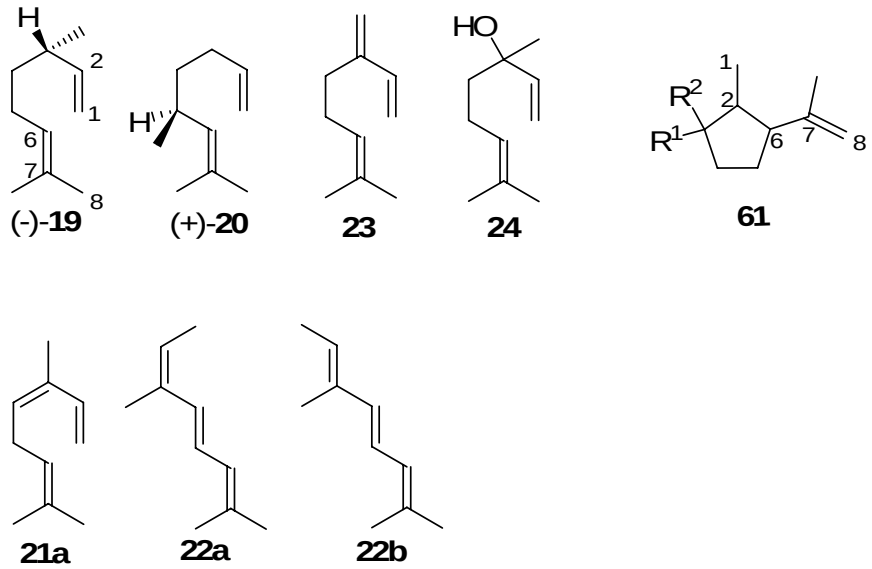

Scheme 7.2. Acyclic main products (**19**-**24**) from the pyrolysis of the pinane-type compounds whose thermal behavior has been investigated (scheme 7.1).

The compounds of the second category listed in scheme 7.2 are characterized by the presence of an additional internal carbon-carbon double bond. Pyrolysis studies performed with 3*Z*-ocimene (**21a**) as substrate revealed that a rapid isomerization to 4*E*,6*Z*-alloocimene (**22a**) occurred only, whereby it is evident from the kinetic results that this reaction proceeds as [1,5]H-shift. The tendency for the formation of fully conjugated **22a** from **21a** is such distinct that it is not possible to find **21a** in the mixture of pyrolysis products resulted from thermal isomerization of **9**. Investigative pyrolyses of **22a** and of the 4*E*,6*E*-isomer (**22b**) as well as the kinetic analysis of the reaction steps responsible for their disappearance allow for the conclusion that the cyclohexane-type products (pyronenes) formed yield from pericyclic concerted reactions as well as from stepwise cyclizations.

The bicyclic compounds subjected to pyrolysis studies herein (scheme 7.1) all have in common that only one of the two positions next to the bridge-head carbon atoms are functionalized. Nevertheless, with respect to the finding it was possible to predict the

pyrolysis products resulted from the thermal gas-phase isomerization of two bifunctionalized compounds very well. The high accordance between prediction and actually found products allows for the conclusion that it is permissible to study the influence of various substituents solely and combine these results to predict the behavior of the substituents combined in one molecule. This procedure is advantageous over the pyrolysis of bifunctional pinane derivatives only because those might lead to complex product mixtures making it difficult or even impossible to assign the products to the discrete reaction pathways.

Abstract in German – Zusammenfassung

Pyrolysereaktionen haben seit der Blütezeit der Alchemie im ausgehenden Mittelalter ihren Platz unter den Methoden, die einem jeden Chemiker zur Verfügung stehen. Mit der Entwicklung der Chemie als eigener anerkannter Zweig der Naturwissenschaften im ausgehenden 17. Jahrhundert rückten Pyrolysereaktionen in den Hintergrund, was sich schlagartig mit der Entstehung der organischen Chemie änderte. Zu jener Zeit dienten Thermolyseprozesse vor allem der Strukturaufklärung, der in immer größerer Zahl synthetisierten organischen Verbindungen. Als ab Mitte der fünfziger Jahre des zwanzigsten Jahrhunderts moderne Analysenmethoden wie IR-Spektroskopie, NMR-, und Massenspektrometrie sowie die Gaschromatographie als leistungsfähige Trennmethode ihren Einzug in die modernen Chemielaboratorien hielten, kam es auch zu einer Renaissance der Gasphasenpyrolyse von organischen Verbindungen. Zur gleichen Zeit entdeckten Gaskinetiker Pyrolysetechniken bei niedrigen Drücken (< 1 mbar) als Methode zur Generierung und *in situ* Charakterisierung von instabilen oder hochreaktiven Molekülen (z.B. Carbene, Nitrene). Aber auch in der organischen Synthese kam es mit der Entdeckung der Fullerene als dritte Kohlenstoffmodifikation zu einer wiederholten Einführung von thermischen Gasphasenprozessen als wichtiger Bestandteil der Synthesechemie.

In den dreißiger bis sechziger Jahren des letzten Jahrhunderts wurden vermehrt Anstrengungen auf dem Gebiet der Pyrolyse von Verbindungen des Pinan-Typs (α-Pinen, β-Pinen) unternommen, mit dem Ziel wichtige Zwischenprodukten für die Synthese von Feinchemikalien auf der Basis nachwachsender Rohstoffe herzustellen. Trotz einiger Arbeiten auf diesem Gebiet mangelt es bis heute sowohl an systematischen, mechanistischen als auch kinetischen Untersuchungen des Substituenteneinflusses am Pinan-Bicyclus unter vergleichbaren Reaktionsbedingungen. Innerhalb dieser Studie wurde das Pyrolyseverhalten von zwei Monoterpenen (α-Pinen **9**, β-Pinen **10**) sowie vier

verschiedenen Monoterpenoiden mit Pinanstruktur (*cis*-Pinan **3a**, *trans*-Pinan **3b**, *cis*-2-Pinanol **11** und Nopinon **12**) sowohl in explorativen als auch kinetischen Pyrolysestudien untersucht (Schema 1). Die sechs ausgewählten Verbindungen repräsentieren die Gruppe der Terpene mit bicyclischer Pinanstruktur, wobei die Edukte hinsichtlich der verschiedenen Substituenten ausgewählt wurden.

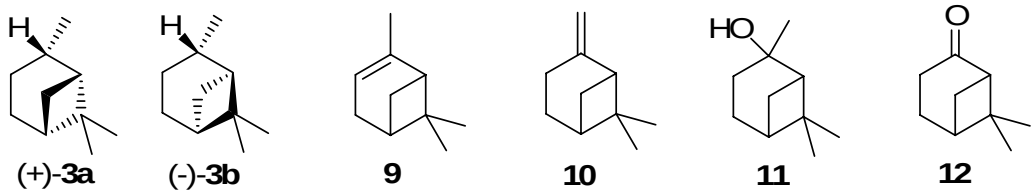

Schema 1. Bicyclen vom Pinan-Typ deren Pyrolyseverhalten untersucht wurde.

Die Pyrolyse bei Normaldruck unter Verwendung von Stickstoff (N_2) als Trägergas diente bei den Pyrolyseversuchen in einem Temperaturbereich von 250-600 °C als experimentelle Basis. Aufgrund der Verwendung von hohen Überschüssen an Trägergas im Vergleich zum Substrat (N_2/Substrat: ca. 3.000 bei 550 °C) konnten intermolekulare Reaktionen, die zu unerwünschter Polymerisation führen können, auf ein Mindestmaß reduziert werden. Im untersuchten Temperaturintervall konnten ausschließlich Umlagerungsprodukte der in Schema 1 dargestellten Substrate in den resultierenden Reaktionsgemischen nachgewiesen werden. Wiederholungsversuche haben gezeigt, dass die Experimente hinsichtlich Umsatz, Ausbeute und Selektivität einen hohen Grad an Reproduzierbarkeit aufweisen. Durch eine Variation der Trägergasgeschwindigkeit war es ohne größeren Aufwand möglich die mittlere Verweilzeit im Reaktor reproduzierbar einzustellen. Dies eröffnete die Möglichkeit für kinetische Untersuchungen der auftretenden Hauptreaktionen bei der Pyrolyse der Edukte **3** und **9-11**. Erstmalig wurden so kinetische Parameter der einzelnen Reaktionen der betreffenden Substrate sowohl nach Arrhenius als auch nach Eyring unter vergleichbaren Bedingungen ermittelt, was Schlüsse zum Reaktionsmechanismus zuließ, aber auch tiefere Einblicke in die Natur der durchlaufenden Übergangszustände lieferte.

Vergleichende Pyrolyseexperimente mit den ausgewählten Monoterpenen und Monoterpenoiden haben gezeigt, dass die unterschiedlichen Substituenten in α-Position zu den Brückenkopfatomen einen signifikanten Einfluss auf die Reaktivität (Umsatz), die Produktspektren und die Selektivität der einzelnen Pyrolyseprodukte ausüben. Dabei

wurde festgestellt, dass die Anwesenheit von C-C-Doppelbindungen in Nachbarstellung zur Verbrückung (**9**,**10**) zu einer deutlichen Reaktivitätserhöhung führt, während die Umsätze bei vergleichbaren Temperaturen im Falle der gesättigten Systeme **3a** und **11** sowie des Ketons **12** sich untereinander wenig unterschieden, aber im Vergleich zu **9** und **10** deutlich niedrigere Werte annahmen. Die Einführung einer Methylgruppe in *trans*-Stellung zur Dimethylmethylenbrücke in **3b** führte zu einem Molekül mit außerordentlich hoher thermischer Stabilität. Die höhere Reaktivität in Hinblick auf thermisch induzierte Umlagerungsreaktionen im Falle von **9** gegenüber **10** ist der Tatsache geschuldet, dass die endocyclische Doppelbindung zu einer höheren Ringspannung führt, die bei der Öffnung des Cyclobutanringes freigesetzt wird und somit zu einer Erniedrigung der Aktivierungsenergie führt.

Neben der Reaktivität traten auch Unterschiede im Produktspektrum der gebildeten Umlagerungsprodukte zu Tage. Während die Pyrolyse der gesättigten Verbindungen **3** und **11** fast ausschließlich zur Bildung von zwei offenkettigen Umlagerungsprodukten führte, wurden im Falle der ungesättigten Vertreter **9**, **10** und **12** neben einem offenkettigen Produkt größere Anteile an monocyclischen Verbindungen des *p*-Menthantyps (*p*-Methylisopropylcyclohexan) gefunden. Offensichtlich führt die Anwesenheit von sp^2-hybridisierten Kohlenstoffatomen zur Eröffnung eines neuen Reaktionsweges und zu einer selektiveren Spaltung des Cyclobutanringes, da jeweils nur ein offenkettiges Isomer gefunden wurde. Im Allgemeinen lässt sich an dieser Stelle festhalten, dass die acyclischen Umlagerungsprodukte aus einer Fragmentierung des Cyclobutanringes im Pinangerüst herrühren, die im Falle der gesättigten Substrate auf zwei verschiedene Weisen erfolgt.

Die kinetische Analyse der Umwandlungsreaktionen der Substrate **3** und **9**-**11** deutet darauf hin, dass die Fragmentierung des Cyclobutanringes im jeweiligen Edukt zur intermediären Bildung eines Biradikals führt, von dem ausgehend die entsprechende Umlagerungsprodukte gebildet werden. Die in Tabelle 1 aufgelisteten Aktivierungs-parameter sind typisch für die degenerative Pyrolyse von viergliedrigen Ringen (Cyclobutan, Oxetan). Aufgrund der Tatsache, dass eine konzertierte Cycloreversion unter Beachtung der Woodward-Hoffmann-Regeln thermisch verboten ist, muss die Reaktion stufenweise unter Ausbildung von biradikalischen Übergangszuständen (**TSA**, **TSB**) erfolgen (Schema 2). Durch weiteren Bindungsbruch können die jeweiligen offenkettigen Isomere gebildet werden, während die cyclischen Umlagerungsprodukte

von Wasserstoffverschiebungen herrühren. Im Falle der ungesättigten Vertreter **9**, **10** und **11** wird dasjenige Biradikal gebildet (**TSA**), welches die Mesomeriestabilisierung eines der beiden Radikalzentren in Form eines Allyl- (**9**,**10**) oder Hetero-Allyradikals (**12**) ermöglicht.

Tabelle 1. Kinetische Daten[a] für die Umwandlung von *cis*-Pinan (**3a**), *trans*-Pinan (**3b**), α-Pinen (**9**), β-Pinen (**10**), *cis*-2-Pinanol (**11**), und von Nopinon (**12**) während ihrer Gasphasenisomerisierung

	E_a (kJ mol^{-1})	$\log_{10}A$ (s^{-1})	$\Delta^{\ddagger}H$ (kJ mol^{-1})	$\Delta^{\ddagger}S$ (J K^{-1} mol^{-1})
(+)-**3a**	201.1 ± 9.1	13.96 ± 0.63	194.8 ± 9.0	6.3 ± 0.4
(-)-**3b**	213.0 ± 6.9	13.94 ± 0.45	206.3 ± 6.9	6.2 ± 0.3
9	170.0 ± 1.7	13.70 ± 0.14	165.2 ± 1.6	3.0 ± 0.04
10	180.8 ± 6.4	13.94 ± 0.48	175.2 ± 6.4	6.8 ± 0.3
11	209.9 ± 6.7	14.70 ± 0.26	203.8 ± 3.7	20.6 ± 0.5
12	166.3 ± 7.3	11.54 ± 0.50	159.9 ± 7.3	-40.1 ± 2.4

[a] Fehlerbereich bezieht sich auf eine Unsicherheit von 95%.

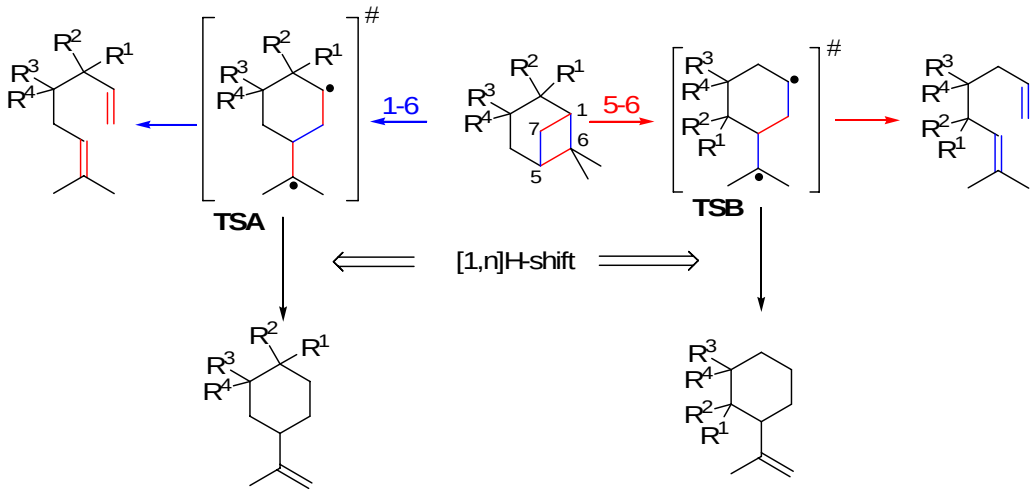

Schema 2. Mögliche Reaktionspfade, die bei der Pyrolyse der in Schema 1 abgebildeten Verbindungen durchlaufen werden können. Die Farben der Reaktionspfeile kennzeichnen diejenigen Bindungen im Bicyclus, deren Bruch zur Bildung der Biradikale **TSA** oder **TSB** führt.

Aufgrund der Tatsache, dass bei der Pyrolyse der in Schema 1 dargestellten Bicyclen ungesättigte offenkettige Verbindungen entstehen, die dazu prädestiniert sind Folgereaktionen einzugehen, wurde das thermische Verhalten dieser Produkte ebenfalls untersucht. Die in Schema 3 abgebildeten primären offenkettigen Pyrolyseprodukte

wurden für weitere Studien herangezogen. Generell lassen sich die Produkte in zwei Gruppen einteilen. Zur ersten Kategorie gehören Verbindungen bei deren thermischer Isomerisierung ausschließlich Cyclopentanderivate (**61**) gebildet werden. Dazu zählen die primären Pyrolyseprodukte von **3**; β-Citronellen (**19**) und Isocitronellen (**20**), Myrcen (**23**) welches das Hauptprodukt der Umlagerung von **10** darstellt, sowie Linalool (**24**) das Umlagerungsprodukt der Pyrolyse von **11**. Bei allen diesen Verbindungen handelt es sich um 1,6-Oktadiene mit einem Wasserstoffatom an C(8) (am Beispiel von **19**) und keiner weiteren internen Doppelbindung. Im Gegensatz zu 1,6-Heptadienen sind diese in der Lage über eine En-Reaktion selektiv das jeweilige Cyclopentan zu bilden. Durch GC-Analyse der erhaltenen Cyclisierungsprodukte an einer β-Cyclodextrinsäule wurde gezeigt, dass die Umlagerung unter Beibehaltung der Konfiguration an C(3) stattfindet.

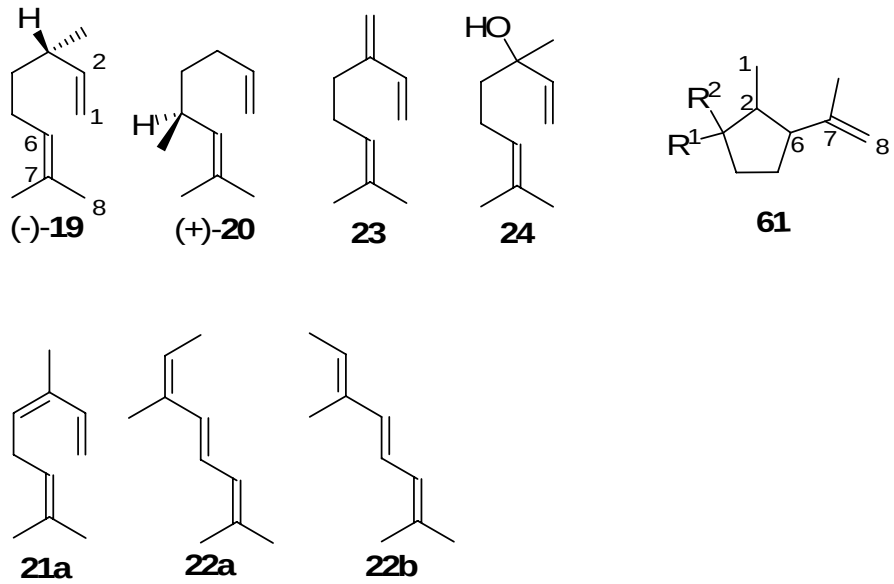

Schema 3. Offenkettige Hauptprodukte (**19**-**24**), die bei der Pyrolyse der in dieser Arbeit untersuchten bicyclischen Verbindungen (Schema 1) gebildet werden.

Im Gegensatz zu den Verbindungen **19**, **20**, **23** und **24** besitzen die drei anderen in Schema 3 dargestellten offenkettigen Pyrolyseprodukte (**21a**,**22**) der thermischen Umlagerung von **9** neben den beiden Doppelbindungen an C(1) und C(6) eine weitere konjugierte interne C-C-Doppelbindung. Die Pyrolyse von **9** führt primär zur Bildung von 3*E*-Ocimen (**21a**) als offenkettiges Produkt, welches allerdings nicht als solches im Produktgemisch nachweisbar ist. Eine schnelle [1,5]H-Verschiebung führt zur selektiven Bildung des vollständig konjugierten 4*E*,6*Z*-Alloocimens (**22a**). Durch Änderung der Konfiguration der 6*Z*-Doppelbindung in **22a** wird 4*E*,6*E*-Alloocimen (**22b**) gebildet,

wobei ausgeschlossen werden kann, dass dieses direkt aus **9** oder **21a** entsteht. Wahrscheinlich verläuft diese *E*-*Z*-Isomerisierung unter Beteiligung der Reaktorwand als basenkatalysierte Umlagerung. Die Gasphasenpyrolyse von **22a** und **22b** führt zur Bildung von Cyclohexadienderivaten (Pyronene).

Den für die Untersuchungen verwendeten bicyclischen Substraten (Schema 1) ist gemein, dass nur eine von zwei möglichen Positionen in Nachbarstellung zu den Brückenkopfatomen funktionalisiert ist. Dennoch sollte es möglich sein, auf Basis der bisherigen Daten Vermutungen darüber anzustellen, wie sich doppelt funktionalisierte Monoterpenoide hinsichtlich der bei ihrer Pyrolyse gebildeten Umlagerungsprodukte verhalten. Anhand von zwei Verbindungen wurde dies mit dem Ergebnis überprüft, dass sich die Rückschlüsse, die aus den vergleichenden Pyrolysen der einfach funktionalisierten Verbindungen gezogen werden können, auch auf die Pyrolyse von bifunktionalisierten Verbindungen übertragen lassen. Dies eröffnet die Möglichkeit, das Pyrolyseverhalten von vielen mehrfach substituierten Pinanverbindungen hinsichtlich der zu entstehenden Produkte vorherzusagen. Daraus ergibt sich ein weiterer großer Vorteil. Aufgrund der in dieser Arbeit vorgestellten Ergebnisse können primäre und sekundäre Pyrolyseprodukte den einzelnen Teilreaktionen eineindeutig zugeordnet werden. Allerdings gilt es zu beachten, dass einige funktionelle Gruppen (z.B. Epoxide) zu Reaktionen neigen, die zu Produkten führen können, welche auf Basis der theoretischen Überlegungen nicht oder nur eingeschränkt vorhersehbar sind.

Es bleibt festzuhalten, dass im Rahmen dieser Arbeit gezeigt werden konnte, dass unterschiedliche Substituenten am Pinangerüst das Umlagerungsverhalten dieser Verbindungen in der Gasphase signifikant beeinflussen. Ferner konnte gezeigt werden, wie vergleichbare Pyrolysebedingungen zu direkt untereinander vergleichbaren Ergebnissen führen. Somit wird die Möglichkeit eröffnet, das Verhalten multifunktioneller Verbindungen mit Pinanstruktur in der Gasphase unter Pyrolysebedingungen vorherzusagen.

References and Notes

Numbers of references attached to this thesis are written in **[boldface]**.

[1] a) S. Fürnsinn, H. Hofbauer, *Chem. Ing. Tech.* **2007**, *79*, 579; b) J.N. Chheda, J.A. Dumesic, *Catal. Today* **2007**, *123*, 59; c) P. Gallezot, *Green Chem.* **2007**, *9*, 295; d) P. Gallezot, *Catal. Today* **2007**, *121*, 76; e) A. Corma, S. Iborraa, A. Velty, *Chem. Rev.* **2007**, *107*, 2411; f) G.W. Huber, A. Corma, *Angew. Chem.* **2007**, *119*, 7320; *Angew. Chem., Int. Ed.* **2007**, *46*, 7184.

[2] C.H. Zhou, J.N. Beltramini, Y.X. Fan, G.Q. Lu, *Chem. Soc. Rev.* **2008**, *37*, 527.

[3] a) R.A. Sheldon, *Green Chem.* **2007**, *9*, 1273; b) J. García-Serna, L. Pérez-Barrigón, M.J. Cocero, *Chem. Eng. J.* **2007**, *133*, 7; c) S. Liu, J. Xiao, *J. Mol. Catal. A: Chem.* **2007**, *270*, 1.

[4] S. Yaman, *Energ. Conv. Manag.* **2004**, *45*, 651.

[5] Y.R. Naves, *Russ. Chem. Rev.* **1968**, *37*, 779.

[6] A.F. Thomas, *Pure Appl. Chem.* **1990**, *62*, 1369.

[7] G. Mehta, *Pure Appl. Chem.* **1990**, *62*, 1263.

[8] K.A.D. Swift, *Top. Catal.* **2004**, *27*, 143.

[9] J.L.F. Monteiro, C.O. Veloso, *Top. Catal.* **2004**, *27*, 169.

[10] E. Mitscherlich, *Justus Liebigs Ann. Chem.* **1834**, *9*, 39.

[11] a) R.B. Woodward, R. Hoffmann, *Angew. Chem.* **1969**, *81*, 797; *Angew. Chem., Int. Ed.* **1969**, *8*, 781; b) R. Hoffmann, R.B. Woodward, *Science* **1970**, *167*, 825; c) R. Ponec, *Top. Curr. Chem.* **1995**, *174*, 1.

[12] D.M. Golden, G.N. Spokes, S.W. Benson, *Angew. Chem.* **1973**, *85*, 602; *Angew. Chem., Int. Ed.* **1973**, *12*, 534.

[13] E. Hedaya, *Acc. Chem. Res.* **1969**, *2*, 367.

[14] G. Seybold, *Angew. Chem.* **1977**, *89*, 377; *Angew. Chem., Int. Ed.* **1977**, *16*, 365.

[15] R.F.C. Brown, *The Place of Flow and Flash Vacuum Pyrolytic Methods in Organic Chemistry*, in *Pyrolytic Methods in Organic Chemistry* (ed. R.F.C. Brown), Academic Press, New York **1980**, pp. 1-20.

[16] R.F.C. Brown, *Pure Appl. Chem.* **2007**, *62*, 1981.

[17] G. Zimmermann, M. Nüchter, M. Remmler, M. Findeisen, H. Hopf, L. Ernst, C. Mlynek, *Chem. Ber.* **1994**, *127*, 1747.

[18] G. Zimmermann, M. Nüchter, H. Hopf, K. Ibrom, L. Ernst, *Liebigs Annalen* **1996**, 1407.

[19] J.J. Gajewski, *Hydrocarbon Thermal Isomerization*, 2nd ed. Elsevier Academic Press, London **2004**.

[20] R.F.C. Brown, *Pyrolytic Methods in Organic Chemistry*, (ed. R.F.C. Brown) Academic Press, New York **1980**.

[21] G. Zimmermann, B. Ondruschka, M. Nüchter, F.-D. Kopinke, M. Remmler, *J. Prakt. Chem.* **1994**, *336*, 415.

[22] J. Hoffmann, G. Zimmermann, K.H. Homann, *Liebigs Ann.* **1995**, 841.

[23] H. Hopf, J. Wolff, *Eur. J. Org. Chem.* **2001**, 4009.

[24] G. Zimmermann, *Eur. J. Org. Chem.* **2001**, 457.

[25] R.F.C. Brown, *Apparatus and Methods*, in *Pyrolytic Methods in Organic Chemistry* (ed. R.F.C. Brown), Academic Press, New York **1980**, pp. 21-43.

[26] L.V. Interrante, K. Moraes, Q. Liu, N. Lu, A. Puerta, L.G. Sneddon, *Pure Appl. Chem.* **2002**, *74*, 2111.

[27] G. Schaden, *J. Anal. Appl. Pyr.* **1982**, *4*, 83.

[28] A.E.M. Gaber, H. McNab, *Synthesis* **2001**, 2059.

[29] a) W.R. Roth, F. Hunold, M. Neumann, F. Bauer, *Liebigs Ann.* **1996**, 1679; b) W.R. Roth, F. Hunold, *Liebigs Annalen* **1996**, 1917; c) W.R. Roth, H. Hopf, A. de Meijere, F. Hunold, S. Börner, M. Neumann, T. Wasser, J. Szurowski, C. Mlynek, *Liebigs Ann.* **1996**, 2141.

[30] L.Ruzicka, *Helv. Chim. Acta* **1971**, *54*, 1753.

[31] D.V. Banthorpe, B.V. Charlwood, M.J.O. Francis, *Chem. Rev.* **1972**, *72*, 115.

[32] a) D.H. Grayson, *Nat. Prod. Rep*. **1998**, *15*, 439; b) D.H. Grayson, *Nat. Prod. Rep.* **2000**, *17*, 385.

[33] The nomenclature of monoterpenes mentioned within this study and the numbering of the carbon atoms are in accordance to general IUPAC recommendations concerning the nomenclature of natural products *cf.* a) D.V. Banthorpe, D. Whittaker, *Chem. Rev.* **1966**, *66*, 643; b) P.M. Giles Jr., *Pure Appl. Chem.* **1999**, *71*, 587; c) H.A. Favre, P.M. Giles Jr., K.-H. Hellwich, A.D. McNaught, G.P. Moss, W.H. Powell, *Pure Appl. Chem.* **2004**, *76*, 1283; d) H. Schick, K.-H. Hellwich, *Angew. Chem.* **2005**, *117*, 7985.

[34] N.L. Paiva, *J. Plant Growth Regul.* **2000**, *19*, 131.

[35] M. Eggersdorfer, *Terpenes*, in *Ullmann's Encylopedia of Industrial Chemistry* (ed. B. Eloers, S. Hawkins) VCH-Weinheim, Weinheim **1996**, A27, p. 267.

[36] K.H. Wagner, I. Elmadfa, *Ann. Nutr. Metab.* **2003**, *47*, 95.

[37] B. Schulze, C. Kost, G.I. Arimura, W. Boland, *Chemie in unserer Zeit* **2006**, *40*, 366.

[38] a) K. Meyer, *Chemie in unserer Zeit* **2002**, *36*, 178; b) W. Bonrath, T. Netscher, *Appl. Catal., A* **2005**, *280*, 55; c) W. Bonrath, M. Eggersdorfer, T. Netscher, *Catal. Today* **2007**, *121*, 45.

[39] N. Ravaiso, F. Zacceria, M. Guidotti, R. Psaro, *Top. Catal.* **2004**, *27*, 157.

[40] W. Hoffmann, *Chemiker-Ztg.* **1973**, *97*, 23.

[41] A. Herrmann, *Angew. Chem.* **2007** *119*, 5938; *Angew. Chem., Int. Ed.* **2007**, *46*, 5836.

[42] a) C.M. Williams, D. Whittaker, *J. Chem. Soc., B* **1971**, 668; b) C.M. Williams, D. Whittaker, *J. Chem. Soc., B* **1971**, 672; c) M. C. Cruz Costa, R.A.W. Johnstone, D. Whittaker, *J. Mol. Catal. A: Chem.* **1998**, *129*, 79.

[43] a) G. Egloff, M. Herrman, B.L. Levinson, M.F. Dull, *Chem. Rev.* **1934**, *14*, 287; b) A.A. Frost, R.G. Pearson, *Die Thermische Isomerisation von α- und β-Pinen*, in *Kinetik und Mechanismus*

homogener chemischer Reaktionen, Verlag Chemie, Weinheim **1964**, pp. 349-354; c) D.V. Banthorpe, D. Whittaker, *Quart. Rev.* **1966**, *20*, 373; d) W. Daniewski, A. Dambska, *Tluszcze, Srodki Piorace, Kosmetyki* **1969**, *13*, 229; CAN 114:6830; e) R.F.C. Brown, *Cleavage of Carbocyclic Systems with Related Heterocyclic Examples*, in: *Pyrolytic Methods in Organic Chemistry* (ed. R.F.C. Brown), Academic Press, New York **1980**, pp. 250-253.

[44] a) D.F. Smith, *J. Am. Chem. Soc.* **1927**, *49*, 43; b) J.B. Conant, G.H. Carlson, *J. Am. Chem. Soc.* **1929**, *51*, 3464.

[45] B.A. Arbuzov, *J. Gen. Chem. (USSR)* **1936**, *6*, 297; CAN 30:36740.

[46] a) L.A. Goldblatt, S. Palkin, *J. Am. Chem. Soc.* **1941**, *63*, 3517; b) T.R. Savich, L.A. Goldblatt, *J. Am. Chem. Soc.* **1945**, *67*, 2027; c) T.R. Savich, L.A. Goldblatt, *Process for producting myrcene from β-pinene*, US-patent 2507546 **1950**; CAN 44:38182.

[47] R.L. Burwell, *J. Am. Chem. Soc.* **1951**, *73*, 4461.

[48] a) R.E. Fuguitt, J.E. Hawkins, *J. Am. Chem. Soc.* **1945**, *67*, 242; b) R.E. Fuguitt, J.E. Hawkins, *J. Am. Chem. Soc.* **1947**, *69*, 319; c) H.G. Hunt, J.E. Hawkins, *J. Am. Chem. Soc.* **1950**, *72*, 5618; d) J.E. Hawkins, J.W. Vogh, *J. Phys. Chem.* **1953**, *57*, 902.

[49] a) A.L. Rummelsburg, *J. Am. Chem. Soc.* **1944**, *66*, 1718; b) V.N. Ipatieff, W.D. Huntsman, H. Pines, *J. Am. Chem. Soc.* **1953**, *75*, 6222; c) H. Pines, N.E. Hoffman, V.N. Ipatieff, *J. Am. Chem. Soc.* **1954**, *76*, 4412; d) R. Rienäcker, G. Ohloff, *Angew. Chem.* **1961**, *73*, 240; e) R. Rienäcker, *Brennstoff-Chemie* **1964**, *45*, 20; CAN 61:61775.

[50] a) J.M. Coxon, R.P. Garland, M.P. Hartshorn, *Chem. Commun.* **1970**, 542; b) J.M. Coxon, R.P. Garland, M.P. Hartshorn, *Aust. J. Chem.* **1970**, *23*, 2531; c) J.M. Coxon, R.P. Garland, M.P. Hartshorn, *Chem. Commun.* **1971**, 1131; d) J.M. Coxon, R.P. Garland, M.P. Hartshorn, *Aust. J. Chem.* **1971**, *24*, 1481; e) J.M. Coxon, R.P. Garland, M.P. Hartshorn, *Aust. J. Chem.* **1972**, *25*, 353; f) J.M. Coxon, R.P. Garland, M.P. Hartshorn, *Aust. J. Chem.* **1972**, *25*, 947; g) J.M. Coxon, R.P. Garland, M.P. Hartshorn, *Aust. J. Chem.* **1972**, *25*, 2409.

[51] K. Riistama, O. Harva, *Finn. Chem. Lett.* **1974**, *4*, 132.

[52] J.J. Gajewski, I. Kuchuk, C.M. Hawkins, R. Stine, *Tetrahedron* **2002**, *58*, 6943.

[53] I.I. Illína, I.L. Simakova, V.A. Semikolenov, *Kinet. Catal.* **2001**, *42*, 686.

[54] a) H. Pines, N.E. Hoffman, *J. Am. Chem. Soc.* **1954**, *76*, 4417; b) W.D. Huntsman, V.C. Solomon, D. Eros, *J. Am. Chem. Soc.* **1958**, *80*, 5455; c) K.H. Schulte-Elte, M. Gadola, G. Ohloff, *Helv. Chim. Acta* **1971**, *54*, 1813.

[55] L. Lemée, M. Ratier, J.G. Duboudin, B. Delmond, *Synth. Commun.* **1995**, *25*, 1313.

[56] a) L. Ning, C. Shan-shan, *Huaxue Shijie* **2001**, *42*, 178; CAN 136:247701; b) J.P. Bain, A.H. Best, R.L. Webb, *J. Am. Chem. Soc.* **1952**, *74*, 4292; c) N.V. Maksimchuk, I.L. Simakova, V.A. Semikolenov, *React. Kinet. Catal. Lett.* **2004**, *82*, 165; d) J.A. Retamar, *Essenze, Derivati Agrumari* **1989**, *59*, 170; CAN 114:6830.

[57] a) J.E. Hawkins, H.G. Hunt, *J. Am. Chem. Soc.* **1951**, *73*, 5379; b) J.E. Hawkins, W.A. Burris, *J. Org. Chem.* **1959**, *24*, 1507; c) T. Sasaki, S. Eguchi, H. Yamada, *Tetrahedron Lett.* **1971**, *12*, 99.

[58] a) J. de Pascual Teresa, I. Sanchez Bellido, M.R. Alberdi Albistegui, A. san Feliciano, M. Grande Benito, *Anal. Quim.* **1978**, *74*, 305; CAN 89:163753; b) C.F. Mayer, J.K. Crandall, *J. Org. Chem.* **1970**, *35*, 2688; c) G. Ohloff, W. Giersch, *Helv. Chim. Acta* **1977**, *60*, 1496.

[59] a) A.F. Thomas, B. William, G. Ohloff, *Helv. Chim. Acta* **1969**, *52*, 1249; b) V.V. Bazyl´chik, P.I. Fedorov, E.D. Skakovskii, L.I. Vinogradov, *J. Org. Chem. USSR* **1981**, *17*, 268; CAN 95:43368.

[60] a) V.I. Anikeev, A. Ermakova, A.M. Chibiryaev, I.V. Kozhevnikov, P.E. Mikenin, *Russ. J. Phys. Chem. A* **2007**, *81*, 771; b) A.M. Chibiryaev, A. Yermakova, I.V. Kozhevnikov, O.I. Sal´nikova, V.I. Anikeev, *Russ. Chem. Bull. Int. Ed.* **2007**, *56*, 1234.

[61] A. Stolle, C. Brauns, M. Nüchter, B. Ondruschka, W. Bonrath, M. Findeisen, *Eur. J. Org. Chem.* **2006**, 3317; ***cf.*** appendix or the following link:
http://www3.interscience.wiley.com/cgi-bin/abstract/ 112609942/ABSTRACT

[62] A. Stolle, B. Ondruschka, W. Bonrath, *Eur. J. Org. Chem.* **2007**, 2310; ***cf.*** appendix or the following link:
http://www3.interscience.wiley.com/cgi-bin/abstract/114190175/ABSTRACT

[63] A. Stolle, B. Ondruschka, W. Bonrath, T. Netscher, M. Findeisen, M.M. Hoffmann, Thermal Isomerization of (+)-*cis*- and (-)-*trans*-Pinane Leading to (-)-β-Citronellene and (+)-Isocitronellene, *Chem. Eur. J.* **2008**, *14*, 6805; *cf.* appendix or the following link:
http://www3.interscience.wiley.com/journal/119880463/abstract?CRETRY=1&SRETRY=0

[64] A. Stolle, W. Bonrath, B. Ondruschka, D. Kinzel, L. González, *J. Phys. Chem. A* **2008**, *112*, 5885; *cf.* appendix or the following link:
http://pubs.acs.org/cgi-bin/asap.cgi/jpcafh/asap/pdf/jp800916b.pdf

[65] J. Tanaka, T. Katagiri, K. Izawa, *Bull. Chem. Soc. Jpn.* **1970**, *44*, 130.

[66] a) A. Stolle, B. Ondruschka, F. Findeisen, (eds: S.K. Starrett, J. Hong, R.J. Wilcock, Q. Li, J.H. Carson, S. Arnold), *Proc. 3rd Int. Conf. Environ. Sci. Technol.*, Houston, TX, August 5-9, 2007, American Science Press, Houston, **2007**, pp. 325; b) A. Stolle, B. Ondruschka, W. Bonrath, (eds: T. Hoffmann, W. Meyerhof, P. Schieberle), *Recent Highlights in Flavor Chemistry & Biology – Proc. 8th Wartburg Symposium*, Eisenach, 27.2.-2.3, 2007, Deutsche Forschungsanstalt für Lebensmittelchemie, Garching, **2008**, pp. 332.

[67] a) F.J. McQuillin, D.G. Parker, *J. Chem. Soc., Perk. Trans. I* **1974**, 809; b) I. Pianet, M. Dolatkhani, H. Cramail, A. Deffieux, G. Bourgeois, *J. Chim. Phys. Phys. Biol.* **1995**, *92*, 1813.

[68] E.F. Weigand, H.-J. Schneider, *Org. Magnet. Res.* **1979**, *12*, 637.

[69] a) B.G. Gowenlock, *Quart. Rev.* **1960**, *14*, 133; b) R. Walsh; *Chem. Soc. Rev.* **2008**, *37*, 686.

[70] W.D. Huntsman, P.C. Lang, N.L. Madison, D.A. Uhrick, *J. Org. Chem.* **1962**, *27*, 1983.

[71] R. Serchelli, A.L.B. Ferreira, L.H.B. Baptistella, U. Schuchardt, *J. Agric. Food Chem.* **1997**, *45*, 1361.

[72] a) V.A. Semikolenov, I.I. Illína, I.L. Simakova, *Appl. Catal., A* **2001**, *211*, 91; b) V.A. Semikolenov, I.I. Illína, I.L. Simakova, *J. Mol. Catal. A: Chem.* **2002**, *182-183*, 383.

[73] H. Strickler, G. Ohloff, E. sz. Kovats, *Helv. Chim. Acta* **1967**, *50*, 759.

[74] a) G. Ohloff, E. Klein, *Tetrahedron* **1962**, *18*, 37; b) R.E. Wellman, W.D. Walters, *J. Am. Chem. Soc.* **1957**, *79*, 1542; c) H.M. Frey, R. Walsh, *Chem. Rev.* **1969**, *69*, 103; d) J.S. Chickos, H.M. Frey,

J. Chem. Soc., Perk. Trans. II **1987**, 365; e) J.J. Gajewski, *Hydrocarbon Thermal Isomerization*, 2nd ed. Elsevier Academic Press, London **2004**, pp.46-50.

[75] The assignment for the cyclopentenols **31a-d** (scheme 3.5) considers the orientation of the alkyl-substituents only. First assignation describes the orientation of the methyl-group at C(1) towards that one at C(2) whereas the second assignment is due to the orientation of the isopropenyl-group at C(3) towards the methyl-group at C(2). In case of cyclopentenes **25a-d** (scheme 3.2) the order of assignment is switched due to switched priority of the carbon atoms.[63]

[76] W.D. Huntsman, T.H. Curry, *J. Am. Chem. Soc.* **1958**, *80*, 2252.

[77] J.J. Gajewski, C.M. Hawkins, *J. Am. Chem. Soc.* **1986**, *108*, 838.

[78] A. Yermakova, A.M. Chibiryaev, I.V. Kozhevnikov, V.I. Anikeev, *Chem. Eng. Sci.* **2007**, *62*, 2414.

[79] Bruker DRX-600 ($CDCl_3$, 600.1 MHz) equipped with a 5-mm TBI probe head in 5-mm-tubes at 27 °C. 1D-NOESY experiments (double gradient spin echo with selective pulse) were carried out using the following parameters: mixing time: 800 ms, repetition time: 3.7 s, selective 180°-pulse ("sinc"-profile), duration: 180 ms, excitation band width: ca. 20 Hz.

[80] J. de Pascual Teresa, I. Sanchez Bellido, M.R. Alberdi Albistegui, A. san Feliciano, M. Grande Benito, *Anal. Quim.* **1978**, *74*, 301; CAN 89:163752.

[81] A. Yermakova, A.M. Chibiryaev, I.V. Kozhevnikov, V.I. Anikeev, *J. Supercrit. Fluids* **2008**, *45*, 74.

[82] a) H.M. Frey, R.G. Hopkins, H.E. O´Neal, *J. Chem. Soc., D* **1969**, 1069; b) W.R. Roth, A. Friedrich, *Tetrahedron Lett.* **1969**, *10*, 2607; c) W.R. Roth, J. König, K. Stein, *Chem. Ber.* **1970**, *103*, 426; d) D.I. Schuster, D. Widman, *Tetrahedron Lett.* **1971**, *12*, 3571; e) K. Dietrich, H. Musso, *Chem. Ber.* **1974**, *107*, 731.

[83] G.W. Shaffer, M. Pesaro, *J. Org. Chem.* **1974**, *39*, 2489.

[84] R. Srinivasan, S.M.E. Kellner, *J. Am. Chem. Soc.* **1959**, *81*, 5891.

[85] G. Frank, *J. Chem. Soc., B* **1968**, 130.

[86] a) T.H. Bates, J.V.F. Best, T.F. Williams, *J. Chem. Soc.* **1962**, 1521; b) F. Cataldo, *J. Radioanal. Nucl. Chem.* **2007**, *272*, 107.

[87] F. Cataldo, personal communication (Rome, 12.2007).

[88] V.A. Mironov, A.D. Fedorovich, A.A. Akhrem, *Russ. Chem. Rev.* **1981**, *50*, 666.

[89] H.M. Frey, B.M. Pope, *J. Chem. Soc., A* **1966**, 1701.

[90] a) E.D. Parker, L.A. Goldblatt, *J. Am. Chem. Soc.* **1950**, *72*, 2151; b) K.J. Crowley, S.G. Traynor, *Tetrahedron Lett.* **1975**, *16*, 3555; c) K.J. Crowley, S.G. Traynor, *Tetrahedron* **1978**, *34*, 2783.

[91] A. Stolle, W. Bonrath, B. Ondruschka, *J. Anal. Applied Pyrol.* **2008**, *83*, 26; *cf.* appendix or the following link:
http://www.sciencedirect.com/science?_ob=PublicationURL&_cdi=5247&_auth=y&_acct=C000056279&_version=1&_urlVersion=0&_userid=2138235&_pubType=J&md5=bd8b8b5b7d1e13b2634f2bcc227f01d7

[92] a) M.B. Kolicheski, L.C. Cocco, D.A. Mitchell, M. Kaminski, *J. Anal. Applied Pyrol.* **2007,** *80*, 92; b) A. Stolle, B. Ondruschka, *J. Anal. Applied Pyrol.* **2008,** *81*, 136.

[93] G.W. Shaffer, A.B. Doerr, K.L. Purzycki, *J. Org. Chem.* **1972**, *37*, 25.

[94] a) C.T. Genaux, W.D. Walters, *J. Am. Chem. Soc.* **1951**, *73*, 4497; b) C.T. Genaux, F. Kern, W.D. Walters, *J. Am. Chem. Soc.* **1953**, *75*, 6196.

[95] W.D. Huntsman, R.P. Hall, *J. Org. Chem.* **1962**, *27*, 1988.

[96] R.F.C. Brown, *Pyrolytic Methods in Organic Chemistry*, (ed. R.F.C. Brown) Academic Press, New York **1980**, p. 300.

[97] J.H. Horner, M. Newcomb, *J. Org. Chem.* **2007**, *72*, 1609.

[98] K.W. Egger, P. Vitins, *J. Am. Chem. Soc.* **1974**, *96*, 2714.

[99] P.D. Hobbs, P.D. Magnus, *J. Chem. Soc., Perk. Trans. I* **1973**, 2879.

[100] Ref. [56d] reports that the reaction proceed *via* different biradical intermediates as pictured in scheme 6.5. With respect to the results presented in this study the presumably correct ones are pictured.

Declaration of Authorship – Selbstständigkeitserklärung

I certify that the work presented here is, to the best of my knowledge and belief, original and the result of my own investigations, except as acknowledged, and has not been submitted, either parts or whole, for a degree at this or any other university.

Ich erkläre, dass ich die vorliegende Arbeit selbstständig und unter Verwendung der angegebenen Hilfsmittel, persönlichen Mitteilungen und Quellen angefertigt habe.

Jena, den 25. 09. 2008 Achim Stolle

Appendix

Curriculum Vitae – Lebenslauf

20. 11. 1980	birth in Eisenach / Germany	Geburt in Eisenach / Deutschland
09/1987- 08/1989	attendance of elementary school in Eisenach	Besuch der Goethe-Schule in Eisenach
09/1989- 08/1991	attendance of elementary school in Eisenach (	Besuch der Liselotte-Herrmann-Schule in Eisenach
09/1991- 07/1999	attendance of high school in Eisenach	Besuch des Ernst-Abbe-Gymnasiums in Eisenach
29. 06. 1999	high school diploma (grade A)	Abitur (Note: 1,4)
11/1999- 08/2000	conscription	Wehrdienst
10/2000- 09/2005	study of chemistry at Friedrich-Schiller-University Jena	Chemiestudium an der Friedrich-Schiller-Universität Jena
15. 08. 2005	acquisition of academic degree: diploma (MSc) (grade: A)	Erwerb des akademischen Grades “Diplom-Chemiker“ (Note: 1,3)
since / seit 10/2005	scientific coworker at the Institute of Technical Chemistry and Environmental Chemistry of the Friedrich-Schiller-University Jena	Wissenschaftlicher Mitarbeiter am Institut für Technische Chemie und Umweltchemie der Friedrich-Schiller-Universität Jena

Documentation of Authorship

This section contains a list of individual author's contribution to the articles in order to document which part of work has been performed by the author of this thesis. In case of collaborative studies with other research groups, authors are collected to groups in order to simplify assignments. Numbering correspond to the reference list are given in brackets.

1. Thermal Behavior of Selected $C_{10}H_{16}$ Monoterpenes by Achim Stolle, Claudia Brauns, Matthias Nüchter, Bernd Ondruschka, Werner Bonrath, and Matthias Findeisen, *European Journal of Organic Chemistry* **2006**, 3317-3325 [61].

A. Stolle: Concept development, pyrolysis experiments with β-pinene and myrcene, manuscript preparation

C. Brauns: Synthesis of β-pinene-D_4 and pyrolysis experiments with it

B. Ondruschka, W. Bonrath, M. Nüchter: Supervision, correction of manuscript

M. Findeisen: NMR-measurements

2. Comprehensive Kinetic and Mechanistic Considerations for the Gas-Phase Behavior of Pinane-Type Compounds by Achim Stolle, Bernd Ondruschka, and Werner Bonrath, *European Journal of Organic Chemistry* **2007**, 2310-2317 [62].

A. Stolle: Concept development, synthesis of nopinone, pyrolysis experiments, kinetic measurements, manuscript preparation

B. Ondruschka, W. Bonrath: Supervision, correction of manuscript

3. Thermal Isomerization of (+)-*cis*- and (-)-*trans*-Pinane Leading to (-)-β-Citronellene and (+)-Isocitronellene by Achim Stolle, Bernd Ondruschka, Werner Bonrath, Thomas Netscher, Matthias Findeisen, and Markus M. Hoffmann, *Chemistry – A European Journal*, **2008**, *14*, 6805 [63].

A. Stolle, Concept development, pyrolysis experiments, manuscript preparation

B. Ondruschka: Supervision, correction of manuscript

W. Bonrath, T. Netscher: Interpretation of NMR-spectra, correction of manuscript

M. Findeisen: NMR-measurements of (+)-*cis*- and (-)-*trans*-pinane

M.M. Hoffmann: Interpretation of NMR-data, correction of manuscript

4. Kinetic Model fort he Thermal Rearrangement of *cis*- and *trans*-Pinane by Achim Stolle, Werner Bonrath, Bernd Ondruschka, Daniel Kinzel, and Leticia González, *The Journal of Physical Chemistry A*, **2008**, *112*, 5885-5892 [64].

A. Stolle: Concept development, pyrolysis experiments, kinetic measurements, evaluation of the kinetic model, manuscript preparation

B. Ondruschka, W. Bonrath: Supervision, correction of manuscript

D. Kinzel, L. González: Interpretation of kinetic measurements and proof of mechanistic considerations by *ab initio* calculations

5. Kinetic and Mechanistic Aspects of Myrcene Production via Thermal Induced β-Pinene Rearrangement by Achim Stolle, Werner Bonrath, and Bernd Ondruschka, *The Journal of Analytical and Applied Pyrolysis*, **2008**, *83*, 26-36 [91].

A. Stolle: Concept development, pyrolysis experiments, kinetic measurements, evaluation of the kinetic model, mechanistic considerations, manuscript preparation

B. Ondruschka, W. Bonrath: Supervision, correction of manuscript

Conference Contributions and List of Publications

Contribution to Conferences:

The 56th Lindau Meeting of Nobel Laureates – 18th Meeting dedicated to Chemistry, 25.-30.6.2006 Lindau am Bodensee (D).

8th Wartburg Symposium on Flavour Chemistry & Biology, 27.2.-2.3.2007 Eisenach (D) – A. Stolle, B. Ondruschka, W. Bonrath, poster presentation: "Thermal Behavior of Selected Monoterpenes".

3rd International Conference on Environmental Science and Technology 2007, 6.-9.8.2007 Houston, Texas (USA) – A. Stolle, B. Ondruschka, M. Findeisen, oral presentation: "Kinetic and Mechanistic Considerations in the Field of Monoterpene Thermal Isomerization".

41. Jahrestreffen Deutscher Katalytiker, 27.-29.2.2008 Weimar (D) – C. Schmöger, T. Szuppa, F. Schneider, A. Stolle, B. Ondruschka, poster presentation: "Pd on Porous Glass – An Easy Recoverable Catalyst for C-C Coupling Reactions".

18th International Symposium on Analytical and Applied Pyrolysis, 18.-23.5.2008 Costa Teguise, Lanzarote (Spain) – A. Stolle, B. Ondruschka, oral presentation: "Prediction of the Isomerization Behavior of Some Monoterpenes Based on the Thermal Rearrangement of Three Major Pinane-Type Monoterpenes".

Publications:

J. Freitag, M. Hermann, M. Nüchter, B. Ondruschka, F. Schneider, A. Stolle, *Optica Applicata* **2005**, *35*, 745.

A. Stolle, C. Brauns, M. Nüchter, B. Ondruschka, W. Bonrath, M. Findeisen, *Eur. J. Org. Chem.* **2006** 3317.

A. Stolle, B. Ondruschka, W. Bonrath, *Eur. J. Org. Chem.* **2007**, 2310.

A. Stolle, B. Ondruschka, F. Findeisen, (eds: S.K. Starrett, J. Hong, R.J. Wilcock, Q. Li, J.H. Carson, S. Arnold), Proc. 3rd Int. Conf. Environ. Sci. Technol., Houston, TX, August 5-9, 2007, American Science Press, Houston, **2007**, pp. 325-329.

A. Stolle, B. Ondruschka, *J. Anal. Appl. Pyrol.* **2008**, *81*, 136.

C. Schmöger, T. Szuppa, A. Tied, F. Schneider, A. Stolle, B. Ondruschka, *ChemSusChem*, **2008**, *1*, 339.

A. Stolle, B. Ondruschka, W. Bonrath, (eds: T. Hoffmann, W. Meyerhof, P. Schieberle), *Recent Highlights in Flavor Chemistry & Biology – Proc. 8th Wartburg Symposium*, Eisenach, 27.2-2.3.2007, Deutsche Forschungsanstalt für Lebensmittelchemie, Garching, **2008**, pp. 332-335.

A. Stolle, W. Bonrath, B. Ondruschka, D. Kinzel, L. González, *J. Phys. Chem. A* **2008**, *112*, 5885.

A. Stolle, B. Ondruschka, W. Bonrath, T. Netscher, M. Findeisen, M.M. Hoffmann, *Chem. Eur. J.* **2008**, *14*, 6805.

A. Stolle, W. Bonrath, B. Ondruschka, *J. Anal. Appl. Pyrolysis* **2008**, *83*, 26.